PEC 84

2025@

Brookhaven
National Laboratory

84th PEC Sponsors

LANGMUIR LEVEL SPONSOR

scientaomicron

FERMI LEVEL SPONSORS

SPECS TII

VST INNOVATIVE VACUUM TECHNOLOG

PHYSICAL ELECTRONICS A DIVISION OF ULVAC-PHI

KORVUS TECHNOLOGY Highly Modular PVD Systems

ANCORP

AUGER LEVEL SPONSORS

AMERICAN ELEMENTS THE MATERIALS SCIENCE MANUFACTURER®

ThermoFisher SCIENTIFIC

Thank you for supporting the Physical Electronics Conference!

Tuesday Morning

9:00 AM – 9:40 AM

Invited Talk

Dario Stacchiola

Operando Surface Chemistry on Copper Oxides

Science and User Support Center (SUSC), Building 101

9:40 AM – 10:40 AM

Contributed Talks I

Science and User Support Center (SUSC), Building 101

- Controlling selective C-O and C-H bond scission of methanol by supporting Pt on TiN and Mo2N model surfaces and powder catalysts - *Marcus Yu, Wenjie Liao, Ping Liu, Jingguang G. Chen*
- Stable Dry Reforming of Methane Enabled by High-Entropy Oxides via Synergistic Redox Exsolution and Strong Metal-Support Interaction Construction - *Zhenzhen Yang, Qingju Wang, Sheng Dai*

10:40 AM – 11:00 AM

Coffee Break (provided)

11:00 AM – 12:20 PM

Contributed Talks II

Science and User Support Center (SUSC), Building 101

- Unlocking Cu+-Activated Reactions via CuGaO2 Delafossite Surfaces - *E. L. Fornero, G. E. Murgida, M. V. Bosco, J. C. Hernández Garrido, A. Aguirre, F. Calaza, D. Stacchiola, M. V. Ganduglia-Pirovano, A. L. Bonivardi*
- Low-Temperature Activation and Coupling of Methane on supported MgO Nanostructures - *Arephin Islam and José A. Rodriguez*
- Towards understanding the Structure/Activity Relationship of Rh/TiO2 Catalysts - *Sabrina M. Gericke, Xiaobo Chen, Amy Wu, Abigail Fearon, Meng Li, Dmitri N. Zakharov, Judith Yang, Ashley R. Head*
- Simultaneous Electron spectroscopy and X-ray scattering on model ceria catalysts. *Baran Eren*

Dario Stacchiola

Group Leader, Interface Sciences/Catalysis, Center for Functional Nanomaterials, Brookhaven National Laboratory

Dr. Dario Stacchiola is the Group Leader for Interface Science and Catalysis at the Center for Functional Nanomaterials at Brookhaven National Laboratory. His research focuses on uncovering structure–reactivity relationships in surface chemistry using in-situ and operando techniques on well-defined model catalysts. He earned his Ph.D. in Physical Chemistry from the University of Wisconsin–Milwaukee and was a Humboldt Fellow at the Fritz Haber Institute. A Fulbright awardee and affiliated faculty member at Stony Brook University, Dr. Stacchiola has authored over 200 publications and patents. His work has advanced the understanding of dynamic catalyst surfaces and supported the development of nanoscale materials for chemicals and energy conversion processes.

Operando Surface Chemistry on Copper Oxides

The chemical and electronic properties of copper combined with its large natural abundance lend this material to impact a wide range of technological applications, including heterogeneous catalysis. The reactivity of copper in its Cu^{1+} oxidation state makes this specific state relevant in various chemical reactions, but the facile redox properties of copper make the isolation of individual states for fundamental studies difficult.[1] I will present our work on model systems including Cu_2O/Cu(111) films, bulk Cu_2O crystals and copper-based mixed-oxides used to study the interaction of Cu^{1+} with small molecules making use of surface science techniques. Advantages and disadvantages of each system are discussed and exemplified through case studies of chemical adsorption and reactivity studies

[1] “The Surface Chemistry of Cuprous Oxide”, *Surf. Sci.* **751**, 122622 (2025)

Controlling selective C-O and C-H bond scission of methanol by supporting Pt on TiN and Mo_2N model surfaces and powder catalysts

Marcus Yu[1], Wenjie Liao[2], Ping Liu[2,*], Jingguang G. Chen[1,2,*]

Author Affiliations:

[1]Department of Chemical Engineering, Columbia University, New York, NY, 10027, USA

[2]Chemistry Division, Brookhaven National Laboratory, Upton, NY, 11973, USA

Email: my2778@columbia.edu

Abstract

Transition metal nitrides (TMNs) have drawn attention as replacements or supports for Pt due to their Pt-like electronic properties. In this work, we investigated the effect of Pt-modification on methanol decomposition pathways on two TMNs, Mo_2N and TiN, using a combination of ultra-high vacuum (UHV) studies and density functional theory (DFT) calculations on model surfaces and correlated these findings with trends in powder catalyst studies. Traditional UHV techniques such as temperature programmed desorption (TPD) and high-resolution electron energy loss spectroscopy (HREELS) experiments were conducted Mo_2N and TiN thin films. Mo_2N was shown to have high selectivity towards C-H scission to form CO as the primary desorption product, while TiN favored C-O scission to form CH_4. The addition of Pt on either TMN surface increased the selectivity towards CO formation. DFT calculations revealed that the binding energy of O (BE_{*O}) was significantly reduced on Pt/TMN surfaces compared to TMN surfaces such that C-O bond scission pathways are suppressed, leading to preferential C-H scission as observed in TPD experiments. Further investigation using powder catalysts showed that Pt-modification of Mo_2N and TiN powders led to similar trends in C-H and C-O scission selectivity to those observed on thin films. Both thin film and powder catalyst studies demonstrated that Pt-modification on Mo_2N and TiN reduces BE_{*O} and BE_{*CO} leading to enhanced CO selectivity. This work further demonstrated that model surface studies can be effectively used to predict selectivity and activity trends in TMN and Pt-modified TMN powder catalysts.

Title: Stable Dry Reforming of Methane Enabled by High-Entropy Oxides via Synergistic Redox Exsolution and Strong Metal-Support Interaction Construction

Zhenzhen Yang,[1]* Qingju Wang,[2] Sheng Dai [1,2]

[1] Chemical Sciences Division, Oak Ridge National Laboratory, Oak Ridge, TN 37831, USA. [2] Department of Chemistry, Institute for Advanced Materials and Manufacturing, University of Tennessee, Knoxville, Tennessee 37996, USA.

Email: yangz3@ornl.gov

Dry reforming of methane (DRM) offers a sustainable pathway to valorize greenhouse gases (CO_2 and CH_4) by converting them into syngas (CO and H_2) for down-stream alkane and methanol/higher alcohols production, and the grand challenge lies in developing coking- and sintering-resistant catalysts from facile synthesis approaches. Here, we report a facile strategy to develop highly active and stable DRM catalysts by transforming rock salt structured high entropy oxide (HEO, $NiMgCuZnCoO_x$) via alkaline earth metal oxide (MO)-doping, without requiring any pretreatment. Key to this success lies in the in-situ exclusion of NiCuCo alloy as active sites, prohibiting alloy sintering via strong metal-support interaction (SMSI) overlayer construction composed of MO_x, and accelerating coking removal by enriching the CO_2 concentration vicinity to the active alloy sites. A suite of spectroscopy, microscopy, x-ray, and neutron-based techniques elucidates the structural evolution of these complex catalysts under DRM reaction conditions.

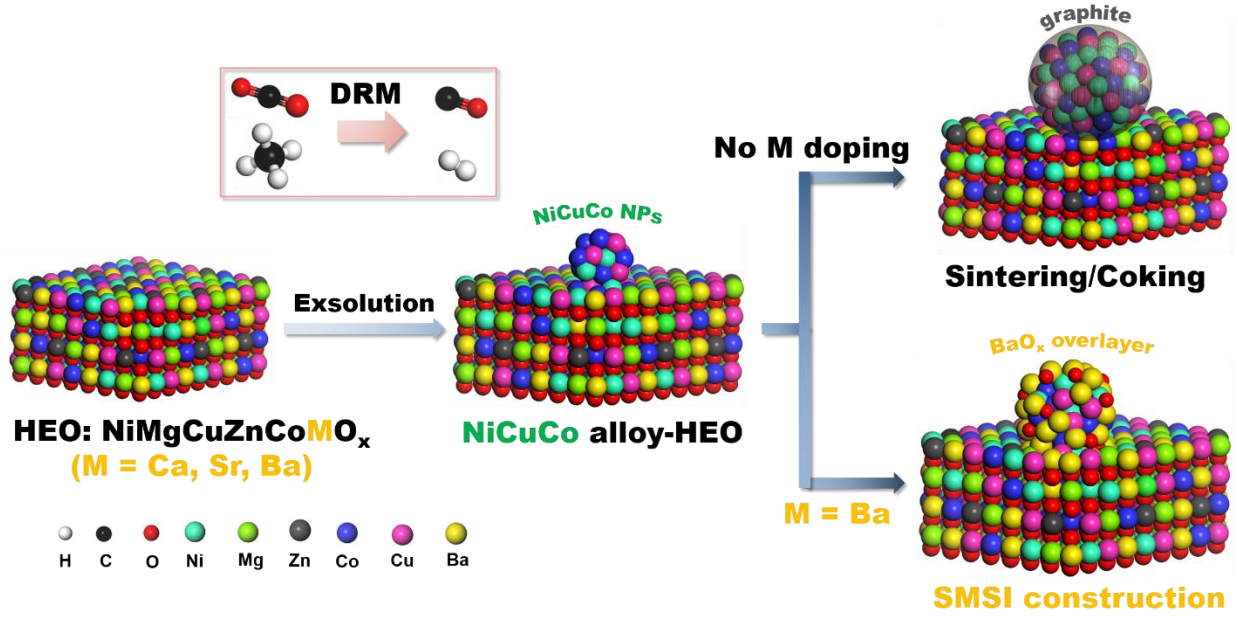

Title: Unlocking Cu^{+}-Activated Reactions via $CuGaO_2$ Delafossite Surfaces

E. L. Fornero[1], G. E. Murgida[2], M. V. Bosco[1], J. C. Hernández Garrido[3], A. Aguirre[1], F. Calaza[1], D. Stacchiola[4], M. V. Ganduglia-Pirovano[5], A. L. Bonivardi[1]

[1]INTEC, Universidad Nacional del Litoral and CONICET, 3000 Santa Fe, Argentina
[2]INN, CNEA-CONICET, Centro Atómico Constituyentes, San Martin, Argentina
[3]Universidad de Cádiz, Campus Universitario Puerto Real, 11510 Puerto Real, Spain
[4]Center for Functional Nanomaterials, Brookhaven National Laboratory, 11973 Upton, USA
[5]Instituto de Catálisis y Petroleoquímica, CSIC, C/Marie Curie 2, 28049 Madrid, Spain

Email: elfornero@santafe-conicet.gov.ar

Copper-based catalysts play a pivotal role in industrial processes, but their stability is a major concern. The active role of various copper species, particularly partially oxidized Cu^{n+} ($0 < n < 2$), remains a subject of debate. Copper delafossites, such as $CuBO_2$ (Cu^{1+} and B^{3+}), offer a promising solution, providing stability and insights into the role of $Cu^{\delta+}$ sites in catalysis. Our study on $CuGaO_2$, a copper delafossite with gallium (Cu^{1+} and Ga^{3+}), combines experiments and theory to unveil the electronic nature of active sites in CO oxidation, a classic heterogeneous catalytic reaction.

Electron microscopy studies have revealed that the $CuGaO_2$ sample primarily consists of porous thin hexagonal nanoplates. These findings, in conjunction with DFT simulations, indicate that the nanoplates' surfaces are predominantly composed of the (110) plane, accounting for approximately 83% of the surface area. These (110) surfaces are characterized by a stacking pattern of O-GaCu-O••• layers. The remaining surface area, constituting less than 17%, is terminated by Ga cations, likely due to reconstructed (111) polar planes with a stacking of O-Ga-O-Cu••• layers. Interestingly, Cu^{1+} and Ga^{3+} are the prevailing surface cations on the $CuGaO_2$ delafossite, even following inert or O_2 pretreatment at 300 °C, as demonstrated by AP-XPS analysis. However, during H_2 pretreatment, approximately 40-50% of the surface copper atoms are reduced to $Cu^{\delta+}$ (where $\delta < 1$) on the $CuGaO_2$(110) surface, leading to $CuGaO_{2-x}$. This reduction was confirmed through DFT calculations.

The IR spectra of adsorbed CO, combined with DFT calculations, have identified two overlapping peaks attributed to distinct species on $CuGaO_2$: t-Cu^{1+} (terminal monocarbonyl) at 2129 cm^{-1} and g-Cu^{1+} (geminal dicarbonyl) at 2112 cm^{-1}. However, when O vacancies are introduced ($CuGaO_{2-x}$), new species emerge, including t-Cu^{1+} or t-$Cu^{\delta+}$, g-$Cu^{\delta+}$, and b-$Cu^{1+/\delta+}$ (bridge carbonyl between 1+ and δ+ sites) at 2122, 2106 (g-sym), 2002 (g-asym), and 1965 cm^{-1}, respectively. Transient DRIFT measurements suggest that when CO adsorbed on $CuGaO_{2-x}$ is exposed to O_2, it undergoes oxidation more rapidly compared to CO on $CuGaO_2$. This difference is attributed to the higher reactivity of g-$Cu^{\delta+}$ species on $CuGaO_{2-x}$ in contrast to g-Cu^{1+} on $CuGaO_2$. The presence of geminal dicarbonyl species on $Cu^{\delta+}$ is considered crucial for CO oxidation.

Light-off curves for CO oxidation over $CuGaO_2$, subjected to sequential calcination and reduction, were compared to pristine treated samples. The findings provide compelling evidence that $CuGaO_2$ serves as an active and stable catalyst for CO oxidation. Furthermore, a reduction pretreatment with H_2 leads to an increase in the reaction rate and a decrease in the apparent activation energy. These results align with the transient DRIFT observations and are associated with the presence of stable Cu^{1+} and $Cu^{\delta+}$ surface sites.

This study underscores the pivotal role of geminal dicarbonyl species located on $Cu^{\delta+}$ sites on $CuGaO_{2-x}$ surfaces in the carbon monoxide oxidation reaction. This exemplifies the vast potential of $CuBO_2$ systems in the exploration of Cu-based heterogeneous catalysis.

Low-Temperature Activation and Coupling of Methane on supported MgO Nanostructures

Arephin Islam and José A. Rodriguez

Chemistry Division, Brookhaven National Laboratory, Upton, New York 11973 (USA)

Email: mislam@bnl.gov

Natural gas, primarily composed of methane, is a versatile energy vector with significant potential for efficient energy utilization. Converting methane into valuable hydrocarbons, such as ethane and ethylene, at low temperatures without deactivation challenges remains a critical objective. MgO nanostructures have emerged as promising candidates for methane activation due to their unique surface properties, while Cu-based catalysts demonstrate potential for selective methane oxidation at reduced temperatures. This study examines the growth and reactivity of MgO nanostructures on Cu_2O/Cu(111) and Au(111) substrate using scanning tunneling microscopy (STM) and synchrotron-based ambient-pressure X-ray photoelectron spectroscopy (AP-XPS). Mg deposition onto the "29" structured copper oxide film promotes oxygen transfer from the Cu_2O/Cu(111) substrate to Mg, forming MgO and CuO_x phases. The resulting structures exhibit diverse morphologies, including embedded MgO nanostructures (1–3 Mg atoms) and randomly dispersed MgO nanoparticles. AP-XPS and STM analyses reveal that MgO nanostructures (0.2–0.5 nm wide, 0.4–0.6 Å high) embedded in Cu_2O/Cu(111) substrates activate methane at room temperature, dissociating it primarily into CH_x (x = 2 or 3) and H adatoms with minimal C adatom formation. At 500 K, these structures facilitate C–C coupling into ethane and ethylene with negligible carbon deposition and no catalyst deactivation, significantly outperforming bulk MgO catalysts, which require temperatures exceeding 700 K. Density functional theory (DFT) calculations support these experimental findings, showing that methane activation is a downhill process on MgO/Cu_2O/Cu(111) surfaces. Methane dissociation is driven by electron transfer from copper to MgO and the presence of under-coordinated Mg and O atoms. The formation of O–CH_3 and O–H bonds lowers the energy barrier for C–H bond cleavage in methane. Furthermore, DFT studies indicate that smaller Mg_2O_2 clusters exhibit stronger binding and lower activation barriers for C–H dissociation, while larger Mg_3O_3 clusters enhance C–C coupling due to weaker $*CH_3$ binding. To understand the role of Cu, MgO was also deposited on inert Au(111) surface followed by similar XPS and STM experiments. These results highlight the critical role of size in optimizing the catalytic performance of MgO nanostructures for selective methane conversion.

Towards understanding the Structure/Activity Relationship of Rh/TiO_2 Catalysts

Sabrina M. Gericke[1], Xiaobo Chen[2,3], Amy Wu[1,4], Abigail Fearon[1], Meng Li[1], Dmitri N. Zakharov[1], Judith Yang[1,2], Ashley R. Head[1]

[1] Center for Functional Nanomaterials, Brookhaven National Laboratory, Upton, NY 11973, USA
[2] Department of Chemical and Petroleum Engineering, University of Pittsburgh, Pittsburgh, Pennsylvania 15261, USA
[3] Department of Mechanical Engineering & Materials Science and Engineering Program, State University of New York at Binghamton, Binghamton, New York 13902, USA
[4] Smith School of Chemical and Biomolecular Engineering, Cornell University, Ithaca, NY 14853, USA

Email: sgericke@bnl.gov

A promising solution to mitigate climate change involves utilizing carbon dioxide as a carbon source and harnessing "green hydrogen" generated from renewable energy sources.[1] This approach enables the production of high-value chemicals from CO_2 through catalytic reactions. One of these conversion reactions is the Reverse Water Gas Shift (RWGS) reaction which converts CO_2 and H_2 into syngas, a vital precursor for various catalytic processes. Nano-sized heterogeneous catalysts, specifically oxide-supported transition metals or oxides, are promising catalysts in the RWGS reaction. While strides have been made in advancing our understanding of the atomic reaction dynamics, one critical aspect tends to be overlooked – catalyst degradation. This phenomenon is the root cause behind the failure of promising catalysts for industrial applications that have shown success in laboratory testing. Hence, addressing catalyst degradation is critical to optimize performance in industrial processes.

Our focus centers on atomically dispersed Rh supported catalysts within low temperature RWGS reactions. The Rh/TiO_2 system is highly active for RWGS, but the selectivity switches to CH_4 production upon Rh sintering.[2] To improve our understanding of the sintering process, we studied Rh/TiO_2 catalysts under different gas conditions using Ambient-Pressure X-ray Photoelectron Spectroscopy (APXPS) and Infrared (IR) spectroscopy to follow changes of the oxidation state and structure of the Rh. We correlate our spectroscopy results with environmental Transmission electron microscopy (TEM) studies to understand the Rh dynamics under gas pressure. Our results show the effect of gas composition and elevated temperature on the size of Rh particles and the occurrence of a strong metal support interaction.

References:

1. W. Y. A techno-economic review on carbon capture, utilisation and storage systems for achieving a net-zero CO_2 emissions future. Carbon Capture Science & Technology 3, 100044 (2022)
2. Matsubu, J. C., Yang, V. N. & Christopher, P. Isolated Metal Active Site Concentration and Stability Control Catalytic CO_2 Reduction Selectivity. J. Am. Chem. Soc., 3076-3084 (2015)

SIMULTENOUS ELECTRON SPECTROSCOPY AND X-RAY SCATTERING ON MODEL CERIA CATALYSTS

Baran Eren

Department of Chemical and Biological Physics, Weizmann Institute of Science, 234 Herzl Street, 76100 Rehovot, Israel

Heterogeneous catalysis is a timely and critical research field in basic and applied energy sciences, due to its potential to provide solutions to global environmental issues. However, there is still a lack of a profound understanding of the molecular and structural processes at the interfaces between solids and reactant gases. A detailed understanding of the correlation between the chemistry, structure, and function in these materials requires a multimodal investigation. Over the past few years, scientists at the at the Advanced Light Source, the Berkeley synchrotron facility, have developed a unique setup attached to an X-ray beamline where chemically-sensitive ambient pressure X-ray photoelectron spectroscopy (APXPS) and structure-sensitive grazing incidence X-ray scattering (GIXS) experiments can be performed simultaneously Here, we showcase that this tool can provide mechanistic insights that are unparalleled in the literature.

Our novel approach allows us to probe the changing surface and bulk chemistry, and surface and bulk structure of the model ceria catalysts in the presence of H_2 and CO_2 gases. In addition to the method itself, the electron density, surface chemistry, and roughness trends observed in ceria during the reaction will be discussed in this talk. Access to such a variety of data from working catalysts in a single experiment can have far-reaching implications, because changes in surface roughness, ability to store hydrogen in the bulk in various forms, and the chemical state of the surface, which all depend on the reactive environment, can directly affect the catalyst performance.

Tuesday Afternoon

2:00 PM – 3:20 PM — **Contributed Talks III**

Science and User Support Center (SUSC), Building 101

- Understanding of non-trivial electronic structure in epitaxial graphene heterostructures on SiC by scanning tunneling microscopy and spectroscopy - *Umamahesh Thupakula and Marek Kolmer, Ames Lab*
- On-Surface Synthesis of Semiconducting-to-Metallic Nanoporous Graphene - *Mamun Sarker, Alexander Sinitskii*
- Impact of external screening on the valence and core-level photoelectron spectra of one-layer WS_2 - *Alex Boehm, Christopher M. Smyth, Andrew R. Kim, Don Bethke, Tzu-Ming Lu, Jose J. Fonseca, Jeremy T. Robinson, Taisuke Ohta*
- Interfacial Design of Two-dimensional Energy-Efficient Nanoelectronics - *Huamin Li*

3:20 PM – 3:40 PM — **Coffee Break** (provided)

3:40 PM – 5:00 PM — **Contributed Talks IV**

Science and User Support Center (SUSC), Building 101

- Metallic Conductivity in Ti3C2Tx and Its Correlation with Photoresponse Behavior - *Alexey Lipatov*
- Atomic-Scale Visualization and Manipulation Polar Domain Boundaries - *Fan Zhang, Zhe Wang, Lixuan Liu, Anmin Nie, Yanxing Li, Yongji Gong, Wenguang Zhu, Chenggang Tao*
- Transition metal silicides: a new class of material candidates for superconducting qubit applications - *Mingzhao Liu*

Understanding of non-trivial electronic structure in epitaxial graphene heterostructures on SiC by scanning tunneling microscopy and spectroscopy

Umamahesh Thupakula,[1#] and Marek Kolmer[1*]

[1] Ames National Laboratory, U.S. Department of Energy, Ames, IA 50011, USA.
Emails: [#]umahere@ameslab.gov; *mkolmer@ameslab.gov

Controlling electronic states in two-dimensional (2D) materials is currently one of the main directions of modern condensed matter physics, aiming for quantum information science applications. Here, we will focus on the epitaxially grown graphene on a silicon carbide (0001) surface, where thermal decomposition of the top silicon carbide layers provides a synthesis of epitaxial graphene layer(s) with exceptional uniformity and control over their structural properties, i.e., number of graphene layers. Subsequent intercalation of heteroatoms under graphene layer(s) becomes a promising strategy for the synthesis of designer 2D quantum materials.

In the talk, we will discuss how control over the graphene interfaces and metal intercalation affects the resulting electronic structure of these model systems, which is studied using the low-temperature (~4.5 K) ultrahigh vacuum scanning tunneling microscopy and spectroscopy. The first part will focus on the less-understood interface states within the unoccupied electronic band regime above the vacuum level. The low-temperature scanning tunneling microscope operating in the high-sample bias voltages reaching ~40 V is used to study the interaction between the interface states and high-bias resonances formed within the triangular tip-sample potential. We show the methodology of how to extract the intrinsic electronic density of states of highly unoccupied bands as a function of graphene thickness and intercalated phase from these high-bias scanning tunneling spectroscopy (STS) experiments. Due to the 2D nature of systematically studied graphene heterostructures, their high-bias STS spectra show pronounced features within this energy regime, which strongly depend on the interlayer couplings between the heterostructure interfaces.

In the second part, we will present the formation of AA stacked lattice "domain walls" within the AB Bernal stacked bilayer graphene (BLG). The differential conductance (dI/dV) maps show two different categories of local density of states behavior of the AA "domain walls", which are expected to host a topologically protected 1D electronic (edge) state in the gapped BLG electronic structure.

Acknowledgements: This work was supported by the U.S. Department of Energy (DOE), Office of Science, Basic Energy Sciences, Materials Science and Engineering Division through a DOE Early Career Project at the Ames National Laboratory, which is operated for the U.S. DOE by Iowa State University under contract # DE-AC02-07CH11358. Part of the research was performed as a User Project at the Center for Nanophase Materials Sciences, which is a DOE Office of Science User Facility.

Preference: Oral Presentation

On-Surface Synthesis of Semiconducting-to-Metallic Nanoporous Graphene

Mamun Sarker*, **Alexander Sinitskii**

Department of Chemistry, University of Nebraska – Lincoln, NE-68588, USA

*Email: msarker2@unl.edu

Molecular design is a powerful tool for growing graphene nanostructures with atomic precision, enabling control over their electronic and physical properties. Precisely tuning these properties is essential for advancing the next generation of graphene-based 2D electronic devices. In this presentation, I will discuss the on-surface synthesis of novel nanoporous graphene (NPG) materials, whose electronic bandgaps can be tuned from semiconducting to nearly metallic through rational molecular design. These NPGs were synthesized using custom-designed polyaromatic precursors deposited on Au(111) and thermally activated under ultra-high vacuum via surface-assisted chemical reactions. Scanning tunneling microscopy (STM) reveals the structural integrity and periodicity of nanoporous networks. Scanning tunneling spectroscopy (STS), in combination with density functional theory (DFT), shows that strategic modifications in the pore size, topology, and connectivity can reduce the bandgap to as low as 0.05 eV, approaching metallic behavior. This work not only demonstrates the feasibility of tailoring graphene's electronic structure with sub-nanometer precision but also establishes a versatile platform for engineering low-bandgap 2D materials.

Impact of external screening on the valence and core-level photoelectron spectra of one-layer WS_2

Alex Boehm,[1] Christopher M. Smyth,[1] Andrew R. Kim,[1] Don Bethke,[1] Tzu-Ming Lu,[1] Jose J. Fonseca,[2] Jeremy T. Robinson,[2] Taisuke Ohta[1]

[1] Sandia National Laboratories, Albuquerque, NM 87185, United States
[2] U.S. Naval Research Laboratory, Washington, DC, 20375, United States

Email: tohta@sandia.gov

In an effectively-screened environment, transition metal dichalcogenides (TMDs) rearrange their charge carriers to screen the added charges, and reduce the electronic band gap. Consequently, when interfaced with dissimilar materials, a sheet of TMD would change its band gap adapted to its local external screening environment. Similarly, a well-screened environment stabilizes photo-holes or core-holes created in the photoemission process and, in turn, boosts the kinetic energy of photoelectrons resulting in the apparent smaller binding energy. Complication arises when determining the electronic band alignment of TMDs using photoelectron spectroscopy since the screening influences the material property of interest as well as its assessment approach concurrently. Using a sample that contains areas of suspended and gold-supported one-layer WS_2, we show how the electronic states of WS_2 under the contrasting effective or ineffective external screening environment align at the built-in junction. The photoelectron spectra point to the breakdown of rigid shifts between the valence states and core-levels with the core-levels shifting more than twice as much as the valence states. Additionally, effectively-screened WS_2 displays a valence state with a substantially larger photoemission linewidth than ineffectively-screened suspended WS_2. Altogether, our result provides key insights into how the local variation of the external screening environment creates essentially a heterojunction within a layer of WS_2, and whether commonly accepted photoelectron spectroscopy practices hold when examining the electronic structures of one-layer TMDs.

The work was supported by the Laboratory Directed Research and Development program at Sandia National Laboratories and Base Programs and the Nanoscience Institute at the Naval Research Laboratory via the Office of Naval Research. A.R.K. acknowledges support from the U.S. Department of Energy, Office of Science, Division of Materials Sciences and Engineering (grant BES 20-017574). Samples were fabricated, in part, at the Center for Integrated Nanotechnologies, an Office of Science User Facility operated for the US Department of Energy, Office of Science. Sandia National Laboratories is a multi-mission laboratory managed and operated by National Technology and Engineering Solutions of Sandia, LLC., a wholly-owned subsidiary of Honeywell International, Inc., for the U.S. Department of Energy's National Nuclear Security Administration under contract DE-NA0003525. Any subjective views or opinions that might be expressed in the paper do not necessarily represent the views of the U.S. Department of Energy or the United States Government.

Interfacial Design of Two-dimensional Energy-Efficient Nanoelectronics

Huamin Li*

Department of Electrical Engineering, Center for Advanced Semiconductor Technologies, University at Buffalo, The State University of New York, New York, USA

Email: huaminli@buffalo.edu

With the rise of graphene (Gr) since 2004, two-dimensional (2D) have been extensively explored for energy-efficient nanoelectronics due to their novel charge transport properties compared to conventional three-dimensional (3D) bulk materials. However, there are still challenges and issues for practical implementation of 2D materials. Here from the perspective of interfacial design, we take 2D semiconducting MoS_2 as an example to review our recent research of energy-efficient nanoelectronics, ranging from synthesis to device demonstration. **First**, by functionalizing the growth substrate, we can achieve on-demand selective-growth of 2D MoS_2 using chemical vapor deposition (CVD) and the electron mobility can be up to 20 cm^2/Vs at room temperature. At the interface between MoS_2 and SiO_2 substrates, an interfacial tension can be induced due to a mismatch of thermal expansion coefficients, which creates an anisotropy of in-plane charge transport [1, 2] as well as a self-formed nanoscroll structure [3]. **Second**, at the interface between MoS_2 and metal contact, a monolayer h-BN decoration can enable novel manipulation of charge transport through quantum tunneling, in contrast with conventional thermionic emission [3]. The contact resistance can be suppressed by both localized and generalized doping using transition metals [4]. **Third**, at the interface between MoS_2 and other 2D materials, band-to-band Zener tunneling and cold-source charge injection can be enabled, giving rise to a superior transport factor (<60 meV/decade) in field-effect transistor (FET) configurations. These novel charge transport can be utilized to overcome the fundamental limit of "Boltzmann tyranny", and realize tunnel FETs and cold-source FETs with sub-60-mV/decade subthreshold swings [5-8] or novel anti-ambipolar FETs [9]. The integration of 2D MoS_2 with 3D Si also shows excellent rectification, even with a sub-1-nm thickness of the monolayer [10]. **Fourth**, at the interface between MoS_2 and ferroelectric or ionic dielectrics, excellent electrostatic gating leads to a superior body factor (<1), and also improves the energy efficiency for transistor operation [11].

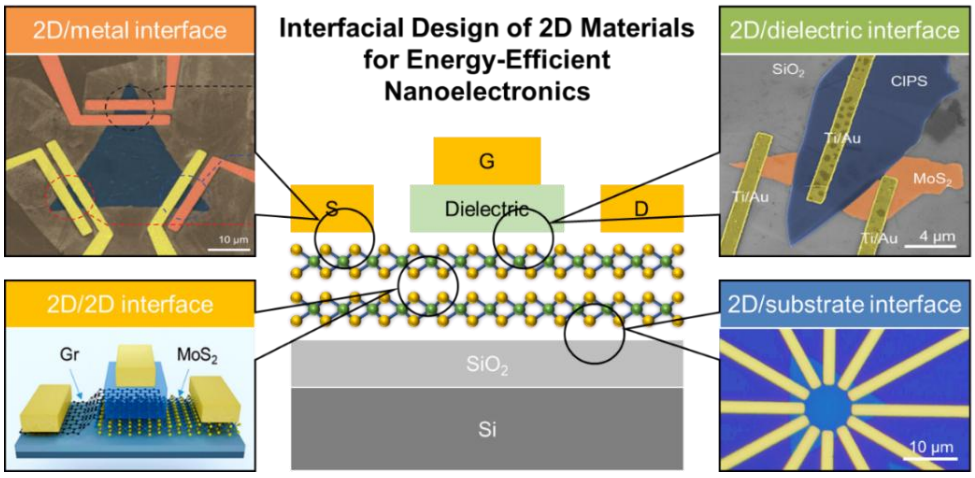

Reference

1. H. Li and co-workers, under review by Nature Communication.
2. H. Li and co-workers, DRC, Ann Arbor, MI, p. 133, 2019.
3. H. Li and co-workers, Adv. Mater., vol. 32, no. 2002716, 2020.
4. H. Li and co-workers, Nanoscale, vol. 12, pp. 17253, 2020.
5. H. Li and co-workers, IEEE IEDM, virtual, p.251, 2020.
6. H. Li and co-workers, ACS Nano, vol. 15, pp. 5762, 2021.
7. H. Li and co-workers, ACS Nano, vol. 11, pp. 9143, 2017.
8. H. Li and co-workers, US Patent 12002877 B2, 2024.
9. H. Li and co-workers, JVST B, vol. 41, no. 053202, 2023.
10. H. Li and co-workers, ACS Nano, vol. 19, pp. 3865, 2025.
11. H. Li and co-workers, Nano Express, vol. 4, no. 035002, 2023.

Metallic Conductivity in $Ti_3C_2T_x$ and Its Correlation with Photoresponse Behavior

Alexey Lipatov[1]

[1] Department of Chemistry, Biology and Health Sciences, South Dakota School of Mines and Technology, Rapid City, SD, USA.

Email: alexey.lipatov@sdsmt.edu

$Ti_3C_2T_x$, the most popular MXene to date, is widely regarded as a metallic material based on numerous theoretical and experimental studies. Yet, despite this consensus, there have not been reports on temperature-dependent resistivity ($\rho(T)$) measurements demonstrating the expected increase of resistivity with temperature ($d\rho/dT > 0$) over a wide temperature range. Instead, all reported $\rho(T)$ data, mainly from macroscopic films of percolating $Ti_3C_2T_x$ flakes, show dependencies with minima in the range of 90–250 K. In this work, we fabricated electronic devices based on individual high-quality $Ti_3C_2T_x$ flakes and measured their temperature-dependent resistivity. Resistivity increased with temperature in the entire 10–300 K range, with $\rho(T)$ accurately fitted by the Bloch–Grüneisen formula, confirming the metallic nature of $Ti_3C_2T_x$. We also show that oxidation of a $Ti_3C_2T_x$ monolayer transforms a monotonically increasing $\rho(T)$ curve into a dependence with a minimum similar to those previously reported. Multilayer $Ti_3C_2T_x$ flakes retain their purely metallic $d\rho/dT > 0$ behavior even after annealing in air, suggesting outer layers effectively protect core layers from oxidation and may improve stability for applications.

Additionally, we investigated the photoresponse of various MXenes and found a distinct correlation between synthesis method, temperature-dependent conductivity, and photoconductive behavior. Due to their high absorption of light energy and low thermal conductivity, these materials exhibit both positive and negative photoresponse depending on preparation conditions, even for $Ti_3C_2T_x$. We show that a simple photoresponse measurement can serve as a rapid indicator of MXene conductivity type.

Title: Atomic-Scale Visualization and Manipulation Polar Doiman Boundaries

Fan Zhang[1], Zhe Wang[2], Lixuan Liu[3,4], Anmin Nie[4], Yanxing Li[5], Yongji Gong[3], Wenguang Zhu[2], Chenggang Tao[6]

[1] Department of Physics, Virginia Tech, Blacksburg, VA 24061, USA.
[2] International Center for Quantum Design of Functional Materials, Department of Physics, University of Science and Technology of China, Hefei, China.
[3] School of Materials Science and Engineering, Beihang University, Beijing 100191, China.
[4] Center for High Pressure Science, State Key Laboratory of Metastable Materials Science and Technology, Yanshan University, Qinhuangdao 066004, China.
[5] Department of Physics, University of Texas at Austin, Austin, TX 78712, USA.
[6] Institute for Critical Technology and Applied Science, Virginia Tech, Blacksburg, VA 24061, USA.

Email: cgtao@vt.edu

Domain boundaries exhibit unique physical properties and have potential applications in nanoelectronics and quantum devices. Polar domain boundaries in bulk ferroelectric bulk and emerging 2D materials have been intensively investigated. Many methods such as electrical, mechanical, and optical approaches have been utilized to probe and manipulate domain boundaries. So far, most research focuses on the initial and final states of domain boundaries before and after manipulation, while the microscopic understanding of the evolution of domain boundaries remains elusive.

In this talk, I will present our controllable manipulation of polar domain boundaries in 2D ferroelectric In_2Se_3 with atomic precision by using scanning tunneling microscopy (STM). We show that the movements of the domain boundaries can be driven by the electric field from an STM tip and proceed by the collective shifting of atoms at the domain boundaries. Our density functional theory calculations reveal the energy path and evolution of the domain boundary movement. The results provide deep insight into domain boundaries in 2D ferroelectric materials and will inspire inventive applications of these materials.

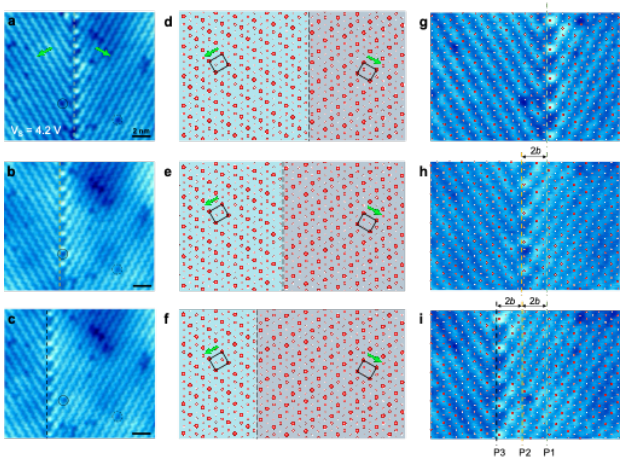

Figure 1 Manipulation of a tail-to-tail polar domain boundary with atomic precision in monolayer In_2Se_3.

References:

1. F. Zhang et al., Nature Communications 15, 718 (2024).
2. F. Zhang et al., The Journal of Physical Chemistry Letters 12, 11902 (2021).
3. F. Zhang et al., ACS Nano 13, 8004 (2019).

Transition metal silicides: a new class of material candidates for superconducting qubit applications

Mingzhao Liu[1]

[1] Center for Functional Nanomaterials, Brookhaven National Laboratory, Upton, NY 11973, USA

Email: mzliu@bnl.gov

For future superconducting qubits development, implementations that are compatible with silicon-based microelectronics (e.g., CMOS), have the best outlook to enable rapid scale-up and high levels of device uniformity and reliability. This vision takes advantage of the vast knowledge obtained from studying transition metal (TM) silicides as gate and low-resistance interconnect materials in CMOS implementations, and that many TM silicides, such as CoSi2, PtSi, and V3Si, are superconductors. The talk will feature the thin film material synthesis and characterization of several superconducting TM silicides that have transition temperatures ranging from just below 1 K to above 10 K. By using standard nanolithography techniques, these TMSi thin films can be turned into relevant quantum information devices, such as Josephson weak links and microwave resonators. In particular I will discuss the application of PtSi, a B31 noble metal silicide that has superior chemical stability and long superconducting coherence length (~100 nm), for application in constriction-type, co-planar Josephson junctions. I will also discuss the perspective of applying superconducting TM sililicides for voltage-controlled qubit applications.

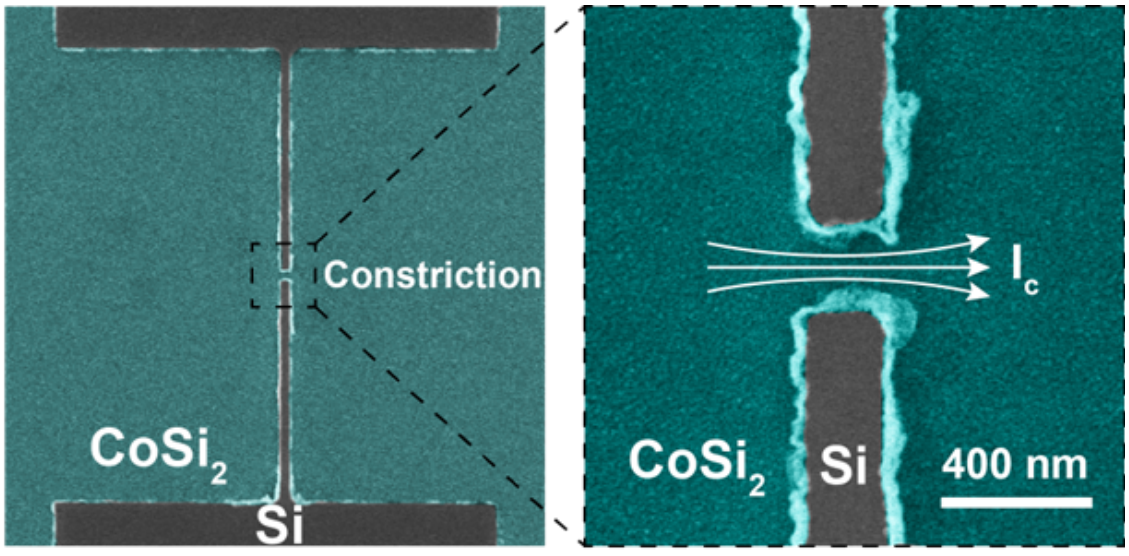

Tuesday Evening

5:30 PM – 8:00 PM

Poster Session & Dinner (provided)

Science and User Support Center (SUSC), Building 101

- Engineering Bandgap of Porous Graphene Nanoribbons - *Mohammad Nazmus Sakib*
- Wafer-Scale 2D MoS2 Transistors Using Transfer-Free Location-on-Demand Selective Synthesis - *Chu-Te Chen, Anthony Cabanillas, Fei Yao, Huamin Li*
- Wafer-Scale 2D MoS2 FETs With Enhanced Contact Resistance and Schottky Barrier Height Achieved by Multipurpose MoO3 - *Anthony M. Cabanillas, Chu Te Chen, Fei Yao, Huamin Li*
- In-situ atomic-scale visualization of Cu2O growth during the oxidation of copper - *Linna Qiao, Jianyu Wang, Shuonan Ye, Zhikang Zhou, Xiaobo Chen, Dmitri N. Zakharov, Kim Kisslinger, Meng Li, Judith C Yang, Guangwen Zhou*
- Machine Learning aided kinetic modeling from transient reaction data - *Jay Shukla*
- Thermal Stability and Decomposition Pathways of ZIF-8 Thin Films Studied via In Situ IRRAS - *Eliseo Perez Gomez, Mueed Ahmad, Jorge Aníbal Boscoboinik, Michael Tsapatsis*
- Unveiling the Impact of Ceria Surface Structure in Ni/CeO2 for Ethanol Steam Reforming - *E. L. Fornero, J. Vecchietti, J. Anibal Boscoboinik, J. C. Hernández-Garrido, A. L. Bonivardi*
- A Reconstructed Cu2O Surface Oxidizes CO at Cryogenic Temperatures - *Burcu Karagoz, Tianhao Hu, Joakim Halldin Stenlid, Markus Soldemo, Frank Abild-Pedersen, Kess Marks, Henrik Öström, Dario Stacchiola, Jonas Weissenrieder, Ashley R. Head*
- Xenon Capture in Silica Nanocages on Metal Substrates - *Kristen M. Burson, Erik Genet, Shabab Kabir, Alexandria Roy, J. Anibal Boscoboinik*
- Advancing Catalysis Research through Theory and Data - *Qin Wu*
- Ion Beam-Engineered Silver Nanoparticles for Controlling Fluorophore Emission: A Surface Photoluminescence Study - *Shahid Iqbal*
- Confinement effects on Surfaces - *J. Anibal Boscoboinik*
- Development of an accurate, efficient, and physically meaningful semiclassical approach to modelling resistivity size effects exhibited by single-crystalline metallic films: from bulk to sub-nm - *William (Bill) Kaden*

Xenon Capture in Silica Nanocages on Metal Substrates

Kristen M. Burson, [1] Erik Genet[1], Shabab Kabir[1], Alexandria Roy[1], Jorge Anibal Boscoboinik[2]

[1] Physics Department, Grinnell College, Iowa, USA
[2]Center for Functional Nanomaterials, Brookhaven National Labs, NY, USA

Email: bursonkr@grinnell.edu

The separation and purification of noble gases is challenging due to their chemical inertness, requiring energy-intensive and expensive processes. A promising alternative involves capturing noble gases within metal-supported nanocages through physical confinement and electronic interactions [1]. In this mechanism, xenon can enter the nanocages when ionized. Once inside, they are neutralized through electron donation from the underlying metal substrate. The process renders it energetically unfavorable for neutral xenon to escape, effectively trapping it within the nanocages. This study explores the impact of various metal supports on the longevity of xenon trapping in silica nanocages. Using a Langmuir–Blodgett trough, near-monolayer films of nanocages were deposited onto single-crystal surfaces of Ag(111), Au(111), and Ru(0001). Post-deposition, samples were calcined to remove ligands and reduced to ensure a clean, metallic support. Samples were exposed to xenon plasma to load the nanocages and X-ray photoelectron spectroscopy (XPS) was subsequently employed to quantify xenon capture. Results showed that all three metal substrates facilitated xenon trapping. The amount of trapped xenon on all metals showed an exponential decay over time, with xenon remaining after 12 hours on all three substrates. These findings highlight the potential of metal substrates to be customized for enhanced noble gas trapping, offering a more energy-efficient and cost-effective alternative to conventional separation techniques.

[1] Xu et al., “Xenon Trapping in Metal-Supported Silica Nanocages,” Small (2021)

Plasma-Powered Xenon Trapping in Nanocages

Laiba Bilal[1,2], J. Aníbal Boscoboinik[2]

[1] Stony Brook University | [2] Brookhaven National Laboratory

Can cold plasma and surface engineering trap one of the most elusive gases; without cryogenics?

Xenon is widely used in nuclear reactors, medical imaging, space propulsion, and isotope production, but its extreme chemical inertness makes capturing it under ambient conditions incredibly challenging. In this work, we introduce a plasma-assisted strategy for xenon confinement using silicate nanocages supported on metal powders.

We use two material preparation methods

1. Chemical vapor deposition (CVD)

2. Wet impregnation (WI)

to explore how synthesis technique, surface composition, and structure influence trapping behavior. Our nanocage-modified metal powders offer high surface area and improved stability, making them promising candidates for scalable noble gas storage.

Using advanced surface characterization techniques, we confirm the successful confinement of Xe and identify key differences in trapping efficiency across samples. The results highlight the importance of surface science and interface engineering in designing materials for selective gas capture and open up exciting possibilities for medical, environmental, and nuclear applications.

Curious how plasma plays a role? Or which method works best? Come find out.

Ion Beam-Engineered Silver Nanoparticles for Controlling Fluorophore Emission: A Surface Photoluminescence Study

Shahid Iqbal

In this study, we investigated the photoluminescence (PL) behavior of optical fluorophores in the presence of ion-implanted silver nanoparticles, with emphasis on surface-mediated interactions. Silver nanoparticles were synthesized through ion implantation at a fixed ion beam energy of 70 keV, with varying fluences to control nanoparticle concentration. Optical absorption spectroscopy confirmed the formation of silver nanoparticles within the near-surface region. Steady-state PL measurements revealed both quenching and enhancement effects, depending on the ion fluence and local nanoparticle density. These variations in PL response are attributed to competing mechanisms, including non-radiative energy transfer leading to quenching, and localized surface plasmon-induced field enhancement promoting emission. The results underscore the critical role of surface modification and nanoparticle–fluorophore interactions in tailoring the optical properties of fluorophores.

Title: Thermal Stability and Decomposition Pathways of ZIF-8 Thin Films Studied via In Situ IRRAS

Eliseo Perez Gomez [1,2], Mueed Ahmad [1,2], Jorge Aníbal Boscoboinik[1,2], Michael Tsapatsis[3,4]

[1] Department of Materials Science and Chemical Engineering, Stony Brook University, Stony Brook, New York 11794-0701, United States.
[2] Center for Functional Nanomaterials, Brookhaven National Laboratory, Upton, New York 11973, United States.
[3] Department of Chemical and Biomolecular Engineering & Institute for NanoBioTechnology, Johns Hopkins University, Baltimore, Maryland 21218-2625, United States
[4] Applied Physics Laboratory, Johns Hopkins University, Laurel, Maryland 20723, United States

Email: eperezgom@bnl.gov

ZIF-8, a zeolitic imidazolate framework formed by zinc ions and 2-methylimidazole ligands, is well known for its thermal and chemical stability. While its bulk properties have been extensively studied, the thermal behavior of ZIF-8 in thin-film form remains less understood. In this work, we explore ZIF-8 thin films synthesized on silicon wafers with a thin layer of gold to examine thermal decomposition pathways with surface-sensitive techniques.

Using in situ Infrared Reflection–Absorption Spectroscopy (IRRAS), we monitor temperature-dependent changes in vibrational modes as the films are heated from room temperature up to ~750–850 K, aiming to identify key spectral signatures of structural breakdown and elucidate the degradation mechanism

Comprehensive surface characterization via X-ray Diffraction (XRD), X-ray Photoelectron Spectroscopy (XPS), Atomic Force Microscopy (AFM), and Scanning Electron Microscopy (SEM) is performed before and after thermal treatment to correlate spectral changes with structural and morphological transformations. These combined techniques aim to provide insight into the stability limits of ZIF-8 thin films and inform their potential use in thermally demanding applications.

Machine Learning aided kinetic modeling from transient reaction data

Jay Shukla

The determination of reaction pathways is a critical step in optimizing and controlling chemical systems. In recent years, data-driven approaches using Artificial Neural Networks (ANNs) have gained attention for this purpose. One such approach previously introduced by our group, PolyODENet models reaction pathways by deriving kinetic differential equations from transient kinetic data, predicting the concentrations of both observed and unmeasured species. More recently, we developed a method based on Chemical Reaction Neural Network by Ji and Deng (JPCA, 125, 1082) that incorporates fundamental chemical kinetics principles, such as the law of mass action, into its architecture. Unlike traditional black-box neural networks, our model features physically interpretable parameters, allowing for deeper insights into reaction mechanisms. With sufficient data, the model autonomously identifies reaction pathways and determines key kinetic parameters, including activation energies and reaction orders, while tracking species concentration profiles over time. To make the model more representative of real conditions, chemical knowledge can be embedded through physical constraints, guiding the optimizer toward plausible solutions. Sensitivity and identifiability analyses are performed to highlight the importance and uniqueness of the model's kinetic parameters. We demonstrate the effectiveness of this approach using experimental infrared spectroscopy data from CO adsorption on a Pd(111) surface. This work was performed at Center for Functional Nanomaterials (CFN), which is a U.S. Department of Energy Office of Science User Facility at Brookhaven National Laboratory under Contract No. DE-SC0012704.

Engineering Bandgap of Porous Graphene Nanoribbons

Mohammad Nazmus Sakib

Abstract

For the post silicon molecular device-based electronics derived from nano-scale materials and exhibiting novel quantum transport mechanisms were theoretically predicted over a decade ago, in terms of reducing the size and energy consumption. Graphene, a single layer of carbon atoms arranged in a honeycomb pattern, has excellent structural and electronic properties, making it a promising material for future nanoelectronics. However, its lack of a natural energy gap and the difficulty of producing high-quality films at scale have limited its use in electronic devices. To overcome these challenges, researchers are exploring ways to modify graphene's electronic structure to create a desired band gap that is called graphene nanoribbons (GNRs). In this poster porous GNR (pGNR) has been discussed. Structurally this pGNR is unique because it has partially zigzag edge structure. Theorical data shows bandgap that is different from the other pGNR, can be useful new devices. As a precursor 3,6-dibromo-10,13-dimethyl-9,14-diphenylbenzo[*f*]tetraphene was used to make the GNR by on surface synthesis method.

Wafer-Scale 2D MoS_2 FETs With Enhanced Contact Resistance and Schottky Barrier Height Achieved by Multipurpose MoO_3

Anthony M. Cabanillas, Chu Te Chen, Fei Yao, Huamin Li*
University at Buffalo, The State University of New York, Buffalo, NY, 14260, USA
Email:huaminli@buffalo.edu / Phone: (716)-645-1026

Introduction

Compatible integration of emerging two-dimensional (2D) materials with mature Si-CMOS technology is promising to enable high-performance energy-efficient electron devices. Among the various 2D materials, transition metal dichalcogenides (TMDs) have been extensively explored with varying levels of success in early fundamental proof-of-concept devices [1,2,3,4]. However, TMD films with good scalability, uniformity, crystallinity, and compatibility on suitable substrates remain a significant roadblock to the realization of commercially viable TMD-based electron devices [5,6].

In this work we utilize wafer-scale, location-on-demand, selective growth of 2D semiconducting TMD, MoS_2 on an SiO_2/Si substrate for transfer-free electron device applications. This method of growth provides a TMD channel directly on a desired area, with definable geometry, which can be used without requiring any wet transfer or etching process which inevitably leads to material degradation. We investigated the impact of SiO_2/MoO_3 dielectric stack on the performance of MoS_2 field-effect transistors (FET) arrays through a comparative study with SiO_2 dielectric by extracting the contact resistance (R_C), transfer length (L_T), and Schottky Barrier Height (SBH). From these results we demonstrate great potential of the selective growth of 2D semiconductors to lower down the technological requirements for practical integration with Si-CMOS technology.

Device Fabrication and Discussion

A controlled growth method is used to form thin films of MoS_2 by limited sulfurization of MoO_3 seedings (Fig. 1a) patterned on p-Si/SiO_2 in an array style by Electron Beam Lithography (EBL) (Fig. 1b, c). Atomic Force Microscopy (AFM) and Raman Spectroscopy are used to confirm the presence of MoS_2 post CVD (Fig. 1a, d). Devices are then formed by EBL and metallization by sputtering Bismuth and Gold in which a back-gate FET configuration is achieved. Two device stacks are formed where two dielectric interfaces are compared, SiO_2 and SiO_2/MoO_3 where both types of devices display similar transfer characteristics (Fig. 1e, f). However, when looking at the distribution of the threshold voltage (V_{Th}), on current density ($J_{D,on}$), and mobility (μ_{FE}) the SiO_2/MoO_3 interface provides a much narrower distribution (Fig. 1g,i).

The back-gate MoS_2 FET arrays can act as 2D phototransistors, and their photoresponsive performance is evaluated, as shown in Fig. 2a-e. Both the power-dependent static photocurrent (PC) generation and time-resolved high-speed photo-switching dynamics suggest excellence photoresponse of MoS_2 FETs in the visible spectrum.

By taking advantage of the definable area of our TMD growth, we can define a long ribbon of MoO_3 (5µm x 100µm) and after growth results in uniform MoS_2 along the ribbon (Fig. 2f). This long ribbon is used for transmission line measurement (TLM) where the results show that the inclusion of the MoO_3 in the interface stack improves the metal contact condition such that R_C and T_L are lowered while maintaining R_{Ch} (Fig. 2g-i). The SHB, evaluated from a temperature-variable measurement, suggests a flat-band barrier height of 12 meV with the MoO_3 interface, which is lower than that with the SiO_2 interface (60 meV) and is consistent with the improvement of metal contact condition (Fig. 2j).

Conclusion

In this work, we presented wafer-scale MoS_2 FET arrays using transfer-free location-on-demand selective growth where we attain consistent device performance and show that the MoO_3 decoration improves the contact resistance and lowers the Schottky barrier height. Our work demonstrates the utilization of wafer-scale, transfer-free, location-on-demand selective growth of 2D TMD in a FET configuration and showcase its potential for integration with Si-CMOS processing paving a feasible way for realizing 2D semiconductor implementation.

[1] S. Das et al., Nat. Electron., 4, 786 (2021).
[2] M. Liu et al., ACS Nano, 15, 5762 (2021).
[3] H. N. Jaiswal et al., Adv. Mater., 32, 2002716 (2020).
[4] M. Liu et al., IEEE IEDM, 251 (2020).
[5] N. Briggs et al., 2D materials, 6, 022001 (2019).
[6] Y. Zhang et al., Adv. Mater., 31, 1901694 (2019)

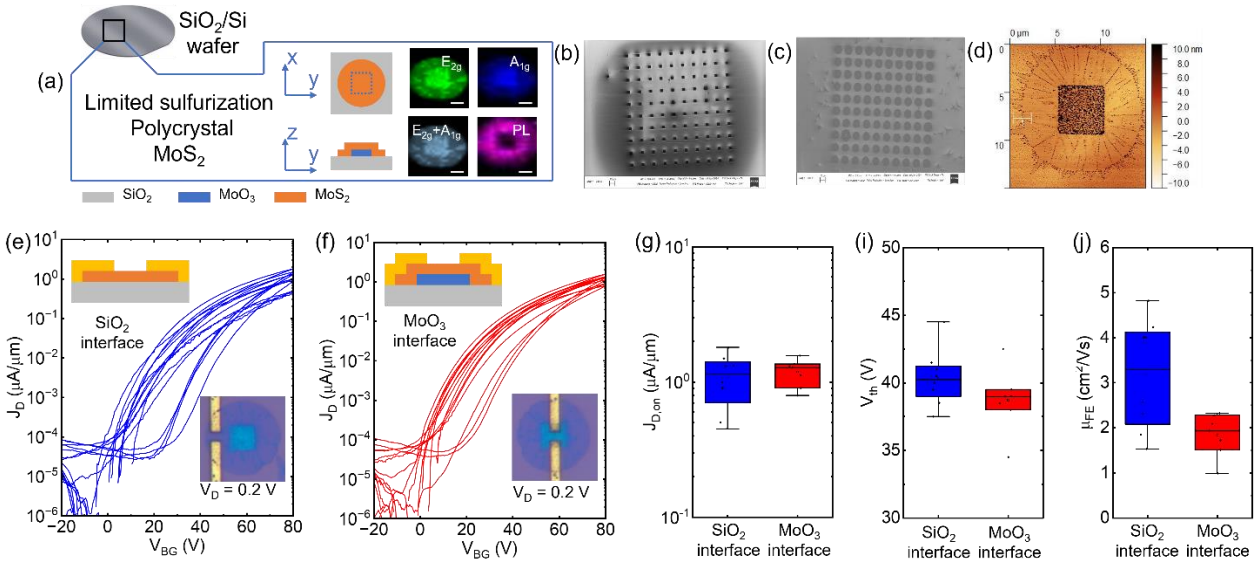

Fig. 1: (a) MoS_2 "circular" polycrystal synthesized by limited sulfurization and its corresponding Raman/PL spectroscopy mapping. (b, c) SEM images of a MoO_3 seeding array before growth and a MoS_2 array after growth. Scale bar: 60 μm. (d) AFM mapping of a circular MoS_2 with the MoO_3 seeding at the center. (e, f) Transfer Characteristics of the MoS_2 FETs with SiO_2 and MoO_3 dielectric interfaces. Insets: The corresponding cross-sectional schematics and microscope images of devices. (g, i, j) Statistical analysis of the MoS_2 FETs with SiO_2 and MoO_3 dielectric interfaces including $J_{D,on}$, V_{th}., and μ_{FE}.

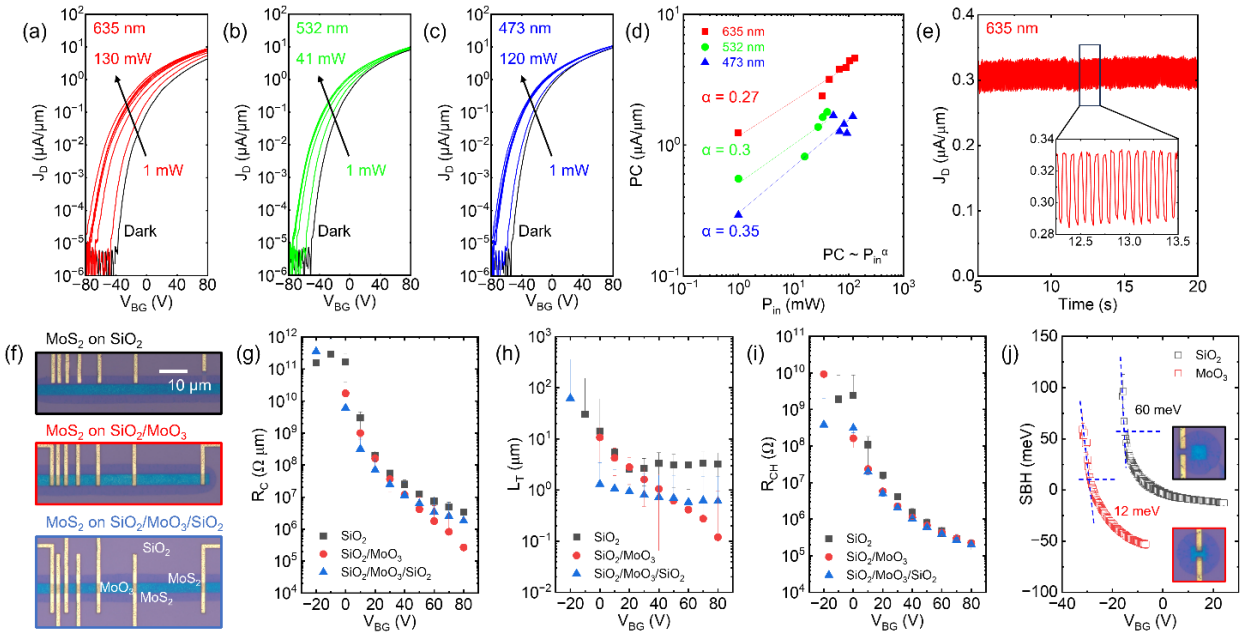

Fig. 2: (a-c) Transfer characteristics of a MoS2 FET under red, green, and blue laser illumination. (d) The extracted PC as a function of the input power (Pin). (e) Time-resolved high-speed photo-switching characteristics under the red laser illumination. (f-i) Microscope images of MoS2 TLM devices with different SiO2 and MoO3 dielectric interfaces, and the extracted RC, LT, and RCH. (j) The extracted SBH as a function of VBG. Inset: Microscope images of the corresponding MoS2 FETs.

In-situ atomic-scale visualization of Cu_2O growth during the oxidation of copper

Linna Qiao[1], Jianyu Wang[1], Shuonan Ye[1], Zhikang Zhou[1], Xiaobo Chen[1], Dmitri N. Zakharov[2], Kim Kisslinger[2], Meng Li[2], Judith C Yang[2], Guangwen Zhou[1*]
[1] Materials Science and Engineering Program & Department of Mechanical Engineering, State University of New York at Binghamton, Binghamton, New York 13902, United States
[2] Center for Functional Nanomaterials, Brookhaven National Laboratory, Upton, New York 11973, United States
* Corresponding author: gzhou@binghamton.edu

Understanding vacancy-mediated oxide growth at gas–solid interfaces is key to controlling defect evolution and nonstoichiometry during metal oxidation. Using environmental transmission electron microscopy, we directly observed atomic-scale Cu_2O growth during the oxidation of Cu, revealing vacancy-assisted lattice diffusion of Cu atoms that drives outward oxide growth. High-resolution, time-resolved imaging reveals that surface oxygen adsorption extracts Cu atoms from the Cu_2O lattice, generating Cu vacancies that self-organize into periodic, vertically aligned structures. These vacancy channels serve as active mass transport pathways, enabling step-flow oxide growth via vacancy-assisted lattice diffusion. Time-resolved imaging further reveals directional migration of vacancies and their role as active structural motifs regulating oxidation kinetics. Our results uncover a fundamental mechanism of point defect generation and transport during oxidation, with implications for tuning ionic conductivity and phase stability in oxide materials through engineered defect dynamics.

A Reconstructed Cu_2O Surface Oxidizes CO at Cryogenic Temperatures

Burcu Karagoz[1], Tianhao Hu[1,2], Joakim Halldin Stenlid[3,4,5], Markus Soldemo[5,6], Frank Abild-Pedersen,[3] Kess Marks,[6] Henrik Öström[6], Dario Stacchiola[*1], Jonas Weissenrieder[*6], Ashley R. Head[*1]

[1]Center for Functional Nanomaterials, Brookhaven National Laboratory; Upon, NY, 11973, United States.
[2]Department of Chemistry, Stony Brook University; Stony Brook, NY, 11974, United States
[3]SUNCAT Center for Interface Science and Catalysis, SLAC National Accelerator Laboratory; Menlo Park, CA, 94025, United States
[4]SUNCAT Center for Interface Science and Catalysis, Department of Chemical Engineering, Stanford University; Stanford, CA, 94305, United States.
[5]Department of Physics, AlbaNova University Center, Stockholm University; Stockholm, SE-106 91, Sweden.
[6]Materials and Nano Physics, Applied Physics, KTH Royal Institute of Technology; Stockholm, SE-100 44, Sweden

Email: ahead@bnl.gov

Conventional low-temperature CO oxidation mechanisms typically require an interface between a metal oxide support and a platinum-group metal. Here, we demonstrate that CO_2 can form on a reconstructed $Cu_2O(111)$ surface at cryogenic temperatures, without the need for noble metals. Using infrared reflection absorption spectroscopy (IRRAS) in combination with X-ray photoemission (XPS) and near-edge X-ray absorption fine structure (NEXAFS) spectroscopies, we provide spectroscopic evidence for CO reacting with lattice oxygen. Density functional theory (DFT) calculations support a low-barrier reaction pathway involving CO interaction with apex oxygen atoms on the pyramidal surface reconstruction. The integration of complementary experimental and theoretical approaches was critical for the correct interpretation of the complex core level C 1s spectra. These results highlight the challenges of spectral assignments in heterogeneous catalysis as characterization methods advance toward more realistic environments. Importantly, the observed reactivity of Cu_2O underscores the potential of earth-abundant oxides to host active sites for both adsorption and reaction steps in catalytic processes.

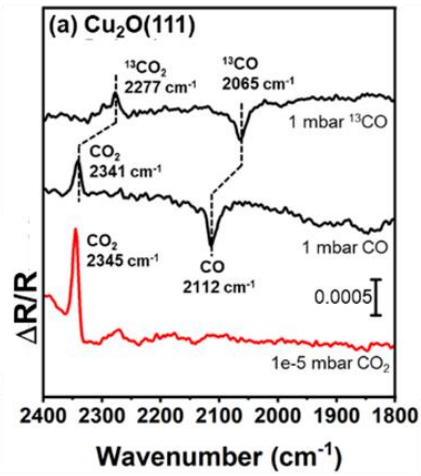

Figure 1. IR spectroscopy data show CO_2 is formed when CO reacts with $Cu_2O(111)$. IRRAS data of the surface species (a) on $Cu_2O(111)$ at the listed pressures of ^{13}CO, CO, and CO_2.

Wafer-Scale 2D MoS_2 Transistors Using Transfer-Free Location-on-Demand Selective Synthesis

Chu-Te Chen[1], Anthony Cabanillas[2], Fei Yao[1], and Huamin Li[2]

[1]*Department of Materials Design and Innovation, University at Buffalo, The State University of New York, Buffalo, NY, USA*

[2]*Department of Electrical Engineering, University at Buffalo, The State University of New York, Buffalo, NY, USA*

Email: feiyao@buffalo.edu and huaminli@buffalo.edu

ABSTRACT

The seamless incorporation of novel two-dimensional (2D) materials into established Si-CMOS technology offers a promising pathway for creating high-performance, energy-efficient electronic devices. In this work, we exploited a wafer-scale, location-on-demand selective growth method for 2D MoS_2 on SiO_2/Si substrates, enabling transfer-free device fabrication. This technique allows precise control over MoS_2 film size and position, with excellent reproducibility. We investigate the impact of MoO_3 and SiO_2 dielectric interfaces on MoS_2 field-effect transistor (FET) performance, finding superior characteristics with MoO_3 interfaces. Our approach significantly simplifies the integration of 2D semiconductors with Si-CMOS technology, paving the way for next-generation electronic devices.

Keywords—2D materials, nanoelectronics

INTRODUCTION

2D semiconducting transition metal dichalcogenides (TMDs) show promise for device miniaturization, but challenges in scalability, uniformity, and substrate compatibility hinder commercial viability [1-7]. We address these issues with a novel location-on-demand selective growth method for high-quality TMD layers. Using MoS_2 as an example, we demonstrate wafer-scale, transfer-free growth of MoS_2 arrays using patterned MoO_3 seeding. We directly observe the chemical vapor deposition (CVD) growth of MoS_2 on micrometer scale within a few seconds and investigate the impact of dielectric interfaces (MoO_3 and SiO_2) on MoS_2 FET performance. We find that polycrystalline MoS_2 with MoO_3 interfaces shows comparable and even superior characteristics to other growth methods. This work establishes a viable approach for integrating 2D semiconductors with Si-CMOS technology, paving the way for advanced electronic devices.

RESULTS AND DISCUSSION

In this study, we demonstrate a controlled growth method for MoS_2 thin films using MoO_3 seedings. The process begins with electron-beam lithography patterning of MoO_3 on p-Si/SiO_2 substrates, followed by controlled sulfurization in a two-zone CVD furnace. By adjusting CVD parameters, we manipulated the spatial morphology and crystallinity of the resulting MoS_2 films. Time-resolved in-situ microscopy revealed rapid MoS_2 growth, achieving a rate of 0.5 μm/s (Fig. 1a,b). Under limited sulfurization, we observed the formation of circular MoS_2 patterns around MoO_3 seedings, indicating isotropic growth on SiO_2 (Fig. 1c). SEM, Raman, PL spectroscopy, and AFM confirmed successful MoS_2 growth from MoO_3 seedings (Fig. 1d-h) across a 1×1 cm^2 area (Fig. 1 i), with excellent uniformity in size and consistent growth even at increased seeding densities (Fig. 1j). Our technique demonstrated precise control over MoS_2 film location, as evidenced by microscopy images of structures synthesized at predefined positions (Fig. 1k-m). These results suggest excellent reproducibility and uniformity of our selective growth method, paving the way for large-scale integration of MoS_2 in electronic devices.

A comparative investigation is performed for the synthetic MoS_2 FETs with the MoO_3 and SiO_2 dielectric interfaces, in terms of output and transfer characteristics (J_D-V_D and J_D-V_{BG}), and a statistical analysis of $J_{D,on}$, μ_{FE}, and on/off ratios, as shown in Fig. 2(a-h). The linear J_D-V_D characteristics suggest Ohmic contact for both FET types. With the identical synthetic process and device geometry, the MoO_3 interface provides comparable FET performance metrics, and more importantly, in much narrower distributions. On the wafer scale, the MoS_2 arrays formed by the controlled sulfurization at on-demand locations are still reproduceable. By optimizing the synthetic parameters, our best MoS_2 FET device possesses $J_{D,on}$ of 3 μA/μm, μ_{FE} of 20 cm^2/Vs, and on/off ratio up to 10^6, as shown in Fig. 2(i).

CONCLUSION

In this work, we presented wafer-scale MoS_2 FET arrays using transfer-free location-on-demand selective growth. This technique allows time- and cost-efficient synthesis (0.5 μm/s) of 2D semiconductor channel arrays at designed locations, and the controlled sulfurization creates MoO_3 dielectric interfaces to enhance FET performance. Our devices show comparable and even superior performance, such as $J_{D,on}$, μ_{FE}, and on/off ratios, compared to other MoS_2 FETs using selective and non-selective growth, and demonstrate great potential to ease the integration of 2D semiconductors for various electron devices.

ACKNOWLEDGMENT

The authors acknowledge support from the SUNY Applied Materials Research Institute (SAMRI) and the National Science Foundation (NSF) under Award ECCS-1944095.

REFERENCES

[1] S. Das et al., Nat. Electron., 4, 786 (2021).
[2] M. Liu et al., ACS Nano, 15, 5762 (2021).
[3] H. N. Jaiswal et al., Adv. Mater., 32, 2002716 (2020).
[4] M. Liu et al., IEEE IEDM, 251 (2020).
[5] N. Briggs et al., 2D materials, 6, 022001 (2019).
[6] Y. Zhang et al., Adv. Mater., 31, 1901694 (2019).
[7] A. Cabanillias et al., ACS Nano., 19, 3865 (2025).

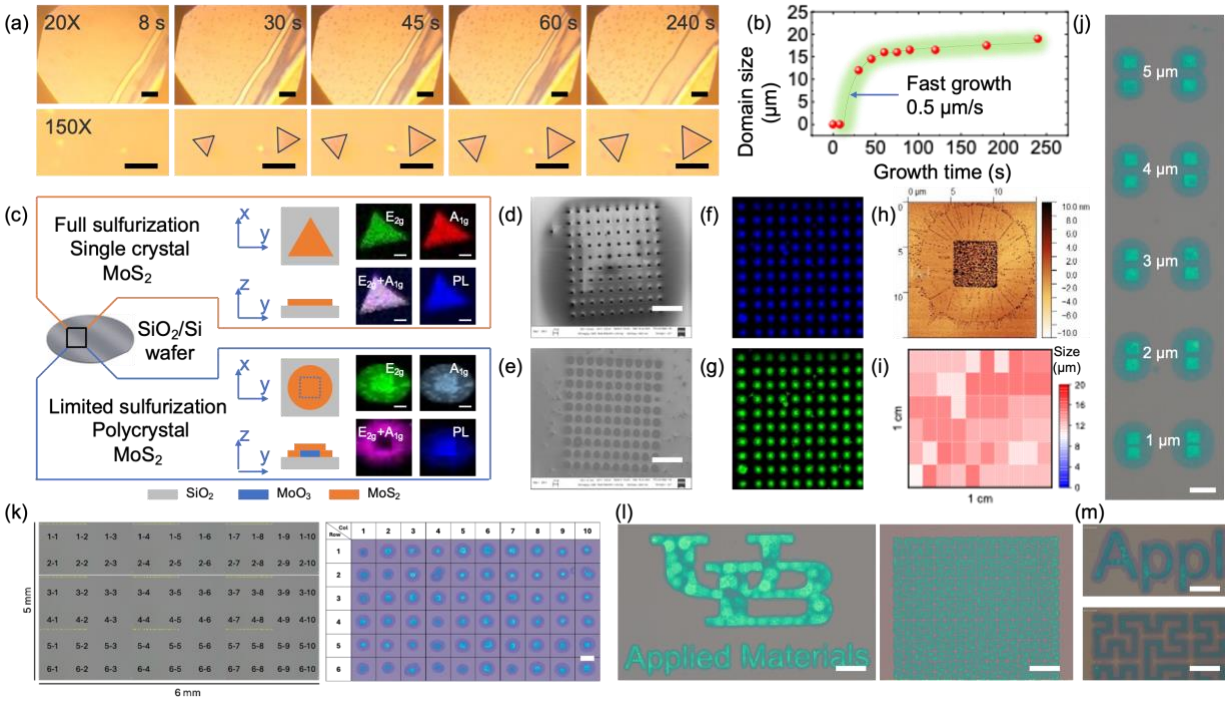

Fig. 1 Synthesis and characterization of wafer-scale location-on-demand MoS_2 growth on SiO_2/Si substrates. (a, b) Time-resolved in-situ microscope images to visualize the MoS_2 growth evolution, and the extracted growth rate up to 0.5 μm/s. Scale bar: 50 μm (top) and 20 μm (bottom). (c) Comparison of single crystal "triangle" MoS_2 and polycrystal "circular" MoS_2 synthesized by full sulfurization and limited sulfurization, respectively, and the corresponding Raman/PL spectroscopy mapping. Scale bar: 5 μm. (d, e) SEM images of a MoO_3 seeding array before growth and a MoS_2 array after growth. Scale bar: 60 μm. (f, g) E_{2g} and A_{1g} Raman spectroscopy mapping for the large-scale synthetic MoS_2 arrays. (h) AFM mapping of a circular MoS_2 with the MoO_3 seeding at the center. (i) Spatial uniformity of the MoS_2 sizes across a 1 × 1 cm^2 area. The average size is about 14 μm. (j) Microscopy image of the circular MoS_2 thin films which merges as the spacing distance of the MoO_3 seedings scales down from 5 to 1 μm. Scale bar: 10 μm (k) Microscopy images of circular MoS_2 thin films grown at predefined locations on a 5 mm × 6 mm wafer, demonstrating spatially controlled growth using MoO_3 seeding. Each position corresponds to a specific row-column coordinate. Scale bar: 10 μm. (l-m) Microscopy images of MoS_2 synthesized at predefined MoO_3 locations, guided by text-based names and a Hilbert pattern. Images include a scale bar of 100 μm, with zoomed-in views showing a scale bar of 10 μm.

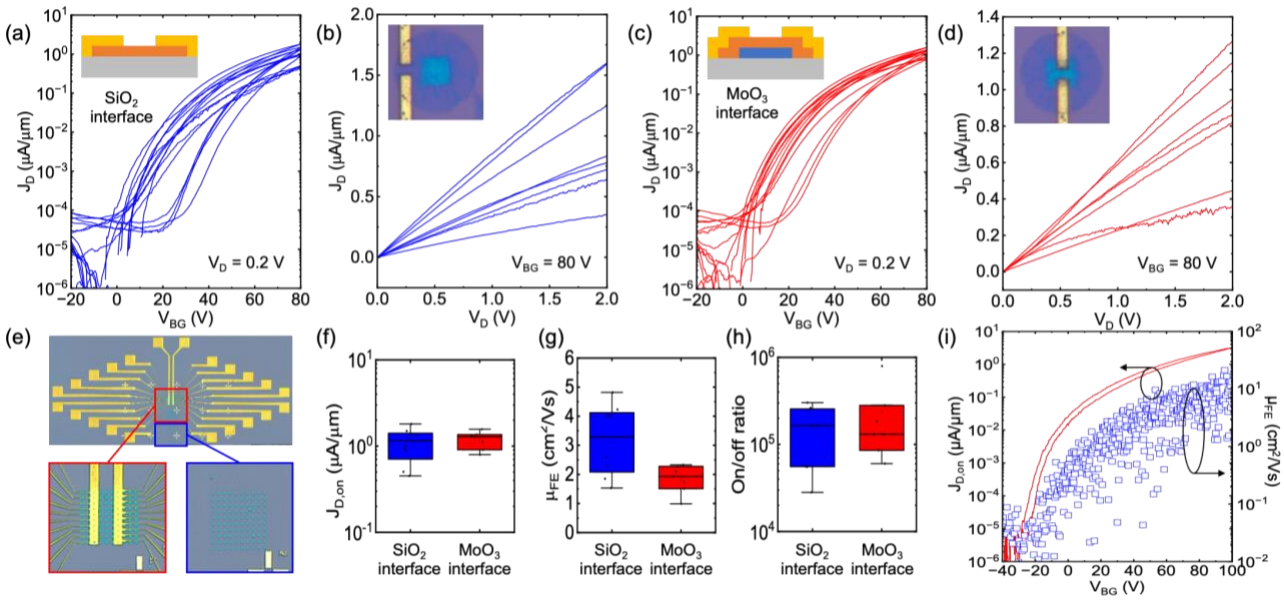

Fig. 2 Comparison of synthetic MoS_2 FETs with SiO_2 and MoO_3 dielectric interfaces. (a-d) Output and transfer characteristics of the MoS_2 FETs with SiO_2 and MoO_3 dielectric interfaces. Insets: The corresponding cross-sectional schematics and microscope images of the devices. (e) Microscope images of the wafer-scale MoS_2 FET arrays with MoO_3 dielectric interfaces (f-h) Statistical analysis of the MoS_2 FETs with SiO_2 and MoO_3 dielectric interfaces, including $J_{D,on}$, μ_{FE}, on/off ratio. (i) The best back-gate MoS_2 FET with MoO_3 dielectric interfaces possesses $J_{D,on}$ of 3 μA/μm, μ_{FE} of 20 cm^2/Vs, and an on/off ratio up to 10^6.

Title: Unveiling the Impact of Ceria Surface Structure in Ni/CeO_2 for Ethanol Steam Reforming

E. L. Fornero [1], J. Vecchietti [1], J. Anibal Boscoboinik[2], J. C. Hernández-Garrido[3], A. L. Bonivardi [1]

[1] INTEC, Universidad Nacional del Litoral and CONICET, 3000 Santa Fe, Argentina
[2] Center for Functional Nanomaterials, BNL, Upton, NY 11973-5000, USA
[3] Universidad de Cádiz, Campus Universitario Puerto Real, 11510 Puerto Real, Spain

Email: elfornero@santafe-conicet.gov.ar

Hydrogen produced from renewable sources like bioethanol is a promising alternative to meet the increasing demand for sustainable energy. Ethanol steam reforming (ESR) is an efficient method for generating H_2 and CO_2, and Ni/CeO_2 catalysts have shown notable activity. However, issues with selectivity and deactivation remain. This study investigates ESR performance of pre-reduced Ni catalysts supported on CeO_2 nanocubes (NC, exposing (100) facets) and nanoctahedra (NO, exposing (111) facets), combining AP-XPS and temperature-programmed surface reaction (TPSR) with infrared spectroscopy (IR) and mass spectrometry (MS) to understand the mechanism of ethanol reaction on Ni/CeO_2-NC (the most active catalyst towards ESR).

Under identical contact times, Ni/CeO_2-NC remains stable, whereas Ni/CeO_2-NO undergoes rapid deactivation. Post-reaction HRTEM analysis of both catalysts reveals that their morphology is preserved; however, STEM-EDS on Ni/CeO_2-NO indicates a lower dispersion of Ni particles after 4 hours of exposure to the ESR reaction mixture. Furthermore, the formation of amorphous carbon deposits surrounding some octahedral particles is observed.

TPSR-IR-MS reveals that pre-reduced Ni/CeO_2-NC catalysts promote faster decomposition of carbon-containing intermediates than pure ceria. Four temperature regions are identified: (I) 100–200 °C – ethoxy decomposition into CH_4 and H_2 with acetate formation and partial ceria reoxidation; (II) 200–270 °C – acetate decomposition near Ni particles yields CH_4, H_2, and CO; (III) 270–330 °C – acetone and CO_2 production via acetate coupling, requiring partial ceria reoxidation; (IV) 330–450 °C – slow decomposition of residual acetates far from Ni-support interphase. On pre-reduced CeO_2-NC, ethoxy species are progressively transformed into acetate species, reaching a maximum concentration at 320 °C. These subsequently decompose, with the formation of CH_4 and an increase in the Ce^{3+} signal, but without CO_2 release. Instead, surface carbonate species are formed. AP-XPS measurements under ESR conditions (500 °C, H_2O/ethanol = 6:1) show that both pre-reduced CeO_2-NC and Ni/CeO_2-NC undergo partial surface reduction of ceria. Additionally, in the case of CeO_2-NC, the O 1s spectrum reveals the presence of carbonaceous surface species, evidenced by a peak at 532.6 eV. These observations are consistent with the TPSR results.

Together with TPSR results obtained from pre-oxidized supports and catalysts, this study demonstrates that the synergy between Ni and partially reduced ceria facilitates key surface reactions during ethanol reforming, promoting both C–C and C–H bond cleavage.

Advancing Catalysis Research through Theory and Data

Qin Wu

Theory and Computation Group, Center for Functional Nanomaterials, Brookhaven National Laboratory

We will present our advances in catalysis modeling from both theoretical and machine learning approaches. First, we introduce a novel electronic descriptor for catalyst activation in transition-metal doped MoS_2 systems, based on the interband distance between the lowest empty Mo/M d-states and the center of occupied S p-states, which successfully captures trends in hydrogen-sulfur binding energies. Additionally, we demonstrate the application of Neural ODE (Ordinary Differential Equations) methods for interpretable machine learning-aided kinetic modeling, enabling direct derivation of rate equations from transient kinetics data without requiring intermediate species information. We envision a combined theoretical and data-driven framework to dramatically accelerate the discovery of catalytic mechanisms and optimize catalyst design for improved efficiency, activity, and selectivity in heterogeneous catalysis applications.

Wednesday Nottingham Sessions

9:00 AM – 9:40 AM — **Invited Talk**

Science and User Support Center (SUSC), Building 101

Steven J. Sibener

Atomically-resolved Dynamical Processes at Surfaces: Materials Oxidation, Single-Molecule Reactivity, and Superconducting Radio Frequency Materials Optimization

9:40 AM – 10:40 AM — **Nottingham Prize Competition I**

Science and User Support Center (SUSC), Building 101

- It's Not a S(KZ)CAM! Accurate Surface Modeling at Low Cost - *Benjamin Shi*
- Atomic-scale Sensing of the Electric Field with a Molecular Sensor - *Yunpeng Xia*
- Atomic-scale terahertz-induced dynamics of van der Waals materials - *Stefanie Adams*

10:40 AM – 11:00 AM — **Coffee Break** (provided)

11:00 AM – 12:20 PM — **Nottingham Prize Competition II**

Science and User Support Center (SUSC), Building 101

- Surface Properties of Zirconium diboride (0001) and Homoepitaxial Growth of Zirconium diboride as Determined by Scanning Tunneling Microscopy - *Ayoyele Ologun*
- High-temperature surface dynamics of NiAl under reactive environments - *Shyam Bharatkumar Patel*
- Defect engineering of metal sulfide surfaces: Where real-world challenges meet Solid-state Physics - *Pablo R A de Oliveira*
- Cold Plasma-Driven Xenon Trapping in Silicate Nanocages on Metal Powders - *Laiba Bilal*

12:30 PM – 2:00 PM — **Lunch Break** (provided)

2:00 PM – 3:00 PM — **Nottingham Prize Competition III**

Science and User Support Center (SUSC), Building 101

- Syngas Conversion to Surface Carbon on Co/CeO_2 - *Matthew Bonney*
- Investigation of Adsorption and Selective Hydrogenation of 1.3-butadiene on Cu(111) and Pd/Cu(111) Single-Atom Alloy Surfaces - *Mohammad Rahat Hossain*
- A Priori designed NiAg Single-Atom Alloys for Selective Epoxidation Reactions - *Elizabeth E. Happel*

3:00 PM – 4:30 PM — **CFN and NSLS-II Tours + Coffee Break** (provided)

Atomically-resolved Dynamical Processes at Surfaces: Materials Oxidation, Single-Molecule Reactivity, and Superconducting Radio Frequency Materials Optimization

Steven J. Sibener
The James Franck Institute and Department of Chemistry
University of Chicago

We have developed the capability to elucidate interfacial dynamics using an arguably unique combination of supersonic molecular beams combined with *in situ* STM visualization. These capabilities are revealing the complex spatio-temporal correlations that govern materials growth, erosion, and modification spanning atomic, nano, and meso length-scales. Illustrative examples include the atomic and multiscale oxidative reactivity of HOPG graphite, Si, and single/multilayer graphene including moiré superlattices. Correlations in the site-specificity of atomic oxygen placement on the moiré lattices are important as they provide a route to creating self-assembled 2D materials platforms for quantum devices. Next, *in situ* studies of nitrogen dissociation dynamics on Ru will be explored. Here, *single molecule* events involving measurement of the distance and angle between nitrogen atoms from the same dissociated N_2 molecule on ruthenium are precisely measured over a range of impinging N_2 kinetic energies and angles, revealing previously unattainable information about spatio-temporal correlations and the energy dissipation channels that govern the reactivity of the system. Such measurements represent a significant extension of gas-surface scattering experiments as they are providing a window into *on-surface chemical processes* that complement more traditional scattering experiments. How energy is dissipated following dissociative chemisorption is an open question in the surface dynamics community, so these results are an exciting step in determining the role that nonadiabatic dynamics (electron-hole pairs) and adiabatic dynamics (phonons) play in dissipating energy. The latter part of this presentation will focus on the optimization of superconducting materials based upon Nb and Nb_3Sn important for superconducting radio frequency (SRF) based accelerators. Topics include the Nb surface oxide, surface phonon dynamics, Nb_3Sn growth and optimization, and the first determination of the surface electron-phonon coupling constants for metallic and oxide covered Nb interfaces.

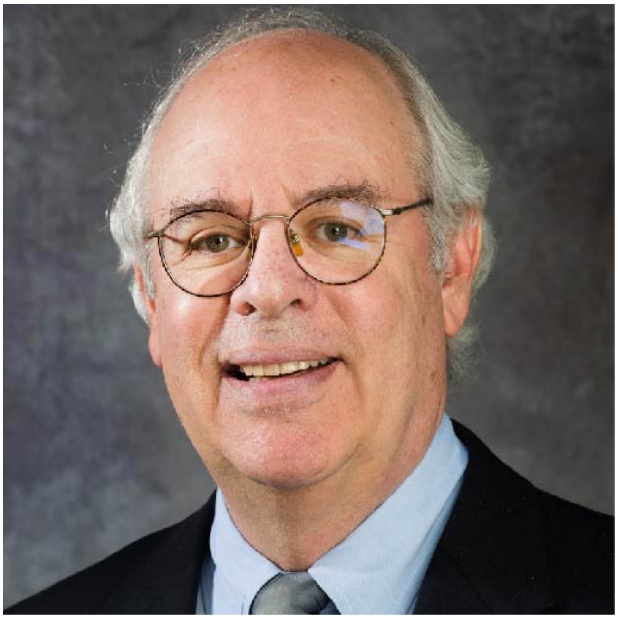

Steven J Sibener

Prof. Steven J. Sibener, the Carl William Eisendrath Distinguished Service Professor in Chemistry and The James Franck Institute at the University of Chicago, and Fellow of the Pritzker School for Molecular Engineering, leads pioneering research at the intersection of chemical physics, surface and materials chemistry, polymer dynamics, nanoscience, astrochemistry, and water sustainability. His group combines state-of-the-art molecular beam scattering, atomic-resolution scanning probe microscopy, numerical simulations, and theory to unravel atomic-level processes at interfaces. Prof. Sibener has received numerous honors, including the Adamson and Remsen Awards from the ACS, and the Marlow Medal of the Royal Society of Chemistry. He is a fellow of five learned societies: The AVS, ACS, APS, AAAS, and the Royal Society of Chemistry.

It's Not a S(KZ)CAM! Accurate Surface Modeling at Low Cost

Benjamin X. Shi,[1] **Angelos Michaelides**[1]
[1]Yusuf Hamied Department of Chemistry, University of Cambridge,
Lensfield Road, Cambridge CB2 1EW, United Kingdom
Email: bxs21@cam.ac.uk

Understanding how molecules interact with surfaces is pivotal towards improving processes underpinning key technologies, including heterogeneous catalysis for chemical manufacturing as well as the fabrication and operation of electronic devices. Computer simulations have the potential to greatly enhance our understanding by providing direct atomic-scale insights into these processes. These insights are particularly useful for complementing experiments, where such resolution is typically hard to obtain. Moreover, they can also accelerate the rational design of new materials via high throughput screening of thousands of hypothetical candidates.

However, inaccuracies of the level of theory used in the computer simulation can make achieving reliable agreement with experiments challenging, underscoring the need for new methods which are accurate while retaining a favorable computational cost. For example, density functional theory (DFT) – the workhorse of computational surface science – is efficient but relies on approximations that make reaching quantitative and even qualitative agreement with experiments challenging. These inaccuracies can lead to an incorrect interpretation of how a molecule interacts with a surface. For example, depending on the chosen DFT approximation (i.e., exchange-correlation functional), six different adsorption configurations have been proposed for how the nitric oxide (NO) molecule binds on the MgO(001) surface (left panel of Figure 1), the important elementary step that influences any subsequent surface reaction.

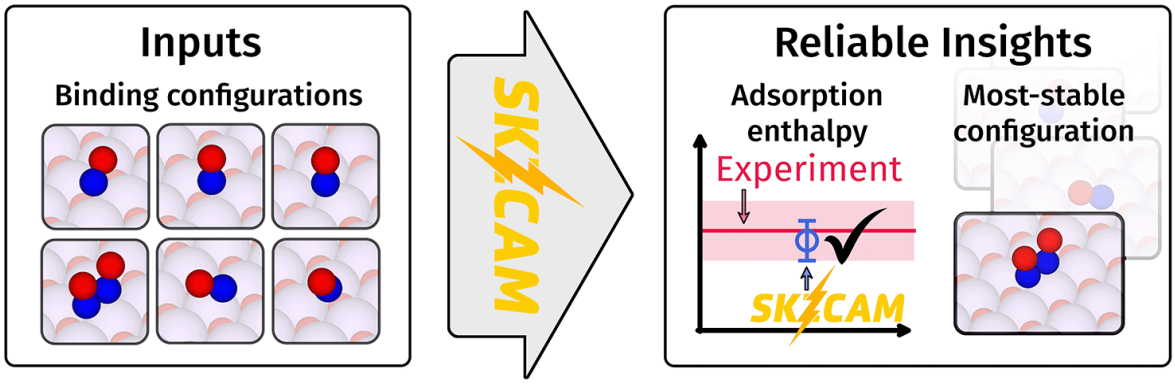

Figure 1. The SKZCAM protocol is a new computational tool for modeling the surface science of ionic materials. It can complement experiments by resolving the adsorption configuration for challenging molecule-surface systems where previous simulation methods have failed. In addition, it can accurately reproduce adsorption energies from (TPD or SCAC) experiments.

Reaching a high accuracy requires methods from quantum chemistry and the method of choice is typically the 'gold-standard' coupled cluster theory with single, double and perturbative triple excitations [CCSD(T)]. While it can routinely reach agreement to experiments on problems in chemistry (typically involving small molecules), its application to surface science has been few and far between as it is prohibitively expensive, particularly when tackling the large system sizes required to model surfaces. For example, even a simple property like the adsorption energy of a molecule-surface system can require months to compute.

My PhD [1–4] focused on developing and applying the SKZCAM protocol (pronounced "scam" and named after the authors of Ref. [1]), which overcomes the traditional cost-accuracy compromise for studying the molecule-surface interactions of ionic materials, particularly the catalytic and gas-storage properties of metal-oxides. The relevant chemistry of these processes is centered on a small region around the interacting molecule and the SKZCAM protocol exploits this property to restrict the application of CCSD(T) to this (quantum cluster) region, embedded within further regions treated at lower levels of theory (Figure 2). This decreases the cost of applying CCSD(T) by more than three orders of magnitude, now enabling experimentally realistic molecule-surface systems to be studied within a day.

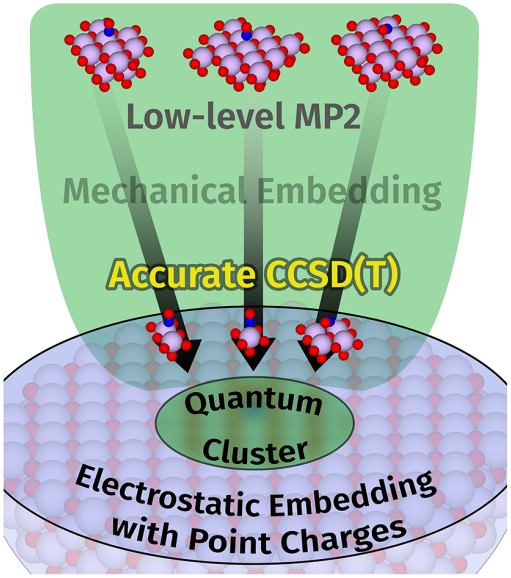

Figure 2. Schematic of the SKZCAM protocol. It computes molecule-surface properties at low cost by employing a multilevel approach, where CCSD(T) is embedded within more affordable levels of theory from perturbation theory (MP2).

The key achievement of the SKZCAM protocol is its ability to reproduce experimental adsorption energies. This is a fundamental measure of the stability of a molecule on a surface and can predict its efficiency as a solid catalyst (through the Sabatier principle) or gas-storage material. Achieving accurate computational predictions of the adsorption energy has been a major challenge within the field, as epitomized by CO adsorbed on the MgO(001) surface – touted as the "hydrogen molecule of surface science" [5] – where computational studies have repeatedly failed to reproduce experiment over decades of research (see panel a of Figure 3). In a publication at JACS [2], the SKZCAM protocol was demonstrated to achieve consensus with experiment for CO on MgO(001). This success sets a new benchmark for the field and has since inspired the application of new methods, including diffusion Monte Carlo (DMC) and quantum embedding method, from other research groups [6,7].

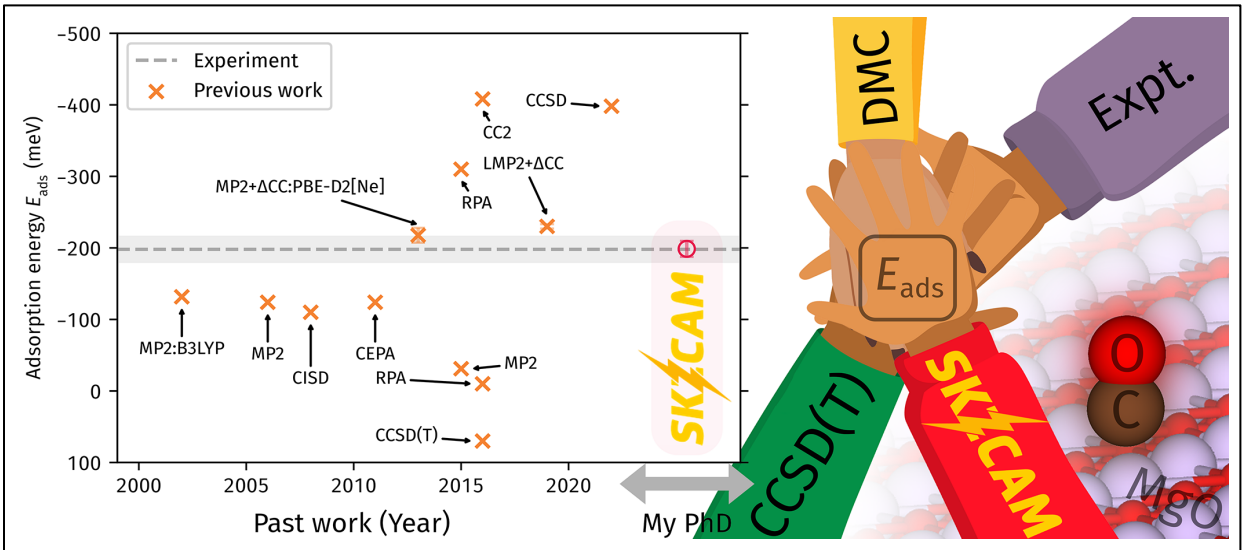

Figure 3. The adsorption energy of CO on MgO(001) has been a decades-long challenge for computational approaches. The SKZCAM protocol can reach consensus with experiment for this system and has motivated further work from reference methods such as periodic coupled cluster theory [CCSD(T)] and diffusion Monte Carlo (DMC).

Paired with its accuracy, the low cost of the SKZCAM protocol expands the range and complexity of systems that can now be tackled reliably. In a publication accepted at Nature Chemistry [4], the SKZCAM protocol was used to study a diverse set of molecule-surface systems (see Figure 4), covering complex adsorbates like benzene or methanol clusters on important metal-oxide surfaces such as TiO_2 rutile(110) and anatase(101) as well as MgO(001). Besides reproducing experimental adsorption energies and enthalpies across all studied systems, the SKZCAM protocol has also resolved the adsorption configuration for each system. In some cases, there had been conflicting interpretations between previous DFT simulations or experiments that it has helped to clarify. For instance, on MgO(001), I found that nitric oxide prefers to pair up as dimers, while carbon dioxide forms a strong chemisorbed structure, and that water and methanol form partially dissociated hydrogen bonded networks. These systems are important for applications ranging from waste gas removal to fuel production and the new insights on their adsorption mechanism is important to enable rational design of enhanced surface processes.

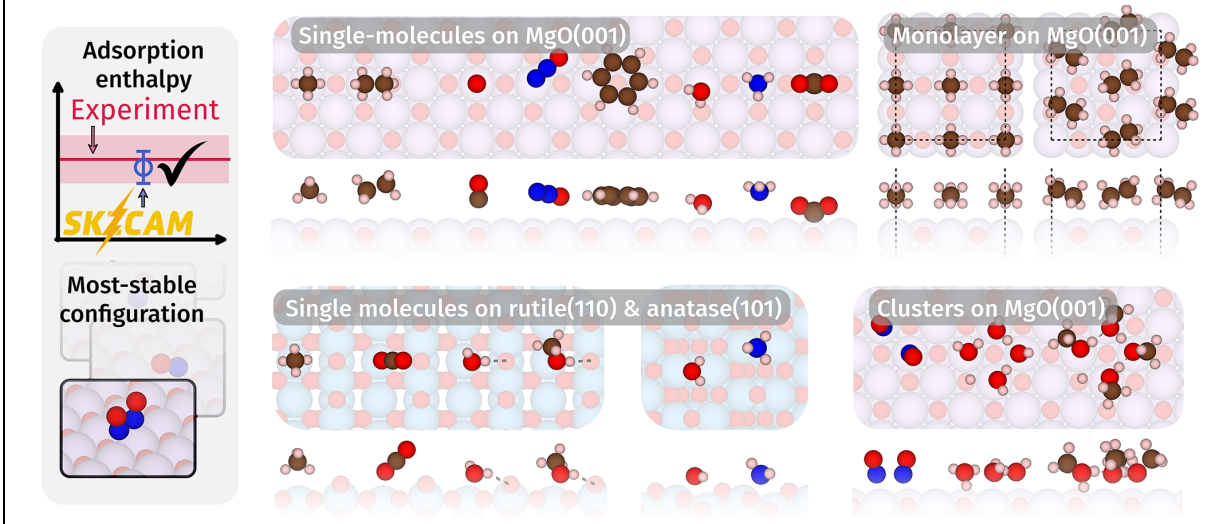

Figure 4. The SKZCAM protocol significantly expands the types of systems which can now be tackled, and I have studied a diverse set of molecule-surface systems, consisting of (a) single molecules on MgO(001), (b) monolayers on MgO(001), (c) single molecules on TiO_2 rutile(110) and anatase(101) surfaces as well as (d) clusters on MgO(001).

With the SKZCAM protocol, it is now possible to generate large reference datasets of molecule-surface adsorption energies, currently sorely lacking within the computational surface science community. This type of reference data is necessary to parametrize and develop new approximations or machine-learned models, particularly for DFT. In a paper published in the Journal of Chemical Theory and Computation [3], I have used the SKZCAM protocol to explain why different DFT approximations can predict drastically different structures, ranging from 2D to 3D, for a 20-atom gold nanocluster on MgO – a model catalyst for carbon monoxide oxidation. These differing predictions can lead to significant changes in the predicted catalytic properties, and I show that this arises from an interplay of errors in the metal-metal and metal-support interactions that govern this system. With these insights, I have proposed a new method (DFT+ΔCC) – as accurate as the SKZCAM protocol while being cheap enough to study larger and more complex systems – which has been applied to this system to show that it forms a 3D tetrahedral structure, resolving previously inconclusive experimental evidence.

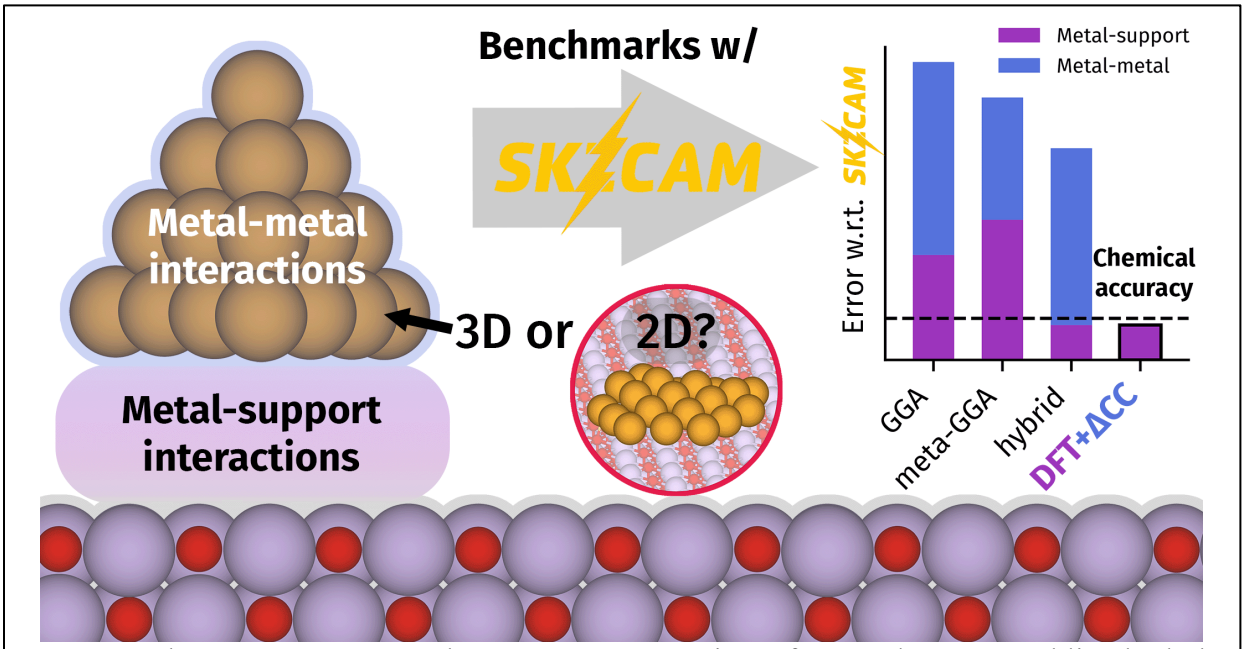

Figure 5. The SKZCAM protocol can generate extensive reference datasets, enabling both the benchmarking of DFT approximations and the development of new, cost-effective methods, as I have shown for gold nanoclusters on MgO(001).

An important outcome of this thesis is the implementation of the SKZCAM protocol into an open-source package [8] where it has been automated to enable integration within high-throughput screening protocols. These developments will facilitate future studies of complex surface phenomena by other research groups, whether to validate experimental interpretations, provide new atomistic insights or generate benchmarks to develop more affordable simulation methods.

References

[1] **B. X. Shi**, V. Kapil, A. Zen, J. Chen, A. Alavi, and A. Michaelides, J. Chem. Phys. **156**, 124704 (2022).

[2] **B. X. Shi**, A. Zen, V. Kapil, P. R. Nagy, A. Grüneis, and A. Michaelides, J. Am. Chem. Soc. **145**, 25372 (2023).

[3] **B. X. Shi**, D. J. Wales, A. Michaelides, and C. W. Myung, J. Chem. Theory Comput. **20**, 5306 (2024).

[4] **B. X. Shi**, A. S. Rosen, T. Schäfer, A. Grüneis, V. Kapil, A. Zen, and A. Michaelides, arXiv:2412.17204 (2025) – Accepted in Nature Chemistry.

[5] J. Sauer, Acc. Chem. Res. **52**, 3502 (2019).

[6] H.-Z. Ye and T. C. Berkelbach, Faraday Discuss. **254**, 628 (2024).

[7] Z. Huang, Z. Guo, C. Cao, H. Q. Pham, X. Wen, G. H. Booth, J. Chen, and D. Lv, arXiv:2412.18553 (2025).

[8] **B. X. Shi**, https://www.github.com/benshi97/autoSKZCAM

Atomic-scale Sensing of the Electric Field with a Molecular Sensor

Yunpeng Xia,[1] **W. Ho**[1,2]

[1]Department of Physics and Astronomy, University of California, Irvine, CA 92697-4575, USA
[2]Department of Chemistry, University of California, Irvine, CA 92697-2025, USA

Email: yunpeng.xia@uci.edu

The ability to probe and control quantum coherence at the atomic scale in both space and time remains a central challenge in nanoscience and quantum measurement. In this work, we introduce a novel approach that integrates ultrashort terahertz (THz) pulses with scanning tunneling microscopy (STM) to perform coherent spectroscopy on a single hydrogen molecule (H_2) confined within the STM junction. This technique enables the direct observation of time-domain quantum coherence and opens new possibilities for atomic-scale electric field sensing and the study of intermolecular interactions.

Experiments were performed in a custom-built 9 K ultrahigh vacuum STM on Cu_2N/Cu(001) surfaces. THz pulses were generated by a plasmonic photoconductive antenna driven by a 1 GHz repetition-rate Ti:Sapphire laser (820 nm, ~ 30 fs), and coupled into the junction via reflective optics and a Tsurupica lens. Modulation at 263 Hz of the high rep-rate source enabled lock-in detection of picosecond dynamics in the THz induced tunneling current with enhanced signal-to-noise.

At the core of this method is the identification of a two-level system (TLS) formed by a hydrogen molecule weakly bound in the STM nanocavity. The molecule resides in an asymmetric double-well potential created by van der Waals interactions with both the metallic tip and the substrate. The two potential wells correspond to distinct adsorption geometries, each associated with a

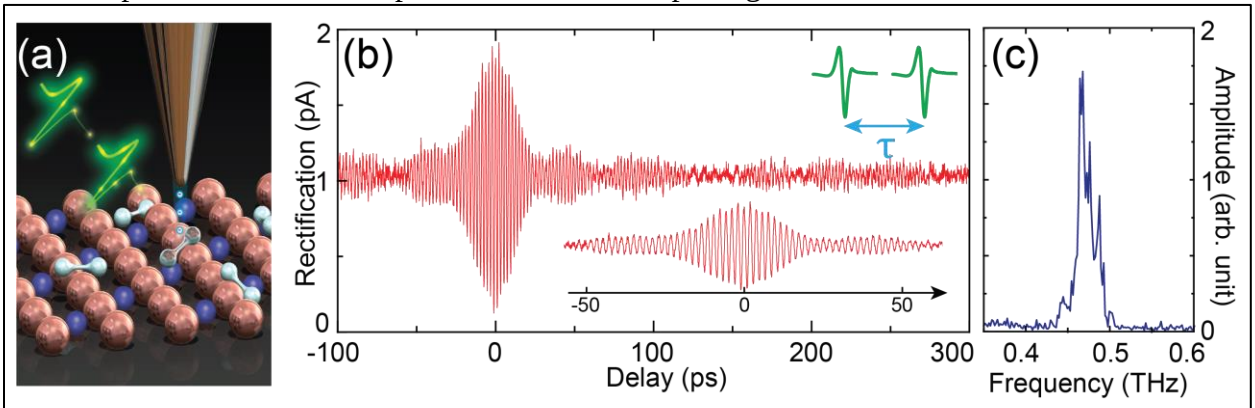

Fig. 1. Coherent dynamics measured from a hydrogen molecule in a THz-STM. (a) A schematic diagram of the experimental setup with hydrogen molecule adsorbed on Cu_2N island. (b) The pump-probe delay scan of the THz induced DC current with fixed tip bias. (c) Fast Fourier Transform (FFT) spectrum of (b).

different spatial configuration of the molecule inside a ~ 6 Å-tall cavity. Quantum tunneling between these geometries gives rise to a discrete energy splitting, defining a TLS. Crucially, these two states possess different dipole moments equivalent to a ~ 0.02e charge difference, making the system highly sensitive to variations in the local electrostatic environment.

When ultrashort THz pulses are delivered to the STM junction, they coherently drive transitions between the two levels of the hydrogen molecule, as shown in Fig. 1. Using a pump-probe scheme, we observe Ramsey-type oscillations in the THz-induced tunneling current, revealing clear evidence of quantum superposition and interference between the two molecular states. The oscillation frequency, approximately 0.5 THz (or ~ 2 meV), directly corresponds to the TLS energy splitting. Notably, in contrast to conventional STM spectroscopy, which probes excitations via inelastic tunneling and is limited by thermal broadening and modulation (~ 4 meV), the coherence-based technique significantly enhances energy resolution, on the order of ~ 0.01 THz (~ 0.04 meV), by measuring the phase evolution between quantum states. This quantum advantage provides a powerful pathway for probing fine energy structures beyond the reach of traditional methods.

The resonance frequency of the hydrogen TLS exhibits a pronounced Stark shift under an externally applied bias across the tunneling gap, stemming from the distinct dipole moments of its two states (Fig. 2). Moreover, as the STM tip is scanned across the surface, variations in the local electrostatic landscape modify the junction environment experienced by the molecule and changes that are directly reflected in the resonance frequency of the hydrogen TLS. For example, electric fields at various $Cu_2N/Cu(001)$ sites are estimated to be: ~ −10 mV/Å at Cu atoms, ~ −60 mV/Å at N atoms, and ~ −25 mV/Å at hollow sites—despite being only a few ångströms apart. These shifts, tracked via changes in the resonance frequency, establish the hydrogen molecule as an ultra-sensitive and spatially localized electric field sensor, capable of mapping nanoscale electrostatic landscapes with sub-ångström resolution.

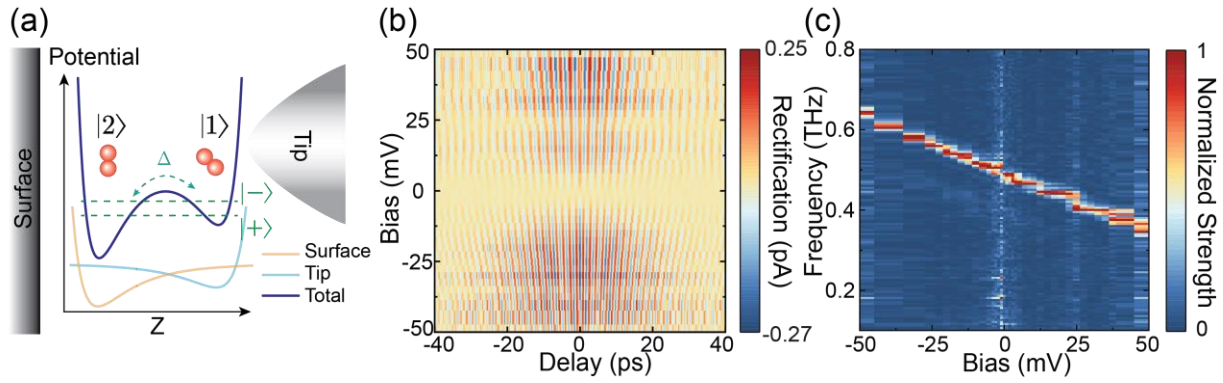

Fig. 2. The TLS of hydrogen molecule and the stark shift of its energy splitting. (a) The schematic diagram of the TLS for H_2 in a STM junction, the potential landscape is formed by van der Waals interaction from both tip and sample surface. (b) Bias dependence of resonance frequencies of H_2. Each horizontal slice of the plot was a –40 to 40 ps delay scan spectrum taken at the corresponding tip bias. (c) FFT results of the delay scans from (b), each normalized to highlight the main frequency component.

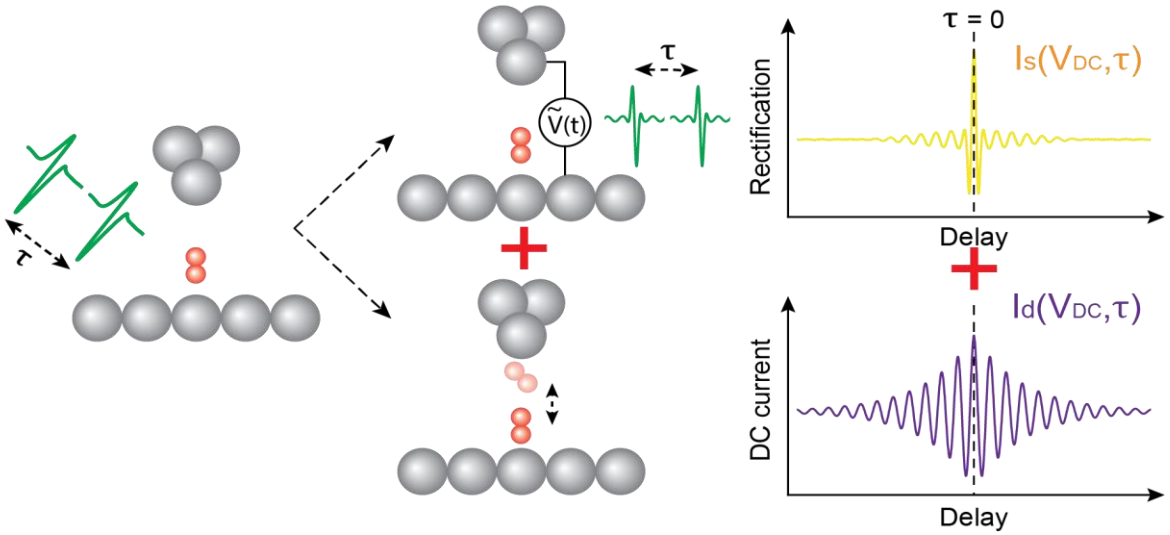

Fig. 3. A schematic diagram showing the two components that contribute to the oscillatory delay-scan signal of THz induced DC current.

The sensing capability extends even further when considering interactions with nearby molecules. When a second hydrogen molecule is close by, dipole-dipole interactions between the two TLSs lead to hybridization and the formation of entangled states. This coupling is experimentally observed as avoided level crossings in the bias-dependent resonance spectra. By adjusting the tip height, we tune the interaction strength and observe coherent transitions between weakly and strongly coupled regimes. These results demonstrate that the hydrogen TLS is not only a sensitive quantum sensor, but also a viable platform for exploring few-body quantum physics and emergent correlations at the atomic scale.

A key insight from this study is that the THz-induced tunneling current contains two physically distinct contributions with each reflecting a different regime of light–matter interaction in the STM junction, as illustrated in Fig. 3. The first is a field-like rectification response, which arises from the nonlinear tunneling I–V characteristics. In this case, the THz electric field transiently modulates the junction bias, and the nonlinearity produces a net DC current. This component dominates at short pump-probe delays when the THz pulses overlap and is sensitive to both the field amplitude and spectral content.

The second component is a photon-like resonant absorption response, which captures the coherent dynamics of the TLS. As the superposition state evolves with varying delay time, the occupation probabilities of the two levels oscillate, modulating the tunneling conductance. This produces Ramsey fringes in the delay-dependent current and reflects the absorption of resonant THz photons. Both contributions are present in our measurements and can be tuned through external bias. The ability to distinguish and analyze these two components provides a comprehensive understanding of the THz-driven signal and highlights the dual nature of the THz excitation as both a classical field and a quantum photon source.

Taken together, we have demonstrated that a hydrogen molecule confined in an STM junction forms a two-level system whose dynamics can be read out electrically with high spatial and temporal resolution, coherently driven by ultrafast THz pulses. The ability to induce and detect coherent quantum oscillations in a single molecule with light pulses, measure electric field distributions with ångström resolution, and probe coupling between quantum states opens exciting possibilities for precision measurements in basic science and applications. Potential extensions include the use of spin-active molecules to study ultrafast magnetic dynamics, the design of molecular-scale quantum bits, and the development of molecule-based quantum sensors capable of resolving charge, spin, and vibrational dynamics in different material systems.

References:

[1] L. Wang, Y. Xia, W. Ho, Science **376**, 401-405 (2022).
[2] L. Wang, D. Bai, Y. Xia, W. Ho, Phys. Rev. Lett. **130**, 096201 (2023).
[3] Y. Xia, L. Wang, D. Bai, W. Ho, ACS Nano **17**, 23144-23151 (2023).
[4] Y. Xia, L. Wang, W. Ho, Phys. Rev. Lett. **132**, 076903 (2024).

Atomic-scale terahertz-induced dynamics of van der Waals materials

S. Adams, T. L. Cocker

Department of Physics and Astronomy, Michigan State University,
East Lansing Michigan 48824, USA

Email: adamsst9@msu.edu

Complex materials are envisioned to drive the development of smaller and faster next-generation nanotechnologies. When such devices approach atomic length scales, it is crucial to understand the local variation in ultrafast electronic dynamics to harness the properties of the materials efficiently. Scanning tunneling microscopy (STM) is a well-established, powerful tool to retrieve the steady-state electronic structure of a material with atomic spatial resolution. Meanwhile, ultrafast pump-probe spectroscopy enables the study of sub-picosecond collective electronic dynamics, where the spatial resolution is generally limited to the spot size. Terahertz scanning tunneling microscopy (THz-STM) combines the high spatial resolution of traditional STM with the ultrafast temporal resolution of terahertz pulses [1-8]. It can probe electronic dynamics at the atomic scale, offering unprecedented insight into the ultrafast processes of materials. This technique is particularly valuable for studying phenomena such as charge transfer, quantum effects on surfaces, and phase transitions, providing a powerful tool for advancing our understanding of material properties at the nanoscale. Despite great achievements in THz-STM over the past decade, many open questions remain including measurement interpretation, its application to quantum materials and potential advances to the technique.

Atomic-scale terahertz time-domain spectroscopy

Until recently, one outstanding challenge was bringing terahertz time-domain spectroscopy (THz-TDS) to the atomic scale. THz-TDS is one of the central technologies of THz science [9]. By measuring the oscillating THz electric field after it has interacted with a sample and comparing it to a reference field, the complex dielectric function at THz frequencies may be determined. Based on the same concept, in THz scattering-type scanning near-field optical microscopy (s-SNOM), THz pulses focused onto a scanning probe tip may be used to spatially map the local complex dielectric function on the 10-100 nm scale [10]. However, many active research directions in surface science require these properties to be determined at yet smaller length scales. For example, THz-TDS of individual atomic sites would allow the role of defects, dopants, and interfaces on charge transport to be studied in unprecedented detail. Although a number of approaches have been reported for characterizing THz pulses at a THz-STM tip apex [11-17], atomic-scale THz time-domain spectroscopy has remained out of reach.

Here, we introduce an experimental method for atomic-scale THz-TDS in a THz-STM junction. Using our technique, we demonstrate atomically resolved THz-TDS of a silicon-doped GaAs(110) sample, revealing a resonator defect with the hallmarks of the elusive DX center [18]. Fig. 1a shows a schematic of the THz-STM setup. A strong-field THz pulse is coupled to the STM tip and acts as an ultrafast bias voltage in the tip-sample junction, inducing a current pulse with a rectified

component that is measured electronically. To perform atomic-scale THz-TDS, we use this induced current pulse to sample a second, weaker THz pulse through a cross-correlation (THz-CC) measurement that captures the near-field waveform. In Fig. 1b, a THz-CC waveform is recorded on an Au(111) surface, which is used as a reference sample because of its flat spectral response. The spectrum of the near-field waveform is displayed in the inset. Fig. 1c shows an STM topography image of our GaAs(110) sample surface; the atomic rows are visible, as are multiple types of atomic defects (e.g., gallium vacancies and silicon substitutional dopants). The inset of Fig. 1c shows a high-resolution THz-STM image of the blue square region, where a particular defect exhibits a strong THz-STM signal. Near-field waveforms were measured 200 pm away from the defect (Fig. 1d; green circle in Fig. 1c) and in the center of the bright feature in the THz-STM scan (Fig 1e). In Fig. 1f, we divide the amplitude spectra of the GaAs(110) near-field waveforms (insets in Fig. 1d and e) by the Au(111) reference spectrum (inset of Fig 1b). Spectroscopically, the most prominent contrast occurs at 0.96 THz, where the defect exhibits a strong resonance that is absent at the location 200 pm away. From this signature resonance and other STM characteristics (not shown), we identify the defect as a silicon-vacancy complex stabilized in a DX center configuration and the resonance as the vibrational motion of the silicon dopant atom. Although DX centers are of significant interest in semiconductor research due to their prominent role in carrier scattering [19], this is the first time one has been observed directly. With atomic-scale THz-TDS we can now study open questions that previously could not be addressed experimentally, such as the simultaneous spatial and spectral description of defect complexes in semiconductors. As a next step, we envision that THz-TDS within a THz-STM junction will enable time-resolved THz spectroscopy of the transient THz dielectric response on the atomic scale.

Terahertz control of surface topology probed with subatomic resolution

Equipped with atomic-resolution THz-TDS, we next turn our attention to quantum materials. The discovery of topologically protected states has had a lasting impact on condensed matter research, leading to countless theoretical and experimental discoveries of new topological phases in materials. Amongst these, the layered van der Waals material WTe_2 has gained attention as a likely Weyl semimetal, with topologically protected linear electronic band crossings hosting massless chiral fermions [20]. A shear mode at 0.26 THz that restores lattice inversion symmetry has been associated with a bulk phase transition from the low-temperature ground state (T_d-WTe_2: probable type-II Weyl semimetal) to the high-temperature state (1T'-WTe_2: trivial semimetal) [21] (Fig 2a). Applying atomic-scale THz-TDS to the surface of WTe_2, we observe four clear resonance peaks within our bandwidth [22], including the phase transition associated motion of the layers (Fig. 2b). Although this mode is in-plane, the enhanced out-of-plane fields at the THz-STM tip apex in our experiments couple to it via a ferroelectric dipole at the interface. These strong THz fields can further induce a localized structural phase transition of the topmost atomic layer, driving it from T_d-WTe_2 to a metastable state characterized by both shear translation and intralayer distortion. As a result, the electronic structure at the vacuum interface undergoes a phase transition, where the top atomic layer can no longer host Fermi arc surface states. We explore this THz-driven phase transition further with subatomically resolved differential imaging combined with hybrid-level density functional theory, which reveals a shift of 7 ± 3 pm of the top atomic plane, consistent with a structural transition in which only the top layer moves (Fig. 2c). The spatial contrast between the phases enables us to achieve this unprecedented spatial resolution and reveals subtle differences

in the surface electronic wavefunctions as the atomic positions distort and the lattice planes shift across the transition [22].

Our study shows that THz-STM can both drive the phase transition of WTe_2 via the enhanced THz fields at the STM tip apex and distinguish the electronic phases. The THz-induced changes to the local density of states and real-space imaging are well supported by hybrid-level DFT calculations [7]. The possibility of finely adjusting the density of states of a material with an ultrafast light field and simultaneously resolving the spatial dependence of the transition on the subatomic scale presents a novel way of studying topological phase transitions. Overall, our finding that THz-STM is extremely sensitive to differences between electronic phases is an exciting prospect for further studies of topological materials with THz-driven transitions.

References:

[1] T. L. Cocker, et al. Nature Photonics **7**, 620-625 (2013).
[2] T. L. Cocker, et al. Nature **539**, 263-267 (2016).
[3] K. Yoshioka, et al. Nature Photonics **10**, 762-765 (2016).
[4] V. Jelic, et al. Nature Physics **13**, 591-598 (2017).
[5] S. E. Ammerman, et al. Nature Communications **12**, 6794 (2021).
[6] L. Wang, et al. Science **376**, 401-405 (2022).
[7] C. Roelchke, et al. Nature Photonics **18**, 595-602 (2024).
[8] S. Sheng, et al. Nature Physics **20**, 1603-1608 (2024).
[9] M. Koch, et al. Nature Reviews Methods Primers **3**, 48 (2023).
[10] T. L. Cocker et al., Nature Photonics **15**, 558–569 (2021).
[11] L. Wimmer, et al. Nature Physics **10**, 432-436 (2014).
[12] S. Yoshida, et al. ACS Photonics **6**, 1356-1364 (2019).
[13] M. Müller et al. ACS Photonics **7**, 2046-2055 (2020).
[14] D. Peller, et al. Nature Photonics **15**, 143-147 (2021).
[15] T. Siday, et al. Nature **629**, 329-334 (2024).
[16] H. Li, et al. ACS Photonics **11**, 1428-1437 (2024).
[17] L. Bobzien, et al. APL Materials **12**, 051110 (2024).
[18] V. Jelic, S. Adams et al. Nature Photonics **18**, 898–904 (2024).
[19] A. Kundu et al. Physical Reviw Materials **3**, 094602 (2019).
[20] A. A. Soluyanov et al. Nature **527**, 495–498 (2015).
[21] E. J. Sie et al., Nature **565**, 61–66 (2019).
[22] V. Jelic*, S. Adams*, D. Maldonado-Lopez* et al., accepted, preprint available arXiv:2411.07545 (2024).

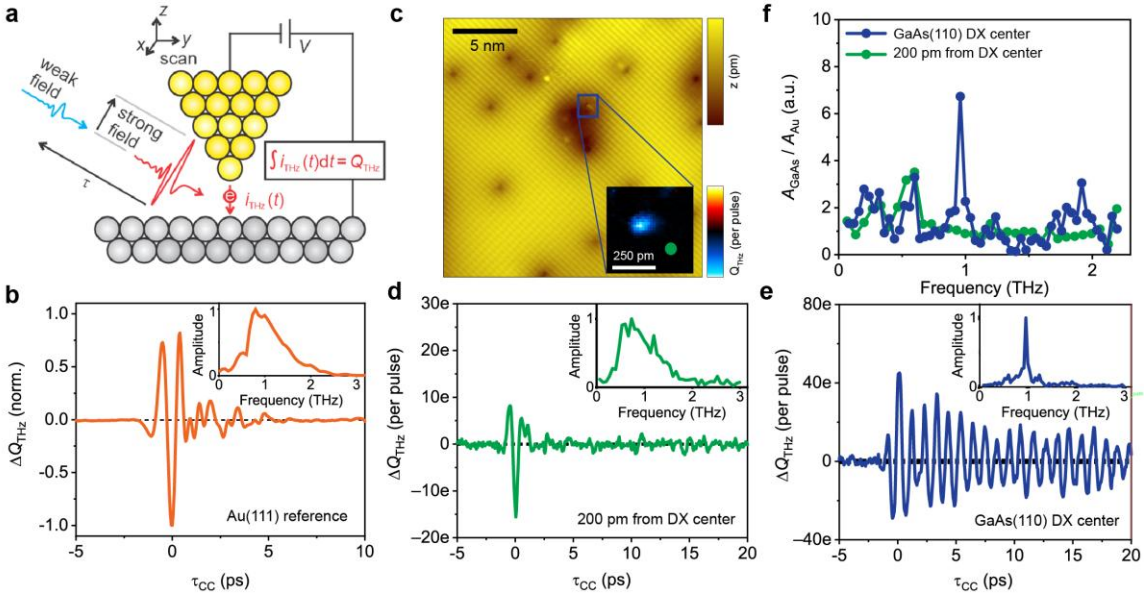

Fig. 1. | Terahertz time domain spectroscopy on the atomic scale on GaAs(110). a, Schematic of atomic-scale THz-TDS based on THz-STM, where a strong-field THz pulse induces a tunnel current that samples the oscillating field of a weak-field THz pulse in the tunnel junction through a cross-correlation (THz-CC) measurement. **b**, THz-CC waveforms measured on a reference Au(111) sample. Inset: Amplitude spectrum of the near-field waveform on Au(111). **c**, STM topography image of the GaAs(110) surface, with atomic rows and multiple types of defects visible. Inset: THz-STM image of a small region of the STM image (blue square), which contains a strong and highly localized THz-STM signal. **d,e**, THz-CC waveforms measured on the GaAs(110) surface 200 pm away from the bright defect (d), which is indicated by a green circle in the inset of c, and on the prominent THz-STM feature, which is associated with a DX center (e). Insets show the normalized amplitude spectrum of the respective near-field waveform. **f**, Amplitude spectra of d and e divided by the gold reference spectrum (inset of b).

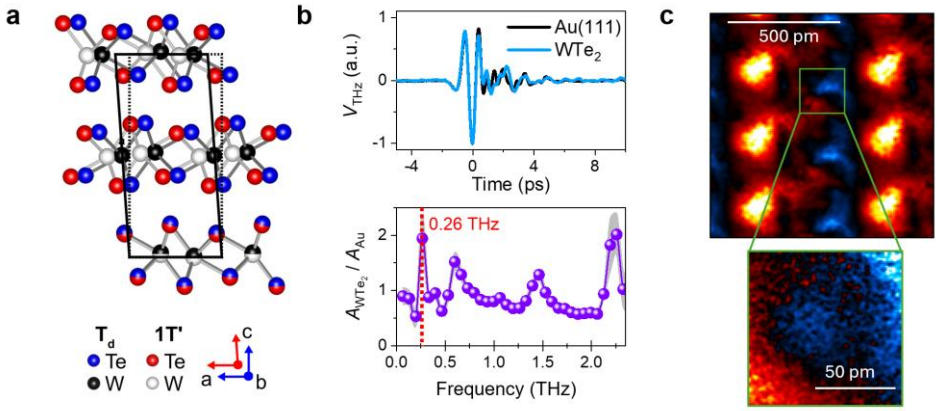

Fig. 2. | Exciting and characterizing a phase transition in WTe_2. a, Schematic of the lattice structure of ground state T_d-WTe_2 (Weyl semimetal candidate) and excited state 1T'-WTe_2 (trivial semimetal). **b**, Atomic-scale THz-TDS of the WTe_2 surface revealing the phase transition associated shear mode at 0.26 THz in the divided Fourier spectrum. **c**, The phase transition enables differential imaging with ultra-high (subatomic) resolution.

Surface Properties of Zirconium diboride (0 0 0 1) and Homoepitaxial Growth of Zirconium diboride as Determined by Scanning Tunneling Microscopy

Ayoyele Ologun[1], Michael Trenary[2].

[1,2] Department of Chemistry, University of Illinois Chicago, Illinois.
845 West Taylor street, Chicago,Illinois, 60607.USA
Email address: aologu2@uic.edu

Keywords: Surface chemistry, Chemical vapour deposition, Zirconium diboride

INTRODUCTION

Many industrial processes require chemical vapour deposition (CVD) to produce high-quality thin films and coatings on solid surfaces. Surface chemical reactions play a central role in these processes. To expand and optimize a more rational approach to applying thin-film growth processes and coatings, a detailed understanding of the surface chemistry at the atomic and molecular level that underlies these processes needs to be better understood. Despite the availability of advanced surface techniques, relatively little fundamental research is being devoted to investigating the underlying surface chemical mechanisms associated with these processes.
Transition metal diborides, MB_2, are known to either have a metal-terminated or boron-terminated surface. While group-V MB_2 has boron-terminated surfaces, group-IV MB_2 has metal-terminated surfaces. Zirconium diboride, ZrB_2, a group-IV metal-terminated diboride, is an extremely hard material with a high melting point of 3246 °C, with applications as ultra-high temperature ceramics, hard refractory coatings, abrasives, and hypersonic vehicles. ZrB_2 can be grown conformally via chemical vapor deposition (CVD) using zirconium borohydride $Zr(BH_4)_4$ as a precursor. The surface chemistry responsible for the molecular transformation of zirconium borohydride, $Zr(BH_4)_4$, to zirconium diboride, ZrB_2, was studied on a $ZrB_2(0001)$ surface using the experimental techniques of reflection absorption infrared spectroscopy (RAIRS), low energy electron diffraction (LEED), x-ray photoelectron spectroscopy (XPS) and scanning tunelling microscopy (STM).

METHODOLOGY

The experiments were conducted in a stainless steel ultra-high vacuum (UHV) chamber equipped with a base pressure of 1×10^{-10} Torr, described in detail elsewhere[1], and the STM images were obtained at room temperature with an Omicron variable-temperature scanning probe microscope. RAIRS spectra were acquired at 95 K. All XPS spectra were obtained using Mg Kα radiation and pass energies of either 50 or 100 eV. The crystal was cleaned by several cycles of Ar^+ sputtering (1.5 kV, 7.0 μA) followed by several annealing cycles for at temperatures ~ 2533 K using a home-built e-beam heater.

$Zr(BH_4)_4$ was synthesized by the reaction between $LiBH_4$ and $ZrCl_4$ using the procedure described by Haaland et al.[2] The purity of the sample was confirmed by infrared spectroscopy, and it was subsequently stored in a glass container at temperatures below 0 °C for later use.

$$ZrCl_4(s) + 4LiBH_4(s) \rightarrow Zr(BH_4)_4(s) + 4LiCl(s)$$

The $Zr(BH_4)_4$ exposures were performed by back-filling the chamber, and the unit of exposure is reported in Langmuir, where 1 L = 1×10^{-6} Torr Sec.

RESULTS

After exposure of $Zr(BH_4)_4$(g) to ZrB_2(0001) at 90 K, a RAIR spectrum that closely matched that of the pure compound was obtained, indicating adsorption without decomposition. Heating to higher temperatures leads to thermal desorption of the compound from the substrate. CVD of $Zr(BH_4)_4$ on ZrB_2(0001) at 1470 K led to an over-stoichiometric thin film of $ZrB_{2.5\pm0.3}$, as revealed by XPS. LEED of this surface revealed a $(\sqrt{3}\times\sqrt{3})$-R30° pattern, which was also observed in a previous study following direct deposition of boron onto a ZrB_2(0001) surface.[3] The $(\sqrt{3}\times\sqrt{3})$-R30° surface is found to be resistant to oxidation in contrast to the zirconium-terminated surface.

Using STM, we investigated the atomic-scale structure of ZrB_2(0001) and the homoepitaxial growth of ZrB_2 on this surface. Annealing over 2000 K e-beam heater led to a rough and smooth surface on each terrace, further annealing to 1470 K for 30 minutes led to mobility of ZrB_2 islands. A smooth surface with a monoatomic step height of Å ~3.54 Å was achieved after further annealing at 1470 K for another 30 minutes.
Zr-terminated bilayer islands of ZrB_2 were observed following the exposures of $Zr(BH_4)_4$ to ZrB_2(0001) at 1473 K and immediately cooling to room temperature. Coalescence of the ZrB_2 islands was observed when the substrate was left for 60 minutes at the deposition temperature before imaging at room temperature. In contrast, exposure of $Zr(BH_4)_4$ to ZrB_2(0001) at 900 K resulted in high-density clusters. Stepwise annealing of these clusters at 1400 K led to the transformation of these clusters into a continuous thin film via thermal-induced coalescence.

FIGURES

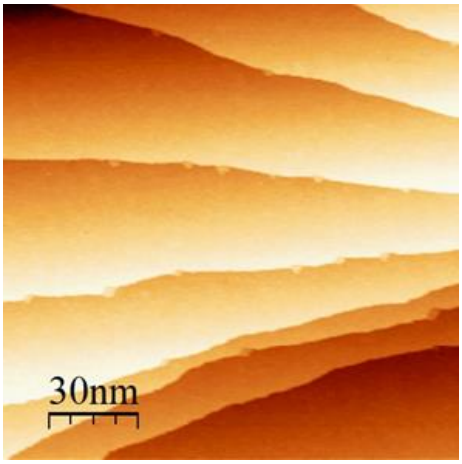

STM image of Clean $ZrB_2(0001)$

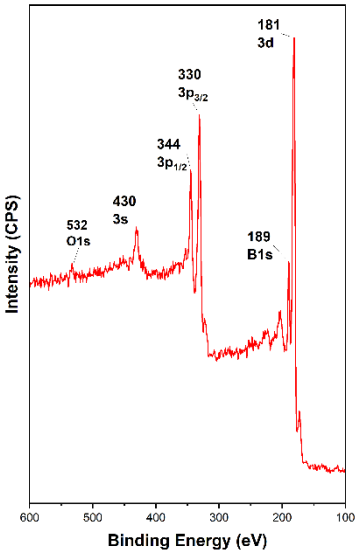

XPS spectrum of $ZrB_2(0001)$

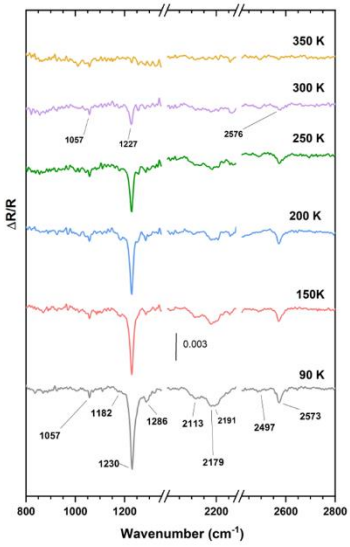

RAIRS Spectra of 50 L exposure of $Zr(BH_4)_4$ on $ZrB_2(0001)$

REFERENCES

(1) Ranjan, R.; Redington, M.; **Ologun, A.**; Zurek, E.; Miller, D. P.; Trenary, M. Identification of a Stable B2H2 Intermediate in the Decomposition of Zr(BH4)4 on the Pd(111) Surface. *J. Phys. Chem. C* **2024**, *128* (30), 12414–12426. https://doi.org/10.1021/acs.jpcc.4c02327.

(2) Haaland, A.; Shorokhov, D. J.; Tutukin, A. V.; Volden, H. V.; Swang, O.; McGrady, G. S.; Kaltsoyannis, N.; Downs, A. J.; Tang, C. Y.; Turner, J. F. C. Molecular Structures of Two Metal Tetrakis(Tetrahydroborates), Zr(BH4)4 and U(BH4)4: Equilibrium Conformations and Barriers to Internal Rotation of the Triply Bridging BH4 Groups. *Inorg. Chem.* **2002**, *41* (25), 6646–6655. https://doi.org/10.1021/ic020357z.

(3) Aizawa, T.; Suehara, S.; Hishita, S.; Otani, S. Surface Phonon Dispersion Of. *J. Phys.: Condens. Matter* **2008**, *20* (26), 265006. https://doi.org/10.1088/0953-8984/20/26/265006.

High-temperature surface dynamics of NiAl under reactive environments.

S.B. Patel[1*], J.T. Sadowski[2], G. Zhou[1]

***Nottingham Contestant**

[1]Department of Mechanical Engineering & Materials Science and Engineering Program, State University of New York at Binghamton, NY 13902, USA
[2]Center for Functional Nanomaterials, Brookhaven National Laboratory, Upton, NY 11973
Email: spate132@binghamton.edu

Intermetallic alloys such as β-NiAl are known for their exceptional mechanical stability under harsh conditions. This robustness largely stems from the formation of a well-ordered phase at an equiatomic Ni-Al ratio, which provides structural integrity at elevated temperatures. A key contributor to its corrosion resistance is the strong affinity of Al for oxygen, which promotes the formation of a uniform passivating Al_2O_3 layer. This oxide layer serves as an effective diffusion barrier, significantly slowing down oxidation and alloy degradation [1]. However, under operando conditions, this protective layer is prone to mechanical failure such as spallation and buckling. These disruptions intermittently expose the underlying NiAl surface to reactive species, leading to compositional and structural degradation over time.

Herein, we investigate the high-temperature surface dynamics of pristine NiAl surface (at ~800 °C) under various gas-phase environments to identify active surface sites and early-stage reaction mechanisms. A suite of advanced in-situ characterization techniques is employed, including UHV LEEM, LEED, High-Resolution TEM, HAADF imaging, and NEXAFS, to track surface segregation behavior and identify atomic-scale structural transformations in real time.

By introducing trace amounts of oxygen, we show that even small variations in temperatures can critically influence surface step pinning and unpinning phenomena, highlighting the delicate thermodynamic balance that governs surface mobility. In separate experiments, we expose the NiAl surface is exposed to CO, a gas typically considered reductive, and demonstrate dissociative adsorption which results in the formation of atomic O and C. This reaction pathway deviates from the classic Boudouard disproportionation reaction, where CO_2 is expected to form. Complementary density functional theory (DFT) calculations provide insight into adsorption energetics and reveal atomistic mechanisms underlying the interaction between CO and the NiAl surface. Furthermore, we investigate the dissociative adsorption of C_2H_4 on the NiAl surface by dosing controlled amounts of C_2H_4, which decomposes to generate surface carbon that subsequently diffuses into the subsurface. By systematically varying both the C_2H_4 partial pressure and the substrate temperature, we establish strategies to tune the nucleation and morphology of carbon-related structures. These findings contribute to a comprehensive understanding of the dynamic surface evolution of NiAl in reactive gas environments and offer mechanistic insights that are critical for guiding the design of more robust intermetallic materials for high-temperature catalytic and corrosive applications.

Intermetallic compounds are known to be resistant to changes in composition. This is even more prominent in the NiAl system, which is known to have a very high order-disorder transition temperature, which is close to its melting temperature of 1640 °C [2]. However, the concentration of thermal vacancies also increases dramatically with an increase in temperature and leads to an increase in mobile atoms within the bulk. In our study, we reveal a thermally activated bulk-to-surface mass exchange that drives surface phase separation, resulting in the formation of a Ni-rich γ'-Ni3Al precipitate on the NiAl surface as characterized by NEXAFS, HAADF, EDS maps and HRTEM (Fig.1). Using DFT, we demonstrate that the asymmetries in diffusion barriers and vacancy formation energies between Ni and Al atoms induce preferential Ni segregation to the surface, which then leads to the formation of the Ni-rich precipitate. We provide experimental evidence in the form of HRTEM images that highlight the role of vacancies in the bulk, and how they can influence the composition of the precipitate due to the bulk-surface coupling of the atoms. Furthermore, we also highlight the role of the misfit strain between the Ni-rich precipitate and the NiAl substrate, which governs the morphology of the precipitate being formed. We show that the precipitate forms a wetting layer on the NiAl(100) facet due to the lower misfit strain as opposed to more spherical precipitates that are formed on the NiAl(110) facet. This bulk-surface coupling mechanism is likely a universal driver of surface phase separation in intermetallic alloys, driven by thermal stress.

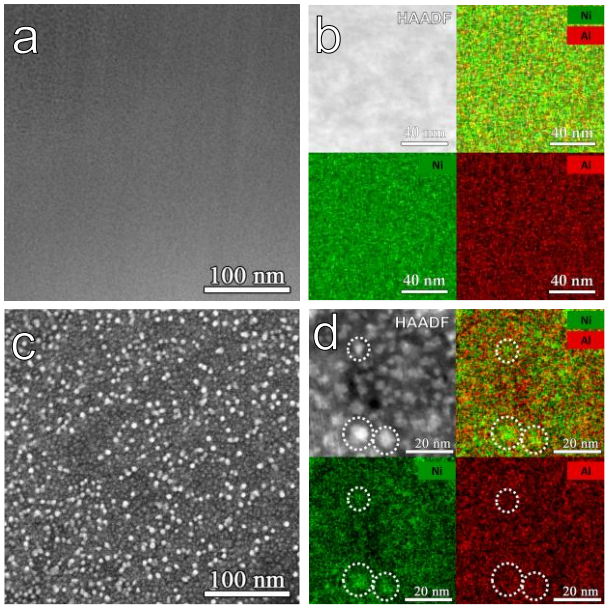

Fig. 1. (a-b) HAADF images and EDS elemental maps showing the even distribution of Ni and Al prior to UHV annealing; (c-d) Formation of Ni-rich precipitates upon annealing under UHV conditions.

Furthermore, the bulk-surface coupling also directly influences the motion of surface steps. We employ *in-situ* LEEM to investigate the bulk-surface coupling and the movement of atoms at elevated temperatures at ~800 °C. Our studies show that an increase in temperatures generally results in an increase in vacancy concentration in the bulk, which then results in the formation of adatoms on the surface [3]. Surface sites such as step edges

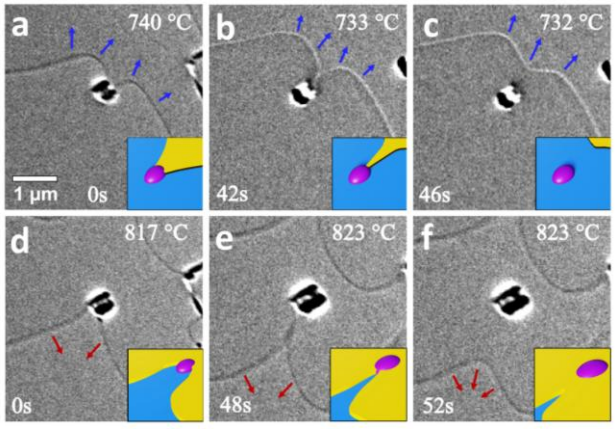

Fig. 2. Time sequence of LEEM images illustrating how surface steps can overcome pinning with persistent (a-c) cooling and (d-f) heating

are well known for their reactivity primarily driven by the undercoordinated atoms in comparison to other sites such as terraces. These step edges act as sinks for adatoms, which appear to grow under heating conditions. On the contrary, cooling leads to the inward diffusion of atoms from the surface to the bulk region, thereby quenching existing thermal vacancies in the process. In this instance, surface steps act as sources for adatoms which subsequently diffuse into the bulk, leading to the retraction motion of step edges. Our studies show that minute changes in temperatures in the range of a few K/min can lead to a distinct outcome due to the direction of adatom diffusion between the surface and the bulk. To investigate the role of surface steps and temperature fluctuations during transient heating and cooling conditions, minute amounts of oxygen was introduced into the chamber. During the initial stages, we found that oxides tend to nucleate along the step edge as the undercoordinated nature of the step edges provide active sites for the nucleation of the oxide. Furthermore, step edges also act as sources for adatoms necessary to sustain oxidation. The oxides formed along the step edges subsequently pin the step edges and leads to the bowing of step edges as they continue to recede (in the case of transient cooling) or grow (in the case of transient heating) in the step edge regions that are oxide free. We demonstrate a mechanism that can subsequently lead to the unpinning of the surface steps with persistent cooling/heating (Fig. 2). Understanding these nuances is critical for accurately predicting and dynamically manipulating the performance of active materials in a plethora of chemical process under transient thermal conditions.

Building on our deeper understanding of the intrinsic behavior of the NiAl surface, we further investigated its chemical stability in CO-rich environments. While CO is widely regarded as a reducing gas, its interaction with structural alloys can result in unexpected surface reactions. In this study, we employed XPS, LEEM, and XPEEM to examine the dissociative adsorption of CO on the NiAl surface. Our findings reveal that CO undergoes dissociation into atomic oxygen and carbon. Liberated oxygen readily reacts with Al to form alumina, whereas the carbon atoms diffuse into the subsurface (Fig. 3). This process results in the formation of spatially distinct surface domains, disrupting the continuity of the protective alumina layer and compromising its passivation effectiveness. Importantly, the data indicate a clear preference for the dissociative CO pathway over the classical Boudouard disproportionation reaction that produces CO_2 [4]. Experimental evidence supports the inward diffusion of carbon and the subsequent nucleation of carbon-rich precipitates on the surface. These carbon islands, influenced by subsurface carbon concentration, highlight the critical role of bulk–surface interactions in

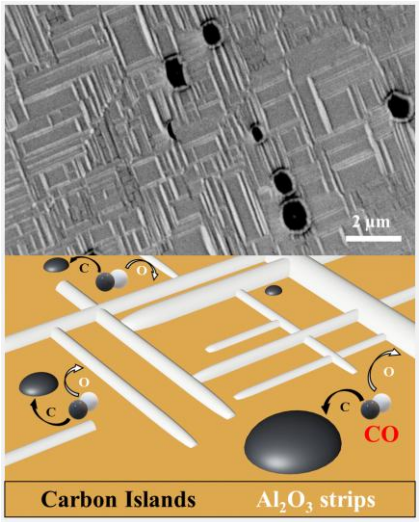

Fig. 3. LEEM image of the NiAl surface following CO exposure, accompanied by a schematic illustration depicting the proposed mechanism of CO dissociative adsorption. The image reveals spatially distinct regions corresponding to reaction products, while the schematic outlines the dissociation of CO into atomic carbon and oxygen, subsequent formation of carbon islands and alumina from oxygen on the surface

determining surface morphology. Overall, our study provides mechanistic insight into CO-induced degradation pathways in intermetallic alloys and underscores the importance of managing carbon ingress for maintaining the long-term structural and chemical integrity of materials used in carbon-rich environments such as petrochemical processing and hydrocarbon combustion systems.

Our studies in CO environments highlight the critical role of subsurface carbon in facilitating the formation of carbon-related species. To further investigate this behavior, we conducted controlled exposures of C_2H_4 on NiAl surfaces at varying temperatures and partial pressures, aiming to develop conditions that selectively promote the formation of either amorphous or graphitic carbon structures. We find that C_2H_4 readily decomposes on the NiAl surface, serving as an effective carbon source. The decomposed carbon diffuses into the subsurface, where an incubation period is required to accumulate a critical concentration of dissolved carbon. Once this threshold is reached, amorphous carbon islands begin to nucleate and grow if the substrate is maintained at relatively low temperatures (~700 °C). Our results show that the amount of pre-dissolved carbon strongly influences both the nucleation density and size of the resulting amorphous islands. At higher temperatures, C_2H_4 exposure promotes the formation of more ordered carbon species, specifically graphitic flakes. These flakes exhibit directional growth at 45° angles due to their epitaxial alignment with the NiAl(100) surface. We demonstrate that both the substrate temperature and carbon chemical potential can be precisely tuned to control the structure and morphology of surface-bound carbon species. Moreover, we introduce a two-step exposure strategy to create hybrid carbon structures: an initial low-temperature exposure produces amorphous carbon islands, which then act as carbon reservoirs during a subsequent high-temperature treatment that induces graphitic flake formation (Fig. 4). This approach enables the engineering of mixed-phase carbon architectures directly on NiAl surfaces. Our findings underscore the diverse forms that carbon can adopt on NiAl under varying environmental conditions—each with distinct structural and chemical implications. While such carbon species may disrupt the formation of a continuous protective alumina scale, they also offer promising opportunities for catalytic applications, particularly as supports for metal nanoparticle deposition [5].

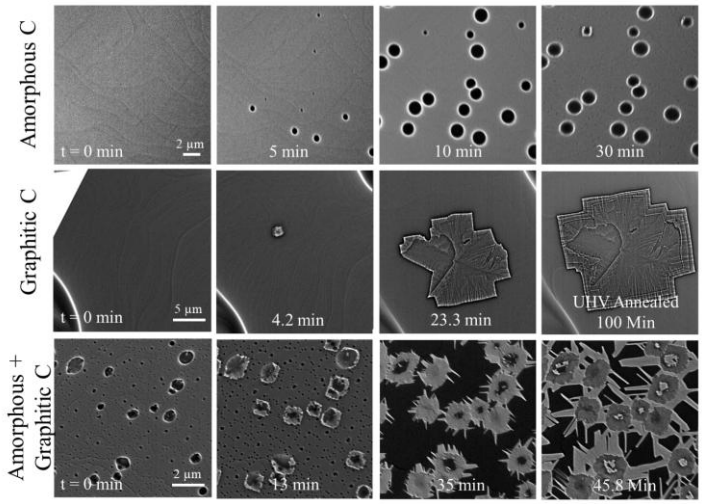

Fig. 4. Time sequence of LEEM images showing the formation of amorphous carbon structures (top row), graphitic carbon structures (middle row) , and a combination of both amorphous and graphitic carbon structures (bottom row) after using a two-step heating process in C_2H_4 on NiAl(100)

References:

[1] K. Bochenek, & M. Basista, Prog. Aerosp. Sci. 79, 136 (2015).

[2] I. Ansara, N. Dupin, H. L. Lukas, & B. Sundman, J. Alloys Compd. 247, 20 (1997).
[3] K. F. McCarty, J. A. Nobel, & N. C. Bartelt, Nature 412, 622 (2001).
[4] P. Lahijani, et al., Renew. Sust. Energ. Rev. 41, 615 (2015).
[5] E. Auer, et al., Appl. Catal. A: Gen. 173, 259 (1998).

Defect engineering of metal sulfide surfaces: Where real-world challenges meet Solid-state Physics

P.R.A de Oliveira,[1] **F.stavale**[2]

[1]Brazilian Center for Physics Research, CBPF, 22290-180, Rio de Janeiro, RJ, Brazil

Email: pabloribeiro@cbpf.br or hninofilho@gmail.com

It is historically observed that scientific breakthroughs often lead to substantial social impact. Reciprocally, solutions to several societal demands rely on the development of innovative platforms with unique properties. Currently, the increase in atmospheric pollutant gases, the urgent need for renewable energy sources, and the pursuit of green energy technologies have drawn significant attention from the scientific community. In this context, solid-state physics approaches emerge as potential strategies for designing new materials platforms capable of addressing these critical challenges. In this thesis, we explore defect engineering in metal sulfide structures, with particular interest on Zinc Sulfide (ZnS) surfaces. By integrating traditional surface-science spectroscopic methods—including ultra-high vacuum and ambient-pressure X-ray photoelectron spectroscopy (XPS and AP-XPS), ultraviolet photoelectron spectroscopy (UPS)—microscopy techniques (Atomic Force Microscopy (AFM), Scanning Tunneling Microscopy (STM)), diffraction methods (Low Energy Electron Diffraction (LEED)), and first-principles Density Functional Theory (DFT) calculations, we have systematically investigated how defects influence ZnS properties. We observed that introducing zinc vacancies transforms the insulating ZnS surface into a more conductive architecture by increasing majority carrier density and band-gap narrowing. In addition, cation-defect engineering significantly enhances the ZnS optical response, extending its absorption and emission properties into the visible range, in contrast to the predominantly UV-visible response observed in defect-free ZnS. The resulting p-type semiconductor character of defect-engineered ZnS proves stable, as confirmed by our calculations. Additionally, ZnS surfaces modified with zinc vacancies present new catalytic active sites capable of enhancing various molecular reactions. Notably, oxidation of these defective surfaces leads to the formation of a type-II ZnO/ZnS heterostructure, which seems promising for photocatalysis due to an efficient charge separation at the interface. Moreover, the formation of zinc vacancies are the driven force for adsorption or co-adsorption of molecules on ZnS surfaces. Through AP-XPS and DFT investigations, we

observed that CO2 exhibit favorable van der Waals interactions with defective ZnS surfaces, while CO molecules stick on oxygen-rich ZnS surfaces, before leaving it as a CO2-like molecule. Although our work has not resulted in a direct industrial application, our deep solid-state physics-driven investigation provides a fundamental understanding of defect-induced phenomena. This research might open new way for the development of ZnS-based catalytic systems and innovative defect-engineered materials platforms, potentially addressing critical environmental and energy-related challenges.

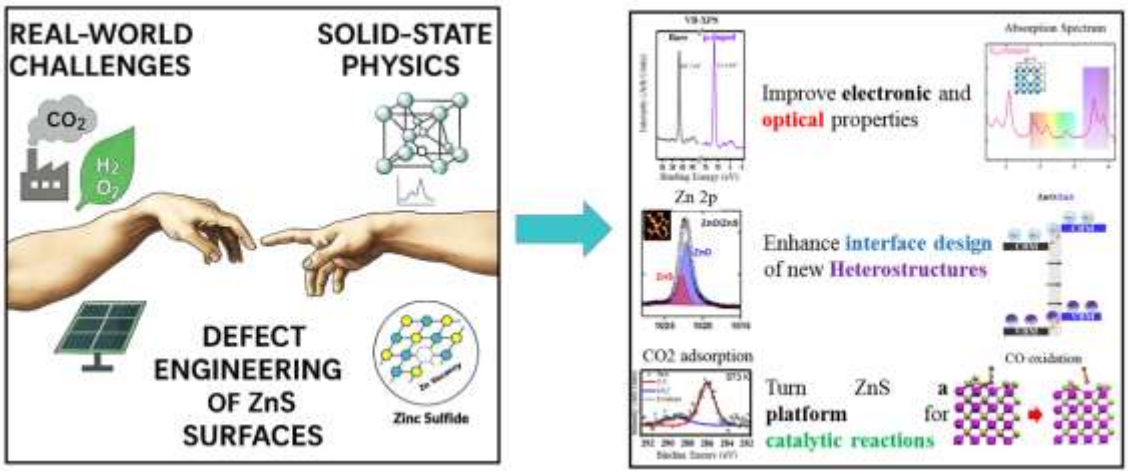

Figure 1. “My Thesis creation”. Graphical abstract illustrating the key-points explored in this thesis.

Cold Plasma-Driven Xenon Trapping in Silicate Nanocages on Metal Powders

Laiba Bilal,[1,2] **Dr. J. Anibal Boscoboinik**[2]

1 Department of Electrical and Computer Engineering, Stony Brook University, NY, USA
2 Centre for Functional Nanomaterials, Brookhaven National Laboratory, NY, USA
Email: laiba.bilal@stonybrook.edu

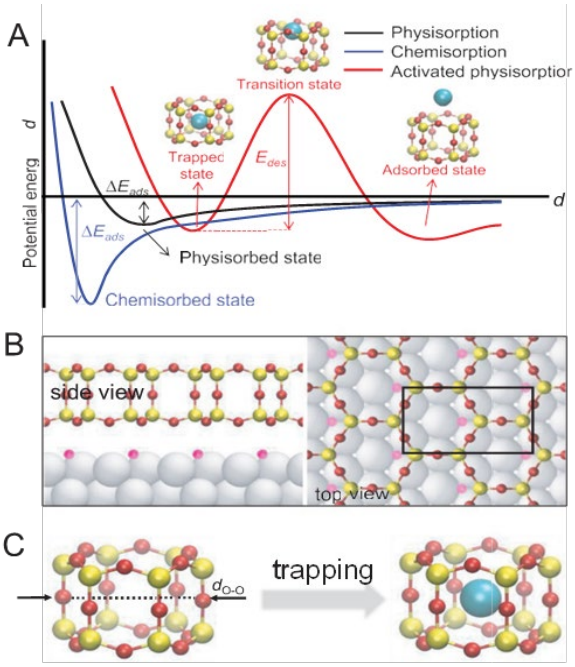

Figure 1. Potential energy diagram and structure of the 2D silica, as a noble gas atom gets trapped in a nanocage within the structure. A) Schematic diagram of the potential energy for a noble gas against the distance from contact surface (*d*) for physisorption, chemisorption, and activated physisorption, respectively. Δ*E*ads represents the adsorption energy; *E*des represents the desorption energy barrier for activated physisorption. B) Side (left) and top (right) views of the 2D silica bilayer film adsorbed on *p*(2x1)-O/Ru(0001) (i.e., (SiO2)8/4O/Ru(0001)). The black rectangle on the top view indicates the unit cell. C) Illustrations of the nanocages in the framework with and without the noble gas atom trapped inside. Color code: Ru (silver), Si (yellow), O in silica (red), and O chemisorbed on Ru (pink)[5].

Xenon (Xe), the heaviest non-radioactive noble gas, plays a critical role in modern technology and scientific research due to its chemical inertness, but this very feature also presents a persistent challenge; so how can we effectively trap or store Xe atoms in a solid matrix at room temperature? Despite its minuscule atmospheric abundance, roughly one part per ten million; xenon is widely used in plasma-based lighting,[1] ion propulsion for spacecraft,[2] medical imaging,[3] and nuclear monitoring. Efficient Xe capture is especially vital in the nuclear energy sector, where xenon isotopes like Xe-135 are produced during fission. Their accumulation can disrupt reactor dynamics, and their uncontrolled release can pose severe safety risks, as highlighted in historical nuclear accidents like Chernobyl.[4] Traditional approaches to Xe separation and capture rely on cryogenic distillation, which is costly, energy-intensive, and complex. The need for a scalable, ambient-condition method to trap xenon led us to explore nanostructured silicate frameworks specifically hexagonal prism-shaped cages that mimic crystalline silica bilayers previously studied at Brookhaven National Laboratory (BNL).[5,6]

Our research builds upon this concept by transitioning from flat, fragile bilayer films to robust, scalable metal powders coated with silicate nanocages derived from dodecaphenyl polyhedral

oligomeric Silsesquioxane (DP-POSS).[7] After cage deposition using chemical vapor deposition (CVD) or wet impregnation (WI), the powders were exposed to xenon gas ionized by a cold plasma. The resulting Xe^+ ions are neutralized by the metal surface and confined within the cages via van der Waals and electrostatic interactions. The activated physisorption model, visualized in Fig. 1A–C,[5] describes how Xe atoms overcome an energy barrier to enter the cage and become kinetically trapped. Figure 1A–C. (A) Potential energy diagram for noble gas trapping. (B) Side and top view of 2D silica bilayer on Ru(0001). (C) Silicate nanocage with and without trapped noble gas atom (adapted from reference [5]).

In our work, characterization via XPS confirmed successful Xe trapping, particularly on Ru powders, with evidence of Xe 3d peaks and Si 2p/Ru 3d ratios. This platform provides much higher surface area (~10 m^2/g) compared to flat films (~1 cm^2), enabling enhanced gas trapping and scalability. Applications include nuclear reactor safety, space propulsion, medical isotope production, and environmental monitoring. This study presents the first demonstration of room-temperature Xe trapping using cold plasma in a scalable material system.[8]

References

[1] T. E. of Encyclopedia. "xenon" Britannica, "Britannica, The Editors of Encyclopedia. 'xenon,'" can be found under https://www.britannica.com/science/xenon, **2021**.

[2] NASA Glenn Research Center, "NASA - Ion Propulsion," can be found under https://www1.grc.nasa.gov/research-and-engineering/space-propulsion/, **2022**.

[3] M. S. Bolmsjö, B. R. R. Persson, *Med Phys* **1982**, *9*, 96.

[4] B. Mercier, D. Yang, Z. Zhuang, J. Liang, *EPJ Nuclear Sciences & Technologies* **2021**, *7*, 1.

[5] J. Q. Zhong, M. Wang, N. Akter, J. D. Kestell, T. Niu, A. M. Boscoboinik, T. Kim, D. J. Stacchiola, Q. Wu, D. Lu, J. A. Boscoboinik, *Adv Funct Mater* **2019**, *29*, DOI 10.1002/adfm.201806583.

[6] Y. Xu, M. Dorneles de Mello, C. Zhou, S. Sharma, B. Karagoz, A. R. Head, Z. Darbari, I. Waluyo, A. Hunt, D. J. Stacchiola, S. Manzi, A. M. Boscoboinik, V. D. Pereyra, J. A. Boscoboinik, *Small* **2021**, *17*, DOI 10.1002/smll.202103661.

[7] B. Handke, Ł. Klita, W. Niemiec, *Surf Sci* **2017**, *666*, 70.

[8] L. Bilal, A. Khaniya, J. A. Boscoboinik, D. Olson, S. Moulton, *Small Science* **2025**, DOI 10.1002/smsc.202500136.

Syngas Conversion to Surface Carbon on Co/CeO_2 Catalysts

Matthew J. Bonney,[1] Michale G. White[2]

1 Department of Chemistry, Stony Book University, Stony Brook, NY
2 Chemistry Division, Brookhaven National Laboratory, Upton, NY

Email: matthew.bonney@stonybrook.edu

The chemical conversion of carbon dioxide has gained significant attention as an alternative route for producing simple liquid fuels and other commodity chemicals while also mitigating greenhouse gas emissions through capture and reutilization. One process involves the reduction of CO_2 via dry reforming of hydrocarbons to syngas ($CO+H_2$), which can be used as a source H_2 or as feed gas for the production of liquid fuels by Fischer-Tropsch catalysis [1]. Alternatively, the CO product can be used to generate solid carbon materials, e.g., carbon nanofibers, via the Boudouard reaction, $2CO \rightarrow C_{(s)} + CO_2$. As an intermediate product in a two-step tandem process involving both reactions, the presence of H_2 can also enhance the conversion of CO to C(s).[2]

In this work we are examining the conversion of $CO + H_2$ to solid carbon on catalysts composed of nanoparticles of early transition metals (Co, Fe) and their alloys supported on ceria (CeO_2). Recent studies suggest that Co and Fe-Co NP's supported on CeO_2 are very active catalysts for the conversion of CO into carbon nanofibers, but the nature of the metal phase and the role H_2 in the reaction remain uncertain.[2] Here we present results to establish the optimum conditions for CO conversion, i.e., temperature and CO/H_2 ratio, and the nature of the metal active phase using ex situ XPS. Results will also be presented for CO conversion on atomically precise Co_n clusters (n = 1-12) supported on ceria that are prepared by mass-selected cluster deposition (Fig. 1). These studies probe the effects of cluster size (structure) and Co-ceria electronic interactions in determining CO reaction pathways.

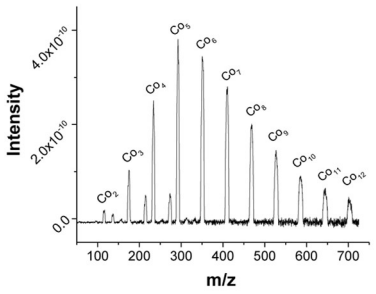

Figure 1. Mass spec of Co_n mass-selected clusters made via Magnetron Sputtering.

Initial work performed on pressed CeO_2 powder; the Co nanoparticles were deposited by evaporating Co rods using an e-beam evaporator(Oxford Applied Research). During the reaction, the samples were exposed to either 100 mbar of CO and H_2(1:1) or 150 mbar of CO and H_2(1:2) and annealed for one hour at different temperatures between 300°C and 600°C. The surface were analyzed via XPS, the samples loaded onto a four-axis manipulator (xyz-Φ) where the sample surface could be positioned for maximum signal. The XPS instrument consists of a hemispherical electron analyzer (Specs HSA 3500) and a non-monochromatized x-ray source (Al Kα, 1486.6eV, Thermo Fisher XR3 Twin Anode X-ray source). Core level spectra were collected at RT for Ce 3d, Co 2p, Fe 2p, O 1s, and C 1s at a 20eV pass energy. The XPS spectra were least-squares fitted with Shirley background contributions using CasaXPS software. The Ce4+ 3d u''' binding energy of 916.7eV was used to calibrate the energy spectra.[2]

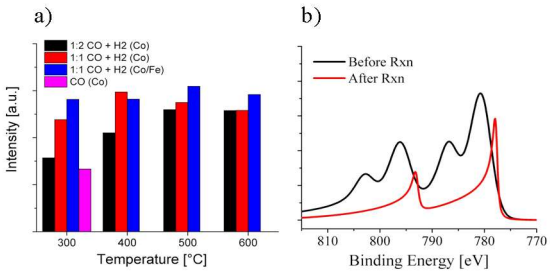

Figure 2. a) The surface carbon is measured on Co/ CeO_2 and Co-Fe/CeO_2 surfaces under varied ratios of CO and H_2. b) The Co 2p XPS of the Co/CeO_2 sample, the Co is reduced from Co(II) to Co(0).

On the bare ceria support, no surface carbon from the reaction was detected even at 600°C. In contrast, the Co/CeO_2 surface is highly active for the conversion of CO to surface carbon, with enough surface carbon to prevent the detection of the ceria support via XPS (Ce 3d) after reaction. Characterization of the C 1s spectra shows that the carbon deposit is primarily atomic carbon with a small percentage of carbon oxygenates observed at higher binging energies. The conversion of CO to surface carbon increases with temperature and higher Co coverage, with the intensity of the surface carbon leveling out at higher values (Fig. 2a). The Co 2p spectra shows that the initially oxidized Co(II) prior to reaction is completely reduced to metallic Co(0) after reaction (Figure 2b).[3]. Further work is being done to explore the impact on Co_n cluster size for the catalytic conversion, as well as further characterization on the structure of surface carbon via Raman spectroscopy.

References:

[1] Xie, Z.; Gomez, E.; Chen, J. G., Simultaneously Upgrading Co and Light Alkanes into Value-Added Products. AIChE Journal 2021, 67, e17249.

[2] Yuan, Y.; Huang, E.; Hwang, S.; et al Converting Carbon Dioxide into Carbon Nanotubes by Reacting with Ethane. Angew. Chem., Int. Ed. Engl. (2024), 63, e202404047.

[3] Kim, K. S. X-Ray-Photoelectron Spectroscopic Studies of the Electronic Structure of CoO. Phys. Rev. B (1975), 11 (6), 2177.

Investigation of Adsorption and Selective Hydrogenation of 1.3-butadiene on Cu(111) and Pd/Cu(111) Single-Atom Alloy Surfaces

Mohammad Rahat Hossain,[1] Ahmad Arshadi,[2] Ye Xu,[2] Michael Trenary[1]

[1]Department of Chemistry, University of Illinois Chicago, 845 W. Taylor Street, IL, 60607, USA
[2]Department of Chemical Engineering, Louisiana State University, Patrick F. Taylor Hall, Baton Rouge, LA 70803, United States. Email: yexu@lsu.edu

Email: mhossa21@uic.edu

The selective hydrogenation of 1,3-butadiene (BD) to 1-butene is a key industrial transformation used to purify C_4 hydrocarbon streams for polymer production. While conventional Pd catalysts are effective, they often suffer from over-hydrogenation and deactivation due to coking [1-4]. In this work, we demonstrate that a Pd/Cu(111) single-atom alloy (SAA) surface exhibits excellent selectivity and reactivity for this transformation under ambient pressure, and we investigate the underlying adsorption modes of BD on Cu(111) that contribute to this behavior. Using reflection absorption infrared spectroscopy (RAIRS), we directly monitored the real-time conversion of BD to 1-butene at 380 K in the presence of 10 Torr of H_2. Gas-phase spectral features confirmed 84% selectivity toward 1-butene with no detectable butane formation, indicating suppression of over-hydrogenation. Kinetic measurements showed the reaction is first-order in H_2 (1.12 ± 0.04) and approximately zero-order in BD (-0.12 ± 0.01), with a turnover frequency of 36 s^{-1} and an activation energy of 63 ± 3 kJ/mol—comparable to values for pure Pd surfaces. No stable surface intermediates were detected during the reaction, suggesting transient adsorption and rapid conversion [5].

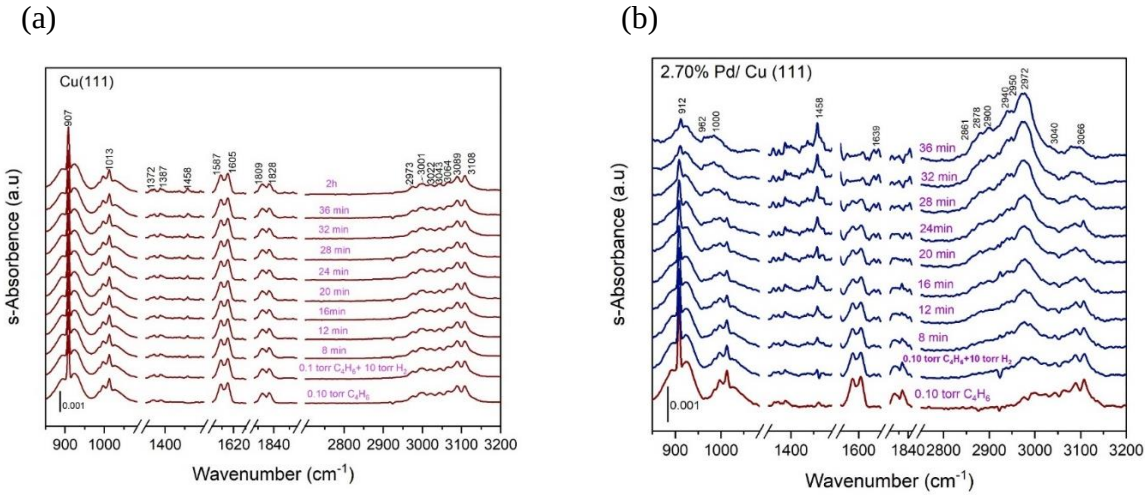

Fig. 1: Gas phase RAIR spectra of 0.1 Torr 1,3-butadiene and 10 Torr H_2 on (a) Cu (111) and (b) 2.7% Pd/Cu (111) at 380 K shown over a reaction time of 36 minutes at 4-minute intervals. 0.10 Torr of 1,3-butadiene and 10 Torr H_2 are introduced successively in a closed reaction vessel with a total pressure of 10.10 Torr. All the vibrational modes are labeled at the final RAIR scan at 36 mins.

To understand the absence of observable surface intermediates and the high product selectivity, we investigated the adsorption of BD on clean Cu(111) using low-temperature RAIRS and temperature programmed desorption (TPD). At low exposures (≤1.0 L) and 85 K, BD chemisorbs to Cu(111) in configurations distinct from physisorbed multilayers, showing unique IR signatures. A combined analysis using TPD, RAIRS, and DFT shows that 1,3-butadiene chemisorbs on Cu(111) with an interaction strength that lies between weak physisorption (as seen on Ag(111) and Au(111)) and strong chemisorption (as on Mo(100), Pd(110), or Pt(111)). On strongly interacting surfaces, the molecule dissociates upon heating, leaving carbon residues. In contrast, on Ag(111) and Au(111), RAIRS spectra closely resemble that of solid butadiene, indicating minimal bonding perturbation. On Cu(111), the bonding is sufficiently strong to alter vibrational features relative to the gas-phase molecule, yet weak enough to allow intact desorption. Comparison of experimental and DFT-simulated spectra suggests that 1,3-butadiene binds as a mixture of *s-trans* di-π, *s-cis* di-π, and *s-trans* tetra-σ species. This discovery provides crucial insights into molecular rehybridization on Cu(111) despite having very low binding energy and how these adsorption modes govern selective hydrogenation pathways [6]

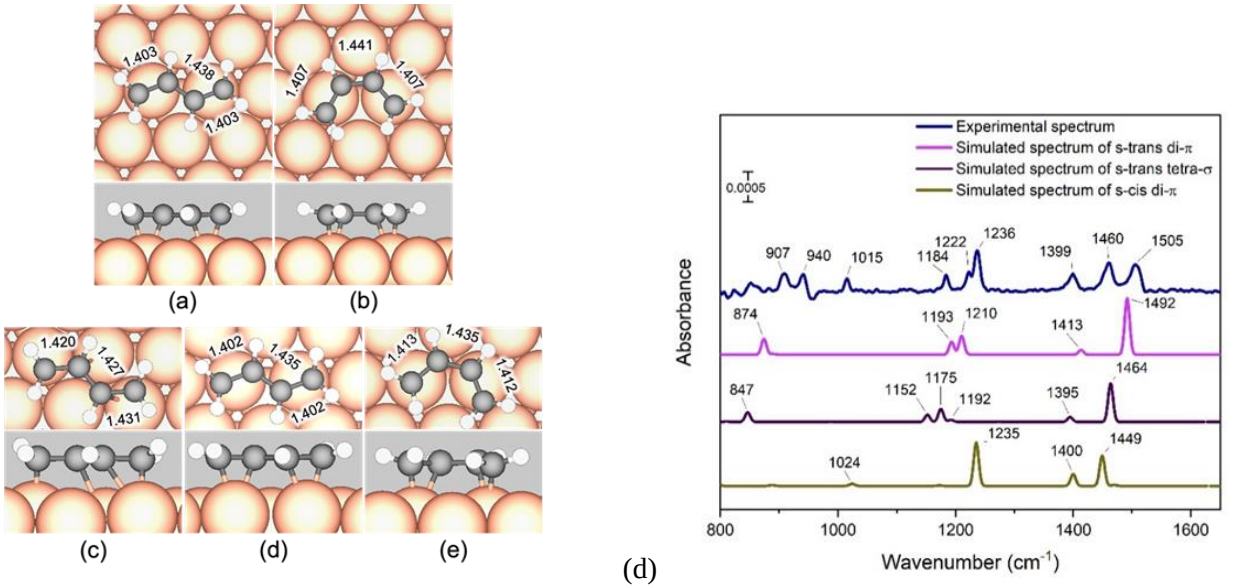

Fig. 2: Minimum-energy adsorption states for 1,3-butadiene calculated using the optB86b-vdW functional, in top (upper panels) and side (lower panels) views: at 1/9 ML, (a) s-trans di- π; (b) s-cis di-π; at 1/6 ML, (c) s-trans tetra-σ, (d) s-trans di-π, and (e) s-cis di-π. The lengths of the C-C bonds (in Å) are as indicated. Color code: brown = Cu, black = C, white = H. (d) Comparison of experimental and simulated spectra for the *s-trans* di-π, *s-trans* tetra-*σ* and *s-cis* di-π structures at 1/6 ML as shown in (c-e). The experimental RAIR spectrum was obtained by exposing the surface held at 130 K to 1.0 L of 1,3-butadiene. The background spectrum was also obtained at 130 K. The intensities of the simulated spectra have been scaled to match the experimental spectrum.

The selective formation of 1-butene on Pd/Cu(111) SAA is likely due to the site-isolated nature of Pd atoms that facilitate H_2 dissociation without over-adsorption of butene products. The weak interaction of BD with Cu(111) allows for rapid desorption of products such as 1-butene before further hydrogenation to butane can occur. The dominance of the 1,2-di-π binding geometry supports 1,2-H addition, explaining the selectivity toward 1-butene.

References

1. M. Pradier, E. Margot, Y. Berthier and J. Oudar, Appl. Catal. **43** (1), 177-192 (1988).
2. G. Tourillon, A. Cassuto, Y. Jugnet, J. Massardier and J. Bertolini, J. Chem. Soc., Faraday Trans. **92** (23), 4835-4841 (1996).
3. T. Ouchaib, J. Catal. **119** (2) (1989).
4. J. Massardier, J. Bertolini, P. Ruiz and P. Delichere, J. Catal. **112** (1), 21-33 (1988).
5. Hossain, M.R. and Trenary, M., J. Phys. Chem. C , 128, 45, 19204–19209.
6. Hossain, M.R., Ahmad A., Xu Y. and Trenary, M, Phys. Chem. Chem. Phys. (manuscript submitted)

A Priori designed NiAg Single-Atom Alloys for Selective Epoxidation Reactions

Elizabeth E. Happel,[1] **E. Charles H. Sykes**[1,2]

[1]Department of Chemistry, Tufts University, Medford, MA 02155, United States

[2]Department of Chemical and Biological Engineering, Tufts University, Medford, MA 02155, United States

Email: elizabeth.happel@tufts.edu

Ethylene oxide, produced via the partial oxidation of ethylene, is among the highest-volume chemicals manufactured globally, yet its production comes with a significant environmental cost. Industrial synthesis using Ag catalysts achieves high ethylene oxide (EO) selectivity (~90%), but this performance is only attainable through the co-feeding of Cl and additional promoters such as Cs and Re. Even with these additives, reactors are limited to low per-pass conversions (<15%) to suppress the total combustion of ethylene and EO to carbon dioxide [1]. This limitation, combined with the volume of production, gives EO one of the largest carbon footprints among commodity chemicals.

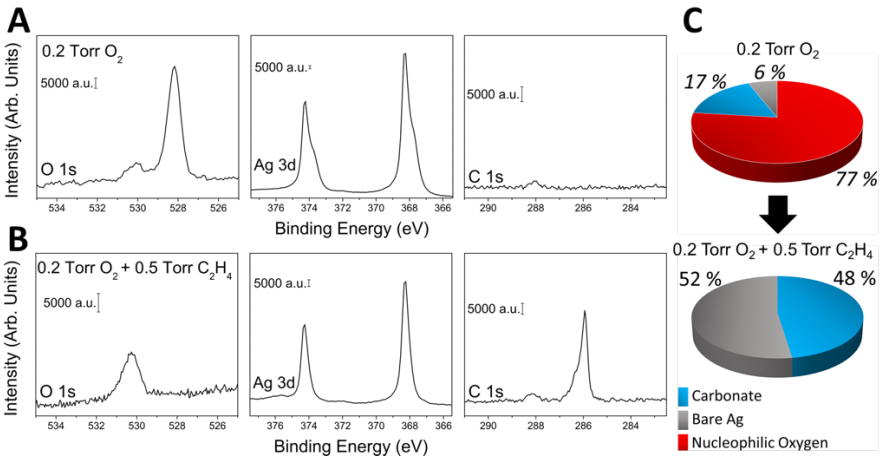

Fig 1. C 1s, O 1s, and Ag 3d spectra of Ag(111) under **(A)** 0.2 Torr O_2 at 433 K and **(B)** 0.2 Torr oxygen and 0.5 Torr ethylene at 433 K. The C 1s and Ag 3d spectra were taken at 500 eV and O 1s at 760 eV photon energies **(C)** shows the surface composition at 0.2 Torr oxygen followed by the composition at 0.2 Torr oxygen and 0.5 Torr ethylene.

To design more selective and environmentally sustainable catalysts, we began by investigating the surface chemistry of Ag under conditions relevant to industrial EO production. A central controversy in the field concerns the oxidation state of the Ag surface under reaction conditions. Proposed mechanisms of epoxidation often invoke either oxidized or metallic silver sites as the active centers [2-4]. Using ambient pressure X-ray photoelectron spectroscopy (AP-XPS), we measured the Ag(111) surface at 433 K and under 0.2 Torr O_2. The resulting spectra reveal a mixture of two oxygen species: electrophilic oxygen (530.2 eV) and nucleophilic oxygen (528.4 eV), yielding a total surface coverage ~94% (Fig 1A) [2]. However, when 0.5 Torr ethylene is introduced (a 5:2 ethylene-to-oxygen ratio representative of industrial conditions), nucleophilic

oxygen is rapidly consumed, and the remaining oxygen signal corresponds largely to surface carbonate, which appears at a similar binding energy to electrophilic oxygen (Fig 1B). The total oxygen content drops with only carbonate remaining and leaving ~50% of the surface as bare metallic Ag (Fig 1C).

This transformation is mirrored in the Ag 3d spectra: under oxidizing conditions, a characteristic low-binding-energy shoulder is observed, consistent with a surface oxide reconstruction. Upon ethylene introduction, this feature disappears, confirming the rapid reduction of the surface. These findings suggest that the active catalyst surface under reaction conditions is primarily metallic, not oxidized. This supports mechanistic models invoking oxametallacycle (OMC) intermediates, which require bare Ag sites for formation [5].

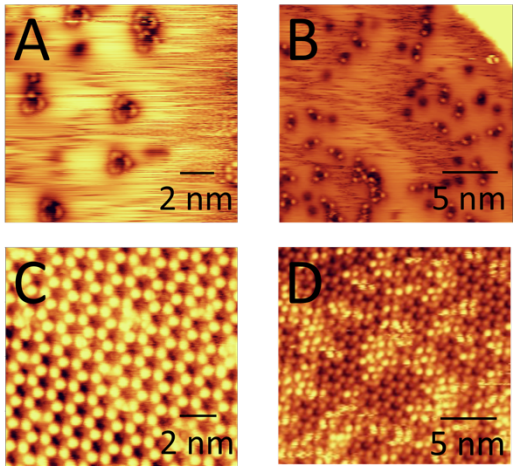

Fig 2. (A) NO_2 exposure to Ag(111) <373 K (image conditions: 0.3 nA, 50 mV) shows the formation of ring structures. **(B)** C_2H_4 is exposed to the same surface <23 K (0.3 nA, 50 mV) and new bright spots form in the existing corners of the triangular structures. **(C)** Ag(111) is exposed to NO_2 between 473-525 K and a honeycomb structure (p(4x4)) forms (0.2 nA, 100 mV). **(D)** C_2H_4 is exposed to the same surface <23 K (0.2 nA, 100 mV) and new bright patches of ethylene cluster on top of the p(4x4) surface.

To investigate the atomic-scale structure of the oxygen species seen in XPS, we employed low-temperature scanning tunneling microscopy (STM). Due to the low sticking probability of O_2 in UHV conditions, we used NO_2 as an oxidant to controllably generate oxygen species on Ag(111). By adjusting the sample temperature during exposure, we selectively formed either electrophilic or nucleophilic oxygen phases. STM imaging of surfaces dosed with NO_2 at ~373 K, a temperature consistent with electrophilic oxygen formation, revealed a triangular ring-like structure consisting of three-lobed protrusions surrounding a central Ag vacancy (Fig 2A). In contrast, NO_2 dosing at ~473 K produced the well-known p(4×4) honeycomb reconstruction, characteristic of nucleophilic oxygen (Fig 2C) [6].

Further, we dosed ethylene onto these oxygen-covered surfaces at cryogenic temperatures (~25 K). On the electrophilic oxygen phase, ethylene preferentially adsorbed at the ring corners, producing brighter STM contrast at those positions and forming extended chain-like assemblies (Fig 2B). DFT simulations of oxametallacycle intermediates support this structural assignment, as the observed ethylene–oxygen binding motifs resemble the OMC geometry. Conversely, on the nucleophilic oxygen-covered surface, ethylene binding was more disordered and lacked consistent adsorption geometry (Fig 2D). These results offer the first direct visualization of distinct surface oxygen phases on Ag(111) and their differing interactions with ethylene, providing a critical experimental foundation for future DFT modeling of reactivity and spectroscopy.

Having established that the active Ag surface under reaction conditions is largely metallic and that electrophilic oxygen forms distinct ring-like structures associated with selective epoxidation,

we sought to improve the catalytic performance through rational design. Motivated by the need to preserve the inherent selectivity of Ag for ethylene oxide formation while overcoming the kinetic limitation imposed by the high barrier to O_2 activation, we hypothesized that a promoter capable of lowering the O_2 dissociation barrier, without over-stabilizing oxygen, could facilitate more efficient oxygen activation and sustain high selectivity without relying on Cl promotion.

Using density functional theory (DFT), our collaborators screened potential dopants for their ability to dissociate O_2 and weakly bind the resulting oxygen atoms. Ni emerged as an ideal dopant: DFT showed that single Ni atoms embedded in Ag(111) drastically lower the O_2 dissociation barrier to <0.05 eV, while maintaining a moderate oxygen binding energy (~-2.2 eV). To test this prediction experimentally, we fabricated single-atom NiAg(111) alloys containing ~1% Ni and characterized their surface chemistry using temperature-programmed desorption (TPD) (Fig 3A) [7]. After dosing 500 L of O_2 at 350 K, TPD spectra of NiAg(111) showed significant O_2 uptake and desorption at ~525 K (a full 50 K lower than on pure Ag(111)). These results confirm facile O_2 activation and spillover of atomic oxygen to the Ag surface at low pressure [7].

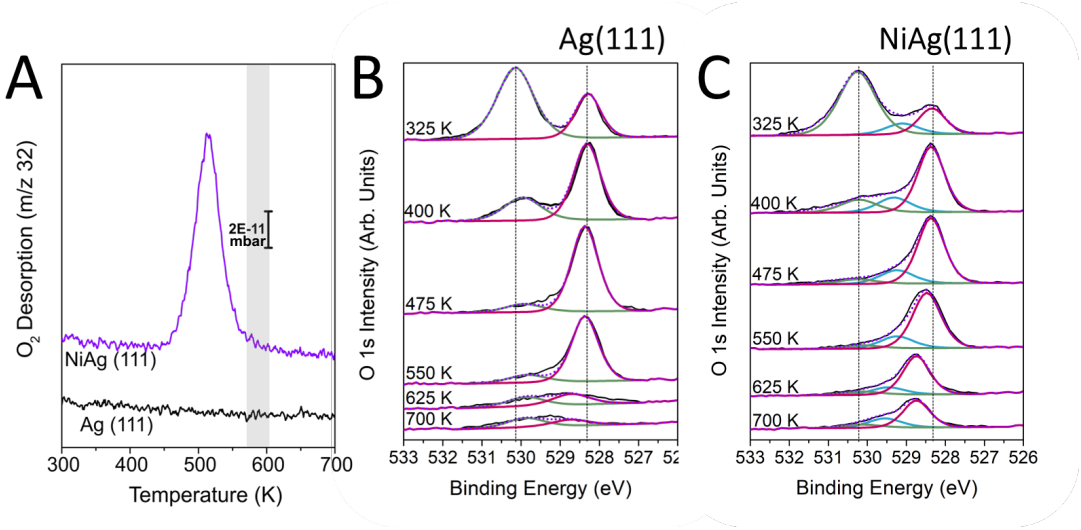

Fig 3. **(A)** O_2 TPD traces for Ag(111) and ~1% NiAg(111) after 500 Langmuirs (L) of oxygen dosed at 350 K, cooling to room temperature, and recording the TPD with a 1 K/s heating rate. AP-XP spectra showing a change in oxygen species from primarily electrophilic oxygen (pink, ~530.2 eV) to more nucleophilic oxygen (red, ~528.5 eV) as the temperature was increased on **(B)** Ag(111) and **(C)** ~5% NiAg(111).

To assess the thermal stability and redox behavior of these alloy surfaces, we conducted multiple annealing and oxidation cycles. The TPD response remained consistent, demonstrating that Ni atoms reversibly segregate to the surface under oxidizing conditions and diffuse back into the subsurface under vacuum. This reversible behavior is particularly attractive for catalyst durability under fluctuating reaction environments.

We next examined the oxygen species formed on NiAg(111) using AP-XPS. Compared to Ag(111), Ni-doped surfaces maintained nucleophilic oxygen signatures at higher temperatures, with the 528.4 eV feature persisting up to 700 K. This enhanced thermal stability of nucleophilic oxygen suggests that Ni stabilizes otherwise reactive oxygen atoms, potentially rendering them

less prone to engage in unselective combustion pathways (Fig 3B/C) [7]. DFT calculations corroborate this interpretation, showing that nucleophilic oxygen becomes less reactive when bound in proximity to Ni.

These atomic-scale insights informed the design of supported NiAg catalysts. Collaborators demonstrated supported NiAg nanoparticles under industrially relevant conditions (10% C_2H_4, 10% O_2, balance He) showed a ~25% increase in EO selectivity compared to pure Ag catalysts. Notably, this enhancement was achieved without any Cl co-flow. Moreover, when Cl was introduced, NiAg catalysts further improved selectivity to >90%, eliminating the need for additional promoters such as Cs or Re [7].

Together, these results demonstrate the power of surface science techniques in unraveling mechanistic questions at the heart of industrial catalysis. Our ability to correlate spectroscopic fingerprints with atomically resolved surface structures and reaction intermediates enabled a more complete picture of the oxygen speciation on Ag surfaces and its reactivity under operating conditions. This understanding, in turn, informed the rational design of a new class of Cl-free, highly selective ethylene epoxidation catalysts based on dilute NiAg alloys.

By revealing that the active Ag surface is metallic and structurally distinct from prior oxidized models, we provide strong evidence supporting mechanisms involving bare Ag and ring-structured electrophilic oxygen, both of which were previously challenging to observe directly. The stabilization of nucleophilic oxygen by Ni and the ability to reversibly populate the Ag surface with reactive oxygen in UHV conditions without plasma sources or aggressive oxidants represents a significant advance in our synthetic control over catalyst surfaces.

Ultimately, this study underscores the relevance of surface science in addressing pressing industrial challenges. Techniques like STM and AP-XPS, though often employed in idealized environments, provide the mechanistic clarity necessary for bridging model systems and applied catalysis. The insights gained here open new directions in selective oxidation catalysis, both in the identification of previously uncharacterized surface species and in the implementation of theory-guided alloying strategies. In doing so, we illustrate the essential role of surface science in the rational design of real-world catalytic processes.

[1] J.H. Miller, A. Joshi, X. Li, A. Bhan, J. Catal. **389,** 714 (2020).
[2] T. Pu, H. Tian, M.E. Ford, S. Rangarajan, I.E. Wachs. ACS Catal. **9,** 12 (2019).
[3] V.I. Bukhiyarov, I.P. Prosvirin, R.I. Kvon. Surf. Sci. **320,** 1-2 (1994).
[4] S. Linic, M.A. Barteau. J. Catal. **214,** 2 (2003).
[5] S. Linic, M.A. Barteau. J. Am. Chem. Soc. **124,** 2 (2002).
[6] M.E. Turano, R.G. Farber, E.C.N. Oskorep, R.A. Rosenberg, D.R. Killelea. J. Phys. Chem. C. **124,** 2, (2020).
[7] E.E. Happel, A. Jalil, L. Cramer, A. Hunt, A.S. Hoffman, I. Waluyo, M.M. Montemore, P. Christopher, E.C.H. Sykes. Science **387,** 6736 (2025).

Thursday Morning

9:00 AM – 9:40 AM

Invited Talk

Science and User Support Center (SUSC), Building 101

Sylvie Rangan

2D organic layers on surfaces: self-assembly, on-surface chemistry and electronic structure

9:40 AM – 10:40 AM

Contributed Talks V

Science and User Support Center (SUSC), Building 101

- Quantitative Comparative Force Spectroscopy on Molecules - *Eric I. Altman, Xinzhe Wang, Percy Zahl, Jara Trujillo Mulero, Hailiang Wang, Rubén Pérez, and Udo D. Schwarz*
- Applications of Scanning Tunneling Microscopy in Heavy Element Studies - *Benjamin R. Heiner, Miles F. Beaux II*
- Imaging Molecules from "Stardust" *Percy Zahl, Martha L. Chacon-Patino, Joseph W., Frye-Jones*

10:40 AM – 11:00 AM

Coffee Break (provided)

11:00 AM – 12:00 PM

Contributed Talks VI

Science and User Support Center (SUSC), Building 101

- In-situ Atomic-Resolution Observations of Formation of Amorphous Iron during Reduction of Iron Oxides in Hydrogen - *Yupeng Wu, Zhikang Zhou, Wenhui Zhu, Linna Qiao, Shuonan Ye, Xiaobo Chen, Renu Sharma, Judith C. Yang, Mengen Wang, Guangwen Zhou*
- Reliability Assessment and Failure Analysis of Vertical-Cavity Surface-Emitting Lasers with Different Oxide Apertures - *G.M. Wu, J.E. Lin*
- An Overview of Surface Science in Semiconductor Industries - *Mueed Ahmad*

2D organic layers on surfaces: self-assembly, on-surface chemistry and electronic structure

S. Rangan

Understanding the basic mechanisms leading to the formation of 2D organic layers on surfaces, either via Van der Waals, ionic or covalent interactions, is a necessary step toward the development of controlled and ordered organic layers, for technological applications such as homogeneous doping of graphene or 2D organic topological insulators. Using a combination of scanning tunnel microscopy, various electron spectroscopy techniques and ab-initio calculations, we have studied several aspects of the self-assembly and reactivity of particularly interesting model systems: Zinc tetraphenylporphyrins (ZnTPP) and their derivatives, on single crystal surfaces.

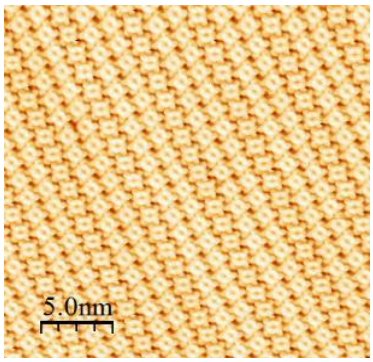

Figure 1. A highly ordered kinetically trapped system: ZnTPP on Ag(100).

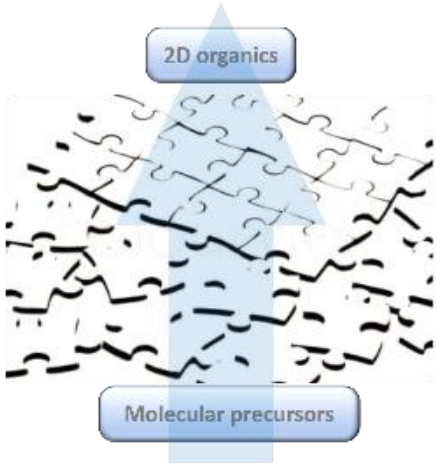

Figure 2. A strategy for 2D organic growth.

First, we have explored the delicate balance of forces during the molecular self-assembly process on metal single crystal surfaces. It is shown that molecule/molecule and molecule/surface interactions, as well as accumulated surface stress, all play an important role in determining self-assembly. In particular, self-assembly can be kinetically trapped into metastable phases different from typical equilibrium outcomes (Figure 1).

Additionally, in order to develop and expand a synthesis toolbox necessary for the directed growth of highly ordered 2D covalent structures (Figure 2), we have studied novel mechanisms of surface-mediated chemistry to form intra- and inter-molecular covalent bonds between functionalized ZnTPPs on metal surfaces. In particular, dehydrofluorination reactions render C-C bond formation chemo-selective as well as potentially regio-selective, if employed with a properly designed molecular precursor.

Sylvie Rangan

Rutgers

Dr. Rangan is the director of the Laboratory for surface modification (LSM) Facilities, housing state-of-the-art electron spectroscopies tools, ion scattering beamlines, transmission electron microscopes as well as an helium ion microscope. She also runs a research group focused on on-surface self-assembly of molecular building blocks for novel 2D materials, energy alignment control at heterointerfaces, and the development of tools aimed at correlating electronic properties to chemical processes in photoresist materials.

Title: Quantitative Comparative Force Spectroscopy on Molecules

Eric I. Altman, [1,2*] Xinzhe Wang,[2] Percy Zahl,[3] Jara Trujillo Mulero,[4] Hailiang Wang,[5] Rubén Pérez,[4] and Udo D. Schwarz[1,2,6]

Affiliation: [1]Department of Chemical & Environmental Engineering, [2]Department of Materials Science, [5]Department of Chemistry, [6]Department of Mechanical Engineering, Yale University, New Haven, CT 06520

Affiliation: [3]Center for Functional Nanomaterials, Brookhaven National Laboratory, Upton, NY 11973

Affiliation: [4]Departamento de Fisica Teorica de la Materia Condensada, Universidad Autonoma de Madrid, Spain

Email: eric.altman@yale.edu

Understanding molecular-scale interactions at surfaces is essential for advancing catalyst design and developing efficient energy conversion processes. Here, we report ongoing efforts to improve the spatial accuracy and quantitative reliability of three-dimensional atomic force microscopy (3D-AFM) by refining data correction techniques for CO-functionalized tips. These developments allow us to minimize tip- and substrate-induced artifacts and isolate the intrinsic molecular interaction at atomic resolution.

As a testbed for this approach, we investigate cobalt phthalocyanine (CoPc) and its amino-functionalized counterpart ($(NH_2)_4$CoPc) adsorbed on Ag(111), both of which are of interest in CO_2 electroreduction catalysis. By identifying and removing asymmetric force contributions caused by the metallic structure of the tip, we obtain corrected force spectroscopy data that reveal equilibrium interaction distances and energies across individual molecules. Our analysis shows that NH_2 substitution alters the spatial distribution of interaction strength, decreasing equilibrium distances near ligand attachment points while broadly reducing interaction energy with the tip.

These experimental observations agree well with DFT-based simulations and suggest that side-group functionalization directly modulates the molecule's chemical landscape. The methodology provides a direct route toward correlating molecular structure with catalytic behavior at the single-molecule level, thereby enabling a deeper understanding of functional molecular systems on surfaces.

Applications of Scanning Tunneling Microscopy in Heavy Element Studies

Benjamin R. Heiner, Miles F. Beaux II

Los Alamos National Laboratory, P.O. Box 1663, Los Alamos, New Mexico 87545 USA

Email: benheiner@lanl.gov

Scanning Tunneling Microscopy and Spectroscopy (STM/S) are powerful techniques for investigating atomic, molecular, and surface properties. At Los Alamos National Laboratory, a specialized instrument designed to contain and probe samples containing heavy elements (i.e. actinides) allows us to study of the most uncharacterized elements on the periodic table. This capability has facilitated new insights into the electronic structure of plutonium oxides, intermetallics, and complexes. Using temperature-resolved STS, we can directly and continuously measure the total density of states of these materials across the Fermi energy, addressing a critical gap in experimental plutonium data. These advancements provide valuable information for understanding the electronic behavior of plutonium, with implications for fundamental science and nuclear materials research. Additionally, our ongoing efforts aim to apply these techniques to molecular complexes containing a single actinide atom, enabling both STM imaging and localized STS probing of individual actinide atoms.

LA-UR-25-22710

Imaging Molecules from "Stardust"

Percy Zahl,[1#*] Martha L. Chacon-Patino [2], Joseph W., Frye-Jones [2]

[1]*Center for Functional Nanomaterials, Brookhaven National Laboratory, NY 11973*
[2]*Ion Cyclotron Resonance User Facility, National High Magnetic Field Laboratory, Florida State University, FL 32310*

Presenting author's e-mail: pzahl@bnl.gov
* Corresponding author's e-mail: pzahl@bnl.gov

Meteorites provide a glimpse into the past of the solar system by preserving snapshots of the universe for millions to billions of years. (1) Organic material forms over this time, creating common molecules seen on Earth such as carboxylic acids, aromatic and aliphatic hydrocarbons, and most importantly for life, amino acids. (1–4) Organic material formed in such a way is often revealed as ultra-complex mixtures, similar to fossil fuels and natural dissolved organic matter seen on Earth.

However, these ultra-complex organic mixtures require ultrahigh-resolution analytical techniques to achieve comprehensive molecular-level characterization.

Very little work has been done so far using HR-AFM (5). Here we analyze highly enriched PAH meteorite sample extracts using our preliminary extraction method similar to that used for fossil fuels. Acetone assists in the extraction of highly aromatic compounds out of a powdered form of meteorite specimens that have already been extracted in a polarity gradient from methanol to toluene. The resulting fraction is enriched in highly aromatic/hydrogen-deficient compounds, as suggested by ultrahigh resolution FT-ICR mass spectrometry.

Comparison with a fraction extracted with chloroform demonstrates a drop in the H/C ratio (a measure of aromaticity) from an average 1.6 for chloroform species down to 0.6 for acetone-extracted compounds. This correlates with the images observed in HR-AFM, where more aliphatic species were observed in the chloroform extract compared to the highly aromatic compounds observed in the acetone fraction. The selected motifs observed in Fig.1 highlight the highly aromatic composition of species from the acetone fraction (Mn), containing complex ring systems vs. (D0) like.

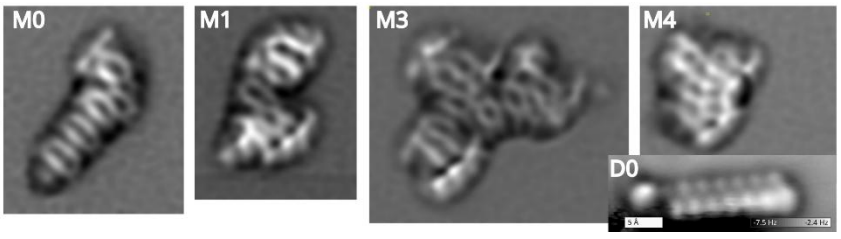

Figure 1. HR-AFMs from our Murchison extracts: Images reveal surprising large and complex molecules.

References:

[1] Sephton, M. A., *Phil. Trans. R. Soc. A: Mathematical, Phys. and Eng. Sci.*, *363* (1837), 2729–2742 (2005)

[2] Pizzarello, S.; Cooper, G. W.; Flynn, G. J., *Meteorites and the Early Solar System II,* 625–651 (2006)

[3] Pizzarello, S., *Acc Chem Res*, *39* (4), 231–237 (2006)

[4] Pizzarello, S.; Shock, *Cold Spring Harb Perspect Biol*, *2* (3), 1–19 (2010)

[5] Kaiser K.; *Meteoritics & Planetary Science 57, Nr 3*, 644–656 (2022)

In-situ Atomic-Resolution Observations of Formation of Amorphous Iron during Reduction of Iron Oxides in Hydrogen

Yupeng Wu[1], Zhikang Zhou[1], Wenhui Zhu[1], Linna Qiao[1], Shuonan Ye[1], Xiaobo Chen[1], Renu Sharma[2], Judith C. Yang[3], Mengen Wang[4], Guangwen Zhou[1]

[1] Department of Mechanical Engineering & Materials Science and Engineering Program, Binghamton University, State University of New York, Binghamton, NY 13902, USA
[2]Materials Measurement Laboratory, National Institute of Standards and Technology, Gaithersburg, MD 20899, USA
[3]Center for Functional Nanomaterials, Brookhaven National Laboratory, Upton, NY 11973, USA
[4]Department of Electrical and Computer Engineering & Materials Science and Engineering Program, Binghamton University, State University of New York, Binghamton, NY 13902, USA

Email: ywu231@binghamton.edu

Hydrogen-based direct reduction (HyDR) offers a sustainable alternative to conventional ironmaking, significantly reducing CO_2 emissions by replacing carbon monoxide with hydrogen. However, the underlying reduction mechanisms of iron oxides in HyDR remain poorly understood, especially at the atomic scale. Using in situ environmental transmission electron microscopy to directly visualize the hydrogen reduction of Fe_3O_4 and FeO, we demonstrate a previously unobserved transient amorphous Fe phase. Our high-resolution imaging captures the stepwise reduction of Fe_3O_4 to FeO, followed by the formation of an amorphous Fe layer, which subsequently crystallizes into α-Fe. The reduction of FeO proceeds faster than Fe_3O_4, resulting in a thicker amorphous Fe overlayer. The amorphous Fe layer stabilizes at ~4 nm thickness, beyond which further reduction drives the nucleation of crystalline Fe particles. These observations provide direct evidence of an interface-strain mediated reduction pathway involving amorphous intermediates. The insights gained from atomic-scale imaging highlight the critical role of microstructural interfaces and transient phases in governing oxide reduction kinetics. This work informs the design of more efficient HyDR processes for low-carbon steel production and contributes broadly to the understanding of gas–solid transformations in energy and materials applications.

Reliability Assessment and Failure Analysis of Vertical-Cavity Surface-Emitting Lasers with Different Oxide Apertures

G.M. Wu,* J.E. Lin

Institute of Electro-Optical Engineering, Department of Electronic Engineering,
Chang Gung University, Taoyuan 333, Taiwan

*Email: wu@mail.cgu.edu.tw

The growth of artificial intelligence (AI) will bring about a large demand for data transmission in high-performance computing (HPC). In this case, the data transmission efficiency and energy consumption of the hardware equipment that maintains AI operation, such as the server, become particularly important. The development of silicon photonics technology is expected to become a technology that can replace traditional copper wires. The laser diode (LD) or vertical-cavity surface-emitting laser (VCSEL) is the core component for light emission, so that understanding their performance degradation and reliability due to thermal and electrical stresses under long-term use is crucial. Thus, it has become the motivation of this investigation. The experimental samples were inserted into the test boards of a burn-in system. The optical output power data were automatically recorded by computer software. The measurements were taken at 200-hour intervals to observe the trend of normalized optical output power over time. The failure criterion was defined as a decrease in the normalized output power to -2 dB, corresponding to 63.1 % of the initial value. Finally, Minitab statistical software was employed to perform the Anderson-Darling test (adjusted), identifying the best-fitting probability distribution (Weibull distribution) for the data and conducting distribution fitting. Finally, the experimental results have shown that the reliability of VCSEL devices decreased with smaller non-oxidized aperture diameters, and only the VCSELs with 6 μm apertures could reach the -2 dB failure criterion.

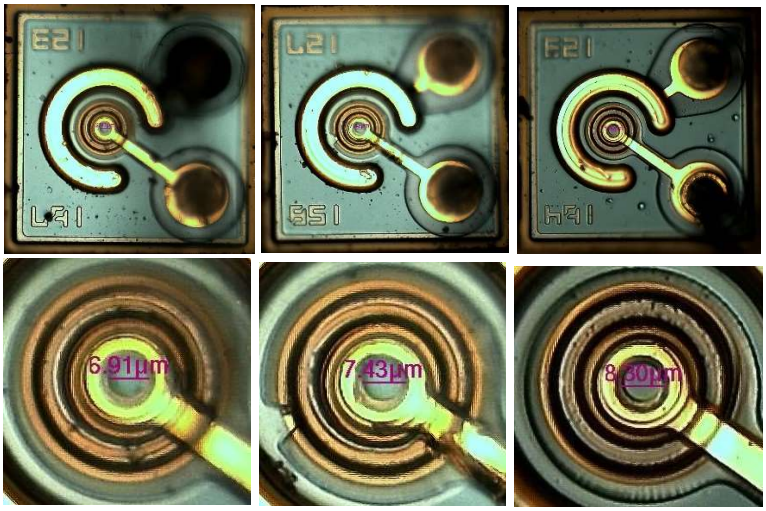

Fig. 1 Top view of VCSEL devices with 6, 7, 8 μm apertures.

An Overview of Surface Science in Semiconductor Industries

Mueed Ahmad[1]

[1]Center for Functional Nanomaterials, Brookhaven National Laboratory, Upton, New York 11973, United States

In an industry where nanometer-scale accuracy dictates performance and yield, understanding surface phenomenon becomes a necessity. The semiconductor sector's relentless drive toward smaller feature sizes and more complex architectures demands an intimate understanding of atomic-scale interactions at material interfaces. As device dimensions shrink below 10nm, surface effects that were negligible at larger scales now dominate process outcomes, making surface science knowledge critical for reliable device fabrication.

With over 1500 process steps on each semiconductor wafer, industries heavily rely on surface science principles that are applied to optimize processes such as thin-film deposition, etching, and lithography. One of the most critical applications of surface science in semiconductor fabrication is in thin-film deposition. Advanced techniques such as atomic layer deposition (ALD) and chemical vapor deposition (CVD) are utilized to grow ultra-thin, uniform layers of dielectrics (e.g., SiO_2, SiN) and conductive materials (e.g., W, Cu). The surface chemistry of these processes must be precisely controlled to ensure proper nucleation, minimal defects, and strong interfacial adhesion.

Lithography, especially extreme ultraviolet (EUV) lithography, majorly benefits from surface science innovations. As patterns shrink sub-10nm, traditional photoresists struggle with resolution and line-edge roughness. Semiconductor manufacturers are exploring novel resist chemistries and surface treatments to improve EUV photon absorption and pattern transfer fidelity. Additionally, anti-reflective coatings (ARCs) and underlayers (Hardmasks) are optimized to minimize light scattering and improve critical dimension uniformity.

Beyond deposition and patterning, surface science is crucial in chemical-mechanical planarization (CMP), where material removal must be uniform and defect-free. CMP is utilized to flatten wafer surfaces after multiple deposition and etching steps, preventing topography-induced issues in subsequent layers. The slurry chemistry, pad surface properties, and downforce parameters are all fine-tuned based on surface interactions to achieve optimal planarization without dishing or erosion. Post-CMP cleaning, another surface-sensitive process, ensures that abrasive particles and chemical residues are completely removed to avoid device failures.

Semiconductor manufacturing begins with purifying silicon and growing it into ingots, which are sliced and polished into wafers. The wafers undergo oxidation to form a protective SiO_2 layer, followed by photolithography to transfer circuit patterns using photomasks and etching to remove unwanted material. Doping and thin-film deposition (CVD/PVD) modify electrical properties, while metal interconnects (e.g., aluminum or copper) link different components. After Electrical Die Sorting (EDS) tests functionality, functional chips are cut, packaged, and wire-bonded into protective casings, then subjected to final performance tests before shipment. This intricate process transforms raw silicon into the chips powering our modern electronics.

Looking ahead, as semiconductor technology advances toward sub-10 nm nodes and beyond, surface science will become even more critical. Challenges such as atomic-level contamination, interfacial diffusion, and quantum effects require deeper understanding and innovative solutions. By mastering surface science, the semiconductor industry will continue pushing Moore's Law forward, unlocking revolutionary leaps in computing power and energy efficiency. These atomic-level breakthroughs will power tomorrow's AI systems, quantum computers, and smart devices - all built on surfaces engineered to perfection.

References:

1. He, Z. (2022). Analysis on the development of semiconductor manufacturing process. *Journal of Physics: Conference Series*, *2295*(1). https://doi.org/10.1088/1742-6596/2295/1/012009

2. Li, J. (2024). Overview of the development of chip manufacturing technology. *Applied and Computational Engineering*, *65*(1), 10-14. https://doi.org/10.54254/2755-2721/65/20240459